

BASIC COURSE ON ACCELERATOR OPTICS

J. Rossbach, Deutsches Elektronen-Synchrotron DESY
P. Schmüser, II. Institut für Experimentalphysik, Universität Hamburg, F.R. Germany

Abstract

The main subject of this introductory course is transverse optics in cyclic high energy accelerators. It is based on three one-hour lectures on "Basic transverse optics" given at the CERN Accelerator Schools (P. Schmüser, 1986 [5], 1988, 1990, and J. Rossbach, 1992). Although the emphasis is on periodic solutions and their stability, application of the formalism to non-periodic structures is also treated. We have not expanded the material beyond what can be covered in 3 lectures, but the proofs are done more carefully and some examples and details have been added which might be useful in practice.

After a brief introduction to the concepts of both weak and strong focusing of relativistic particle beams, types of magnetic lenses are discussed, followed by a careful treatment of the multipole expansion of transverse magnetic fields. Linear transverse single-particle dynamics is treated both in terms of transfer matrices and betatron oscillations. Transfer matrices of the most common accelerator lattice modules are explicitly given, including a brief introduction to quadrupole doublet imaging. Dispersion is treated, but no linear coupling. The concept of beam emittance, including Liouville's Theorem, is discussed from different points of view. Also effects of linear field errors, stability criteria and chromaticity are dealt with. FODO cells are treated in various respects. Finally, strong and weak focusing are compared quantitatively.

1 INTRODUCTION

In any kind of accelerator there is exactly one curve – the design orbit – on which ideally all particles should move, see Fig. 1. If this design orbit is curved, which may be required for many reasons, *bending* forces are needed.

In reality, most particles of the beam will deviate slightly from the design orbit. In order to keep these deviations small on the whole way (which might be as long as 10^{11} km in a storage ring), *focusing* forces are required. Both bending and focusing forces can be accomplished with electromagnetic fields. The Lorentz force is

$$\mathbf{F} = e(\mathbf{E} + \mathbf{v} \times \mathbf{B})$$

For velocities $v \approx c$, a moderate magnetic field of 1 Tesla corresponds to a huge electric field of $3 \cdot 10^8$ V/m. Therefore only transverse magnetic fields are considered.

Now consider the total energy E of a particle:

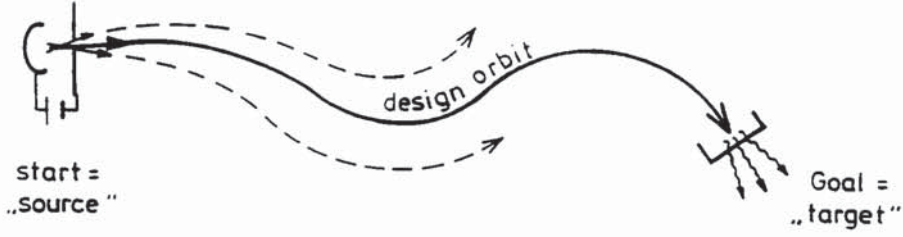


Figure 1: To guide particles on a curved design orbit, bending elements are required.

$$E = \frac{m_0 c^2}{\sqrt{1 - \frac{v^2}{c^2}}}$$

Relativistic mechanics describes its rate of change in the presence of an external force by

$$\frac{dE}{dt} = \mathbf{v} \cdot \mathbf{F}$$

Since \mathbf{v} is perpendicular to $\mathbf{v} \times \mathbf{B}$, the energy and the relativistic mass $m = m_0 / \sqrt{1 - v^2/c^2}$ are not changed in static magnetic fields. So the equation of motion is

$$\dot{\mathbf{v}} = \frac{e}{m} \mathbf{v} \times \mathbf{B} \quad (1.1)$$

The particles have to make a large number of revolutions in a circular accelerator or storage ring. Stability of motion is an important criterion and puts stringent requirements on the magnetic field in the vicinity of the equilibrium orbit. Depending on the magnitude of the focusing forces we can distinguish between weak and strong focusing.

The first machines were built with weak focusing and a guide field which does not depend on the azimuthal angle. If \mathbf{B} is independent of the azimuth angle Θ the equilibrium orbit is a circle of radius $\rho = mv/eB$ which we choose to be in the plane $z = 0$. The motion is stable if for small deviations of the particles from this orbit restoring forces arise which lead to oscillations around the orbit. These are called betatron oscillations.

Consider the motion in the horizontal plane $z = 0$ containing the equilibrium orbit (Fig. 2). Stability requires that the Lorentz force is smaller than the centrifugal force for $r < \rho$ and larger than it for $r > \rho$

$$evB_z(r) \begin{cases} < \frac{mv^2}{r} & \text{for } r < \rho \\ > \frac{mv^2}{r} & \text{for } r > \rho \end{cases} \quad (1.2)$$

For small deviations from the equilibrium orbit we have

$$r = \rho + x = \rho \left(1 + \frac{x}{\rho} \right) \quad (1.3)$$

$$\frac{mv^2}{r} \approx \frac{mv^2}{\rho} \left(1 - \frac{x}{\rho} \right)$$

$$evB_z(r) \approx ecB_0 \left(1 - n \frac{x}{\rho} \right) \quad (1.4)$$

with $B_0 = B_z(\rho)$. In Equation (1.4) we have introduced the *field index* n

$$n = -\frac{\rho}{B_0} \left(\frac{\partial B_z}{\partial r} \right)_{r=\rho} \quad (1.5)$$

Inserting (1.3) and (1.4) into (1.2) we obtain the condition $n < 1$.

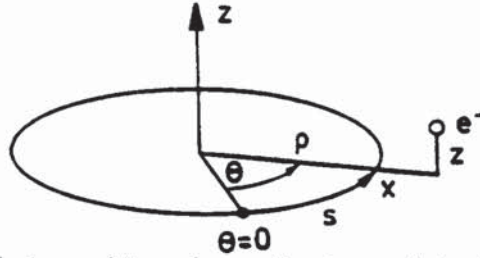


Figure 2: Circular design orbit and coordinates used to describe particle trajectories

It is worth noting that Eq. (1.2) is satisfied even with $n \equiv 0$, that is with a homogeneous field. This reflects the fact, that in a homogeneous field all plane orbits are circles, so that particles diverging from one point will meet again after 180° of revolution (see Fig. 3).

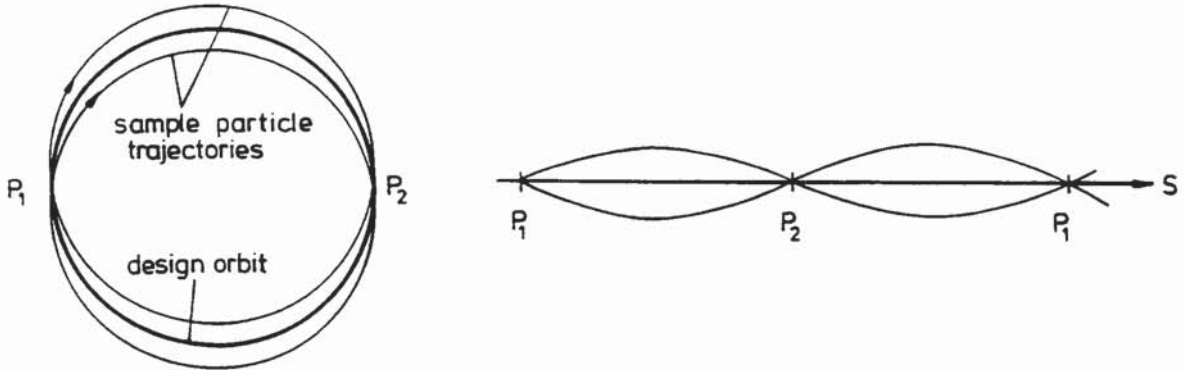


Figure 3: Geometrical focusing in a homogeneous magnetic field. All particles starting at P_1 with slightly different angles α move on circles with the same radii and meet again at P_2 . With respect to the design orbit, this looks like focusing, which can be seen more clearly from the right-hand part of the figure where the design orbit has been developed into a straight line. The maximum deviation from the design orbit (i.e. the amplitude of betatron oscillations) is easily estimated at $\alpha \cdot \rho$. Thus for a typical beam divergence of $\alpha = 1$ mrad it will be 1 mm at $\rho = 1$ m but as large as 1000 mm in a high energy ring with $\rho = 1000$ m.

This is called geometrical focusing, and it is an essential contribution to the weak focusing in the horizontal plane. It is, however, not sufficient:

Consider a particle in a homogeneous field with initial conditions such that it moves on a circle in the horizontal plane $z \equiv 0$. If it now gets an infinitely small kick into the vertical direction, it will spiral away to infinity and will be lost. To achieve stability in the vertical plane we need a restoring force

$$F_z = -C \cdot z \quad (C = \text{const.})$$

and therefore a horizontal field component

$$B_x = -C' \cdot z$$

Now from $\nabla \times \mathbf{B} = 0$: $\partial B_x / \partial z = \partial B_z / \partial x = \partial B_z / \partial r$. So B_z has to decrease with increasing r , see Fig. 4. $\partial B_z / \partial r < 0$ is equivalent to a positive field index, $n > 0$.

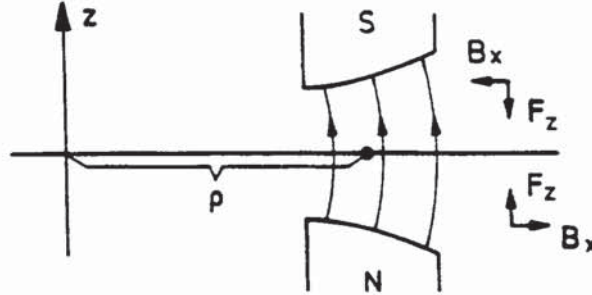


Figure 4: Shape of magnetic field around design orbit

Stability in both horizontal and vertical motion is achieved if the field index fulfils the inequalities

$$0 < n < 1 \quad (1.6)$$

The restoring forces are linear in the deviations x and z from the equilibrium orbit, if x and z are small. We therefore obtain harmonic oscillations. The differential equations will not be derived here, because they are special cases of the equations in section 3.

$$\begin{aligned} \ddot{x} + \omega_0^2(1 - n)x &= 0 \\ \ddot{z} + \omega_0^2 n \cdot z &= 0 \end{aligned} \quad (1.7)$$

with $\omega_0 = eB_0/m$. $f_0 = \omega_0/2\pi$ is the revolution frequency (cyclotron frequency) of the particles. Since $0 < n < 1$ we see that in a weakly-focusing machine the frequency of betatron oscillations is lower than the revolution frequency, i.e. there is less than one oscillation per revolution.

$$f_x = \sqrt{1 - n} f_0, \quad f_z = \sqrt{n} f_0 \quad (1.8)$$

The principle of weak focusing has one serious drawback: Since the betatron oscillation wavelength is larger than the circumference of the machine one gets large deviations from the orbit if the circumference is large. The magnet apertures must be very big. The apertures can be drastically reduced if one applies strong focusing ($|n|$ much larger than 1). This is impossible in a machine which has a guide and focusing field independent of the azimuthal angle, since in that case the condition $0 < n < 1$ has to hold, as we have just shown. It is, however, possible if we split up the machine into a series of magnetic sectors in which in alternating order the magnetic field increases strongly with increasing radius ($n \ll -1$) or decreases strongly with increasing radius ($n \gg +1$) (see Fig.5).

An alternating series of focusing and defocusing lenses leads to an overall focusing because the focusing lenses are, on the average, traversed at larger distance from the axis than the defocusing ones. This is shown in Fig. 6. In section 3 we shall see that focusing is indeed obtained in both planes.

The Brookhaven AGS and the CERN PS were the first large alternating-gradient synchrotrons. In the PS the field index is $n=288$ and there are 6.2 betatron oscillations per revolution. Note

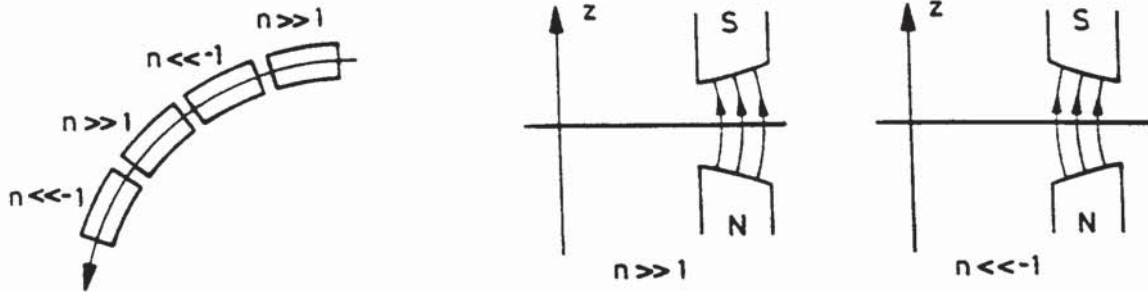


Figure 5: Alternating-gradient focusing

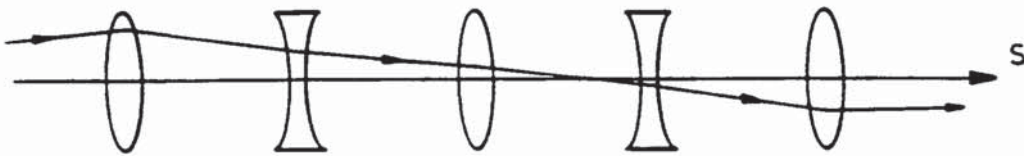


Figure 6: An alternating series of focusing and defocusing lenses leads to overall focusing if the distances between the lenses are not too large.

that Eq. (1.8) is not applicable to strong focusing.

2 ACCELERATOR MAGNETS

Many of the older alternating gradient synchrotrons like the CERN proton synchrotron PS or the DESY electron synchrotron have been built with “combined-function” magnets, i.e. magnets which combine a dipole field for deflection and a quadrupole field for focusing. The new large accelerators and storage rings are equipped with “separated-function” magnets: dipoles for deflection, quadrupoles for focusing. These allow higher particle energies because the iron yoke of a pure dipole magnet saturates at higher field levels than the yoke of a combined-function “synchrotron” magnet and moreover there is more flexibility in optimizing the optical properties of the machine.¹

Traditionally, soft iron of high permeability is used to concentrate the field into the small region where it is needed. This also reduces electric power consumption and easily allows to guarantee high field quality. In those cases where the required field strength is either very small ($B \ll 0.1$ T) or above the saturation level ($B > 2$ T), “air coil” magnets are used. Some remarks relevant

¹In circular electron accelerators, combined-function magnets have another big disadvantage as compared to separated-function magnets. The electrons suffer a permanent energy loss because of the emission of synchrotron radiation which is compensated by the energy gain in the accelerating cavities. In a separated-function electron machine both effects together lead to a damping of the horizontal and vertical betatron oscillations. In a pure combined-function machine, however, only the vertical betatron oscillation is damped whereas the horizontal oscillation will blow up (see the lectures by R. Walker, these proceedings).

for the construction of these magnets are found at the very end of this section.

a) Dipole magnet

A magnet with flat pole shoes generates a homogeneous field B_0 . (Fig. 7).

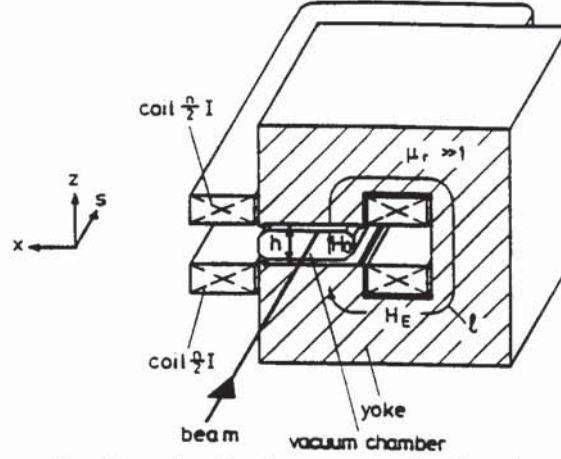


Figure 7: Schematic view of a dipole magnet, showing the path of integration to compute the field in the gap.

The field is computed from the formula

$$\oint \mathbf{H} \cdot d\mathbf{s} = hH_0 + lH_E = nI$$

$$H_E = \frac{1}{\mu_r} \cdot H_0$$

For $\mu_r \gg 1$ we obtain

$$B_0 = \frac{\mu_0 nI}{h} \quad h = \text{gap height} \quad (2.1)$$

Formula (2.1) is only approximate. In particular it neglects fringe fields and iron saturation. The radius of curvature for a particle of charge e and momentum p is given by

$$\frac{1}{\rho} [\text{m}^{-1}] = \frac{eB_0}{p} = 0.2998 \frac{B_0 [\text{T}]}{p [\text{GeV}/c]} \quad (2.2)$$

b) Solenoid lens

A relatively simple magnetic lens arises from the magnetic field of a rotationally symmetric coil, see Fig. 8.

Due to the Maxwell equation $\text{div } \mathbf{B} = 0$, the magnetic field, which is purely longitudinal in the inner part of the coil, must contain radial components in the outer part. While particles moving exactly on the axis do not experience any force, the others suffer an azimuthal acceleration due to the radial component while entering and leaving the lens. Because of the azimuthal motion there is a radial force in the longitudinal field. As required for imaging, this force is, indeed, proportional to the radial distance r if r does not change too much during the passage of the lens. To increase the field close to the axis and to concentrate it into a small area, the coil is usually surrounded by an iron yoke. The focal length f_{sol} is given by

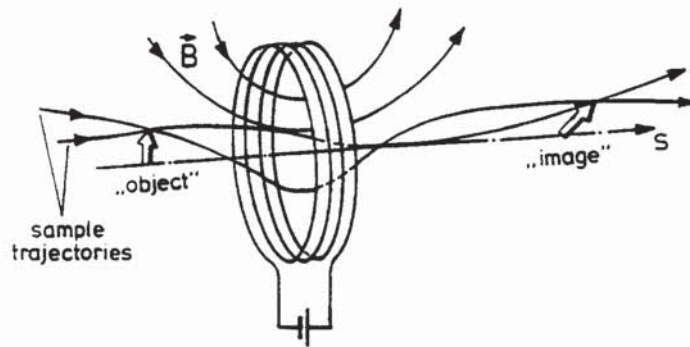


Figure 8: Particle trajectories and field lines in a “thin” lens formed by the solenoidal field of a coil (according to Bergmann/Schäfer: Optik)

$$\frac{1}{f_{sol}} = \int \left(\frac{eB_s}{2p} \right)^2 ds \quad (2.3)$$

In contrast to optical lenses, the image is rotated with respect to the object. As seen from Eq. (2.3), f_{sol} increases with the *square* of the momentum p . Therefore a solenoid lens is effective for small momenta only. At $p \gg 1 \text{ MeV}/c$, a quadrupole magnet is a much more effective lens, see the next section.

c) Quadrupole magnet

Quadrupole magnets have four iron pole shoes with hyperbolic contour (Fig. 9).

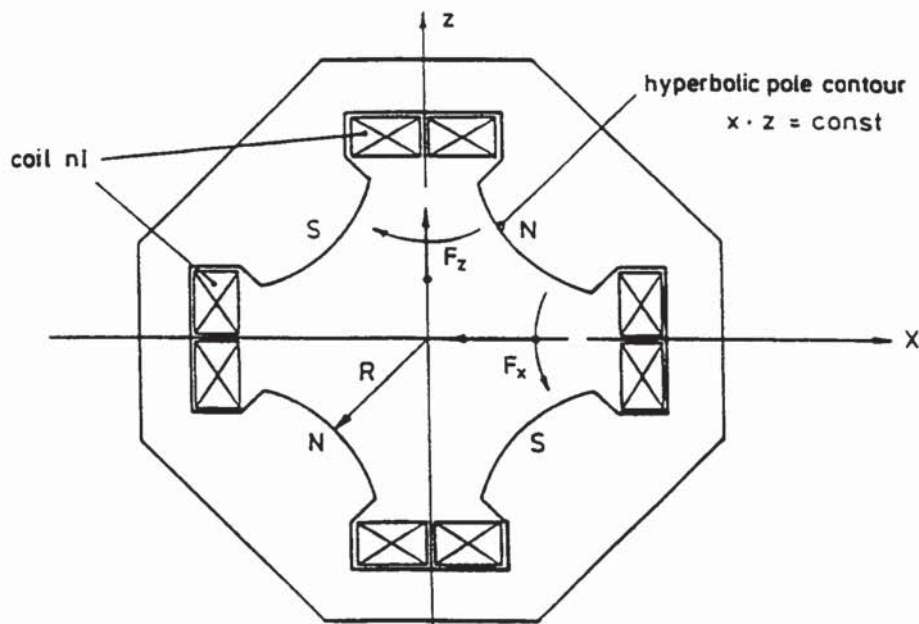


Figure 9: Cross-section of a quadrupole magnet. (Figs. 9,10,12 from K. Wille, Maria Laach lectures.)

With the polarity shown, the horizontal component of the Lorentz force on a positively charged

particle, moving into the plane of the drawing, is directed towards the axis, the vertical component is directed away from the axis. The magnet shown is thus horizontally focusing, vertically defocusing. The opposite holds when the current direction, the particle charge or its direction of motion is reversed.

The field is linear in the deviation from the axis:

$$B_z = -gx, \quad B_x = -gz \quad (2.4)$$

In the air space of the magnet which contains neither iron nor current conductors we have the Maxwell equation

$$\nabla \times \mathbf{B} = 0$$

Here the field can be written as the gradient of a potential

$$\mathbf{B} = -\nabla V \quad \text{with } V(x, z) = gxz \quad (2.5)$$

The equipotential lines are the hyperbolas $xz = \text{const.}$ The field lines are perpendicular to them. If the relative permeability of the iron is large, $\mu_r \gg 1$, iron pole shoes with hyperbolic contour generate a rather pure quadrupole field (2.4).

The gradient g and the current I in the coils can be related by the integral theorem

$$\oint \mathbf{H} \cdot d\mathbf{s} = nI.$$

The path of integration is shown in Fig. 10.

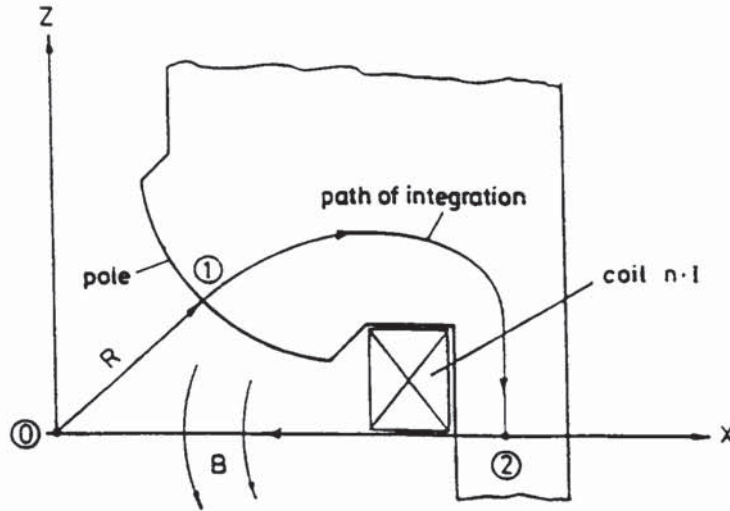


Figure 10: Path of integration used to compute the quadrupole gradient as a function of the current

$$nI = \oint \mathbf{H} \cdot d\mathbf{s} = \int_0^R H(r) dr + \int_1^2 \mathbf{H}_E \cdot d\mathbf{s} + \int_2^0 \mathbf{H} \cdot d\mathbf{s}$$

On the first path $H(r) = gr/\mu_0$. The second integral is very small for $\mu_r \gg 1$. The third integral vanishes identically since $\mathbf{H} \perp d\mathbf{s}$. So we get in good approximation

$$nI = \frac{1}{\mu_0} \int_0^R g r dr \quad r = \sqrt{x^2 + z^2}$$

$$g = \frac{2\mu_0 nI}{R^2} \quad (2.6)$$

In analogy to the bending strength $1/\rho$ of a dipole magnet (see Eq. (2.2)), it is convenient to relate the field gradient to its optical effect. To this end, the field gradient is normalized to the momentum of the particle, thus defining the quadrupole strength

$$k = \frac{eg}{p}$$

Numerically

$$k [\text{m}^{-2}] = 0.2998 \frac{g [\text{T/m}]}{p [\text{GeV}/c]} \quad (2.7)$$

If l denotes the length of the quadrupole, its focal length f is given by

$$\frac{1}{f} = k \cdot l \quad (2.8)$$

Generally, a lens with $f \gg l$ is called a “thin lens” —irrespective of the absolute value of l . An interesting property of the quadrupole is that the horizontal force component depends only on the horizontal position and not on the vertical position of the particle trajectory. Similarly, the vertical component of the Lorentz force depends only on the vertical position.

$$F_x = evB_x(x, z) = -evgx$$

$$F_z = -evB_z(x, z) = evgz \quad (2.9)$$

The important consequence is that in a so-called *linear machine*, containing only dipole and quadrupole fields, the horizontal and vertical betatron oscillations are completely *decoupled*. This is of great importance for an e^+e^- storage ring where the vertical betatron oscillation usually has a much smaller amplitude than the horizontal oscillation. This decoupling would be lost if quadrupole magnets were rotated by some angle around their longitudinal axis. With those rotated quadrupoles a flat beam would not remain flat.

Therefore: *Don't rotate quadrupoles unless you know what you are doing!*

d) ”Synchrotron” magnet

As mentioned earlier, this magnet, sketched in Fig. 11, combines a dipole and a quadrupole magnet.

It can be considered as part of a quadrupole which is traversed at a distance $d = B_0/g$ from the axis. The field can be derived from the potential

$$V(x, z) = -B_0 z + g \cdot xz \quad (2.10)$$

The bending strength $1/\rho = eB_0/p$ and the quadrupole strength $k = eg/p$ can be combined into the dimensionless “field index” n , see Eq. (1.5)

$$n = k \cdot \rho^2 \quad (2.11)$$

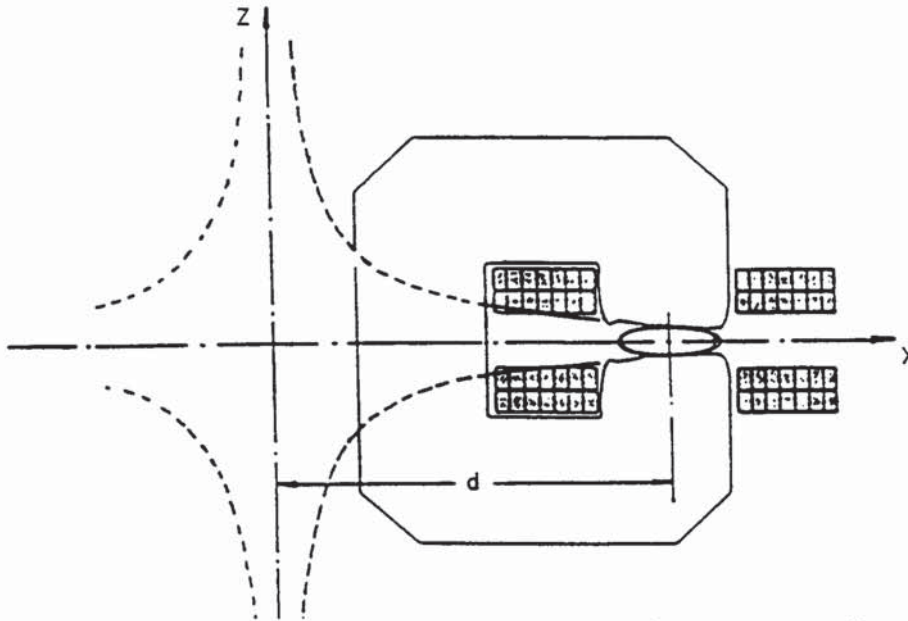


Figure 11: Cross-section of a horizontally focusing synchrotron magnet (from K. Steffen, Orsay lectures [4]).

e) Sextupole magnets

The focal length of a quadrupole depends on the particle momentum. Sextupole magnets (Fig. 12) are used to correct the resulting "chromatic" errors. A sextupole generates a nonlinear field

$$\begin{aligned} B_z &= \frac{1}{2}g'(x^2 - z^2) \\ B_x &= g'x \cdot z \end{aligned} \quad (2.12)$$

The field can be written as gradient of the potential

$$V(x, z) = -\frac{1}{2}g' \left(x^2 z - \frac{1}{3}z^3 \right)$$

A momentum-independent sextupole strength is defined by

$$m = \frac{eg'}{p_0}, \quad m [\text{m}^{-3}] = 0.2998 \frac{g' [\text{T/m}^2]}{p_0 [\text{GeV}/c]} \quad (2.13)$$

g' is related to the current in the coils by

$$g' = 6\mu_0 nI/R^3$$

f) General multipole expansion

In the literature you may find various kinds of multipole expansions for the guide field: expansion of the magnetic field \mathbf{B} , expansion of the magnetic vector potential \mathbf{A} , expansion of the scalar potential, and using cylindrical as well as cartesian coordinates. People use whatever is most

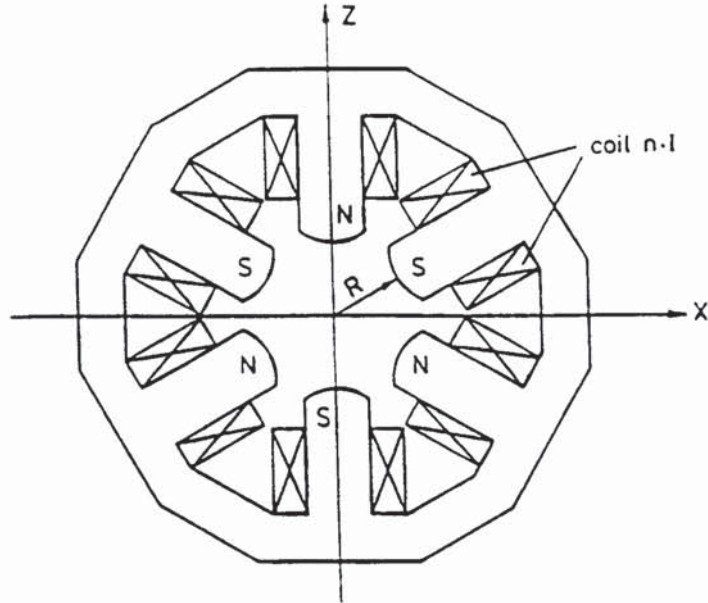


Figure 12: Sextupole magnet

appropriate for the specific problem, but the physics content is always the same as will be shown in the following.

In this paragraph we denote the vertical coordinate by y instead of z because we want to keep the conventional notation $z = x + iy$ for complex numbers.

The length of modern accelerator magnets is usually much larger than their bore radius. The end field contribution is then rather small and the magnetic field has to a good approximation only transverse components. (This is of course not the case for the large solenoids in the experimental areas which need a special treatment. The same applies for wigglers and undulators which are special magnets for generating synchrotron radiation.)

For two-dimensional fields one can apply the theory of analytic functions. From

$$\operatorname{div} \mathbf{B} = 0$$

it follows that a vector potential \mathbf{A} exists such that

$$\mathbf{B} = \operatorname{rot} \mathbf{A} \quad (2.14)$$

Because of the transversality of the field, the vector potential has only a component A_s in the longitudinal direction s . In vacuum, for example inside the beam pipe, we have furthermore

$$\operatorname{rot} \mathbf{B} = 0$$

This implies that \mathbf{B} can also be written as the gradient of a scalar potential V :

$$\mathbf{B} = -\operatorname{grad} V \quad (2.15)$$

Combining both equations (2.14, 2.15) we get:

$$B_x = -\frac{\partial V}{\partial x} = \frac{\partial A_s}{\partial y} \quad B_y = -\frac{\partial V}{\partial y} = -\frac{\partial A_s}{\partial x} \quad (2.16)$$

Now we define a complex potential function of $z = x + iy$ by

$$\bar{A}(z) = A_s(x, y) + iV(x, y) \quad (2.17)$$

The equations (2.16) are just the Cauchy-Riemann conditions for the real and imaginary part of an analytic function. So the complex potential is an analytic function and can be expanded in a power series

$$\tilde{A}(z) = \sum_{n=0}^{\infty} \kappa_n z^n \quad \kappa_n = \lambda_n + i\mu_n \quad (2.18)$$

with λ_n, μ_n being real constants.

From complex analysis we know that this series expansion converges for all z inside a circle $|z| < r_c$. The radius of convergence r_c is the closest distance between the origin of the expansion and the iron yoke or the coil where the Eqs. (2.16) break down and $\tilde{A}(z)$ is no more analytic, see Fig. 13.

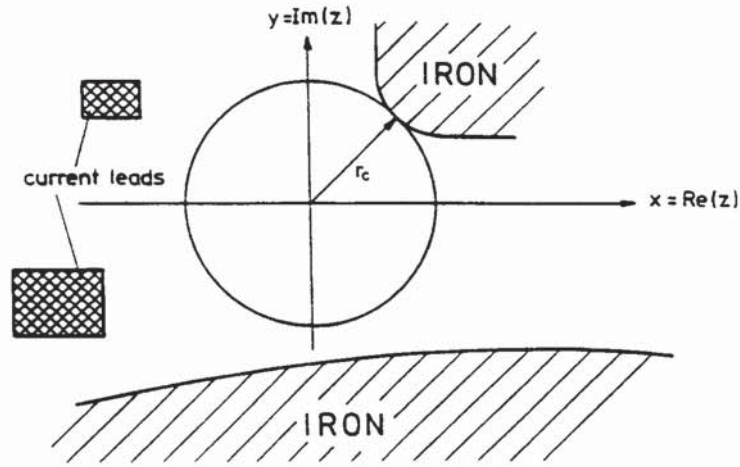


Figure 13: The multipole expansion with respect to $z = 0$ is only valid inside the circle r_c (radius of convergence).

Cylindrical coordinate representation

For superconducting magnets, it is practical to express the field in cylindrical coordinates (r, φ, s) , see Fig. 14:

$$x = r \cos \varphi \quad y = r \sin \varphi \quad z^n = r^n \cdot e^{in\varphi} = r^n (\cos n\varphi + i \sin n\varphi) \quad (2.19)$$

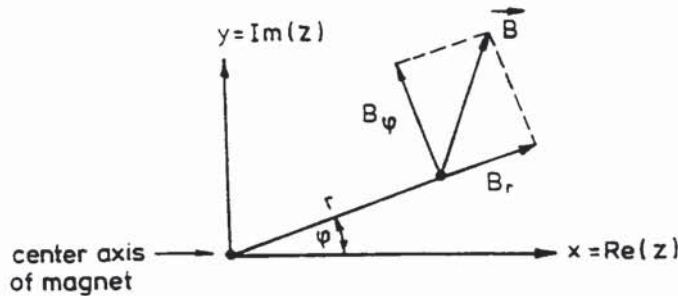


Figure 14: Cylindrical coordinate system used in the multipole expansion

The scalar potential is given by the imaginary part of Eq. (2.18)

$$V(r, \varphi) = \sum_{n=0}^{\infty} (\mu_n \cos n\varphi + \lambda_n \sin n\varphi) r^n \quad (2.20)$$

Similarly, we get from the real part of Eq. (2.18)

$$A_s(r, \varphi) = \sum_{n=0}^{\infty} (\lambda_n \cos n\varphi - \mu_n \sin n\varphi) r^n \quad (2.21)$$

Taking the gradient of $-V(r, \varphi)$, we get the multipole expansion of the azimuthal and radial field components, respectively

$$B_\varphi = -\frac{1}{r} \frac{\partial V}{\partial \varphi} = -\sum_{n=1}^{\infty} n(\lambda_n \cos n\varphi - \mu_n \sin n\varphi) r^{n-1}$$

$$B_r = -\frac{\partial V}{\partial r} = -\sum_{n=1}^{\infty} n(\mu_n \cos n\varphi + \lambda_n \sin n\varphi) r^{n-1}$$

Now it is convenient to define a ‘reference radius’ r_0 for the multipole expansion and to denote the magnitude of the main field component of the magnet in question by B_{main} . A useful choice for r_0 is the largest conceivable deviation of beam particles from the design orbit (25 mm in HERA, that is the inner radius of the beam pipe). Furthermore we introduce the ‘normal’ multipole coefficients b_n and the ‘skew’ coefficients a_n by

$$b_n = -\frac{n\lambda_n}{B_{main}} r_0^{n-1} \quad a_n = +\frac{n\mu_n}{B_{main}} r_0^{n-1} \quad (2.22)$$

Then the multipole expansions read (note that a_0, b_0 are set to zero as they don’t contribute to the magnetic field)

$$V(r, \varphi) = -B_{main} r_0 \sum_{n=1}^{\infty} \left(-\frac{a_n}{n} \cos n\varphi + \frac{b_n}{n} \sin n\varphi \right) \left(\frac{r}{r_0} \right)^n \quad (2.23)$$

$$A_s(r, \varphi) = -B_{main} r_0 \sum_{n=1}^{\infty} \left(\frac{b_n}{n} \cos n\varphi + \frac{a_n}{n} \sin n\varphi \right) \left(\frac{r}{r_0} \right)^n \quad (2.24)$$

$$B_\varphi(r, \varphi) = B_{main} \sum_{n=1}^{\infty} (b_n \cos n\varphi + a_n \sin n\varphi) \left(\frac{r}{r_0} \right)^{n-1} \quad (2.25)$$

$$B_r(r, \varphi) = B_{main} \sum_{n=1}^{\infty} (-a_n \cos n\varphi + b_n \sin n\varphi) \left(\frac{r}{r_0} \right)^{n-1} \quad (2.26)$$

Remember that these multipole expansions are only valid within a circle of radius r_c containing neither iron nor current! For an ideal $2n$ -pole magnet we have $b_n = 1$ and all other $a_n, b_n = 0$. We call

$n = 1$	Dipole
$n = 2$	Quadrupole
$n = 3$	Sextupole
$n = 4$	Octupole
$n = 5$	Decapole
$n = 6$	Dodecapole or 12 – pole

It is instructive to consider $B_\varphi + iB_r$:

$$B_\varphi + iB_r = B_{main} \sum_{n=1}^{\infty} \left(\frac{r}{r_0} \right)^{n-1} [b_n (\cos n\varphi + i \sin n\varphi) - ia_n (\cos n\varphi + i \sin n\varphi)]$$

$$B_\varphi + iB_r = B_{main} \sum_{n=1}^{\infty} \left(\frac{r}{r_0}\right)^{n-1} (b_n - ia_n) e^{in\varphi} \quad (2.27)$$

Thus

$$(|\mathbf{B}|)_n = \left(\sqrt{B_r^2 + B_\varphi^2}\right)_n = B_{main} \left(\frac{r}{r_0}\right)^{n-1} \sqrt{a_n^2 + b_n^2} \quad (2.28)$$

i.e. the magnitude of the $2n$ pole field component *does not* depend on the azimuth and scales with the $(n-1)$ th power of r . Equation (2.28) also illustrates a simple interpretation of the fractional multipole field coefficients a_n, b_n : They are just the relative field contribution of the n th multipole to the main field at the reference radius r_0 . This is the reason why the coefficients λ_n, μ_n have been normalized with Eqs. (2.22).

Conventional accelerator magnets with iron pole shoes are limited to dipole fields of about 2 T and quadrupole gradients of about 20 T/m. Significantly higher values (> 6 T, > 100 T/m) are possible with superconducting magnets. In these magnets the field distribution is entirely determined by the conductor arrangement and the coils have to be built with extreme accuracy to keep field distortions below the required level of 10^{-4} . Figure 15a shows schematically the layout of a superconducting dipole.

Ideally, the current as a function of the azimuthal angle φ should follow a $\cos\varphi$ -distribution to generate a pure dipole field and a $\cos 2\varphi$ ($\cos 3\varphi$) distribution for a quadrupole (sextupole) field (Figs. 15b,c,d). Since these ideal distributions are technically difficult to realize one approximates them by an arrangement of current shells. The cylindrical coordinate representation is particularly useful for magnet design from current shells. Figure 16 shows a cross section through the HERA dipole coil.

Another application of the cylindrical coordinate representation is the technique of measurement of the multipole components with a coil rotating in the field: The n th Fourier component of the induced voltage is proportional to $\sqrt{a_n^2 + b_n^2}$ while its phase is related to a_n/b_n .

In a good dipole or quadrupole magnet the unwanted multipole coefficients a_n, b_n are typically a few 10^{-4} or less.

Finally it is noted that within the cylindrical coordinate representation one easily understands which multipole components are forbidden if specific symmetry properties of the field are assumed. For instance, for a quadrupole with perfect constructional symmetry only *odd* harmonics of the 4-pole are allowed. Or, as another example, if mirror symmetry with respect to the $x-y$ plane is assumed, all skew components are forbidden since B_φ must behave purely *cos*-like. A similar reasoning shows that any normal $2n$ -pole magnet transforms into a skew $2n$ -pole magnet if rotated by $\pi/2n$.

Cartesian coordinates

In cartesian coordinates, Eq. (2.18) reads

$$A_s(x, y) + iV(x, y) = \sum_{n=0}^{\infty} \kappa_n z^n = \sum_{n=0}^{\infty} (\lambda_n + i\mu_n)(x + iy)^n \quad (2.29)$$

Separation of real and imaginary part and use of Eq. (2.22) yields

$$\begin{aligned} A_s(x, y) = \Re \sum_{n=0}^{\infty} \kappa_n z^n = & -B_{main} \left[b_1 x + a_1 y + \frac{b_2}{2r_0} (x^2 - y^2) + \frac{a_2}{r_0} xy + \frac{b_3}{3r_0^2} (x^3 - 3xy^2) + \right. \\ & \left. + \frac{a_3}{3r_0^2} (3x^2y - y^3) + \frac{b_4}{4r_0^3} (x^4 - 6x^2y^2 + y^4) + \frac{a_4}{r_0^3} (x^3y - xy^3) \pm \dots \right] \end{aligned} \quad (2.30)$$

$$V(x, y) = \Im \sum_{n=0}^{\infty} \kappa_n z^n = B_{main} \left[a_1 x - b_1 y + \frac{a_2}{2r_0} (x^2 - y^2) - \frac{b_2}{r_0} xy + \frac{a_3}{3r_0^2} (x^3 - 3xy^2) - \right.$$

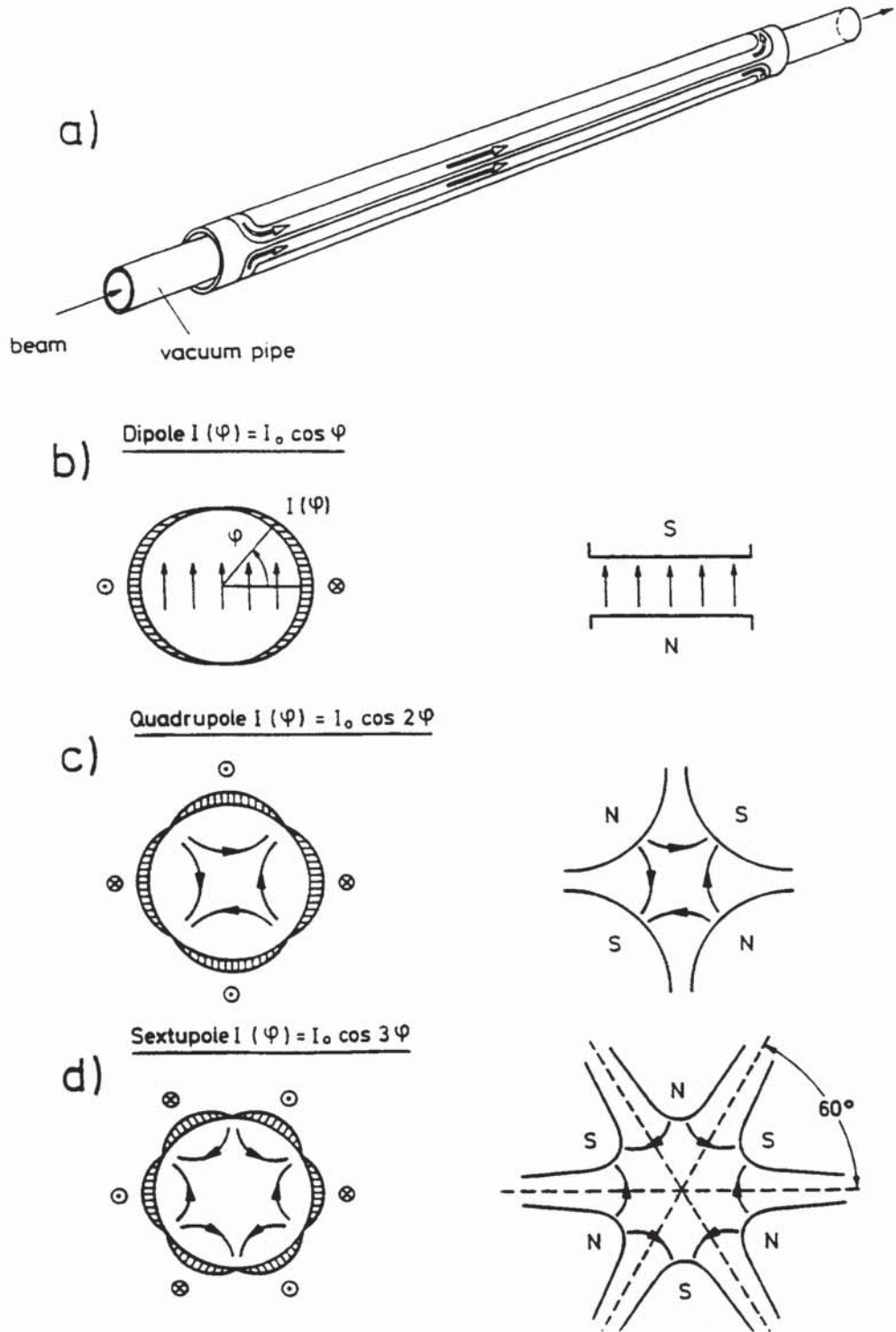


Figure 15: a) Schematic view of a superconducting dipole
b, c, d) current distributions for pure dipole, quadrupole and sextupole fields
and the corresponding yoke profiles of conventional magnets.

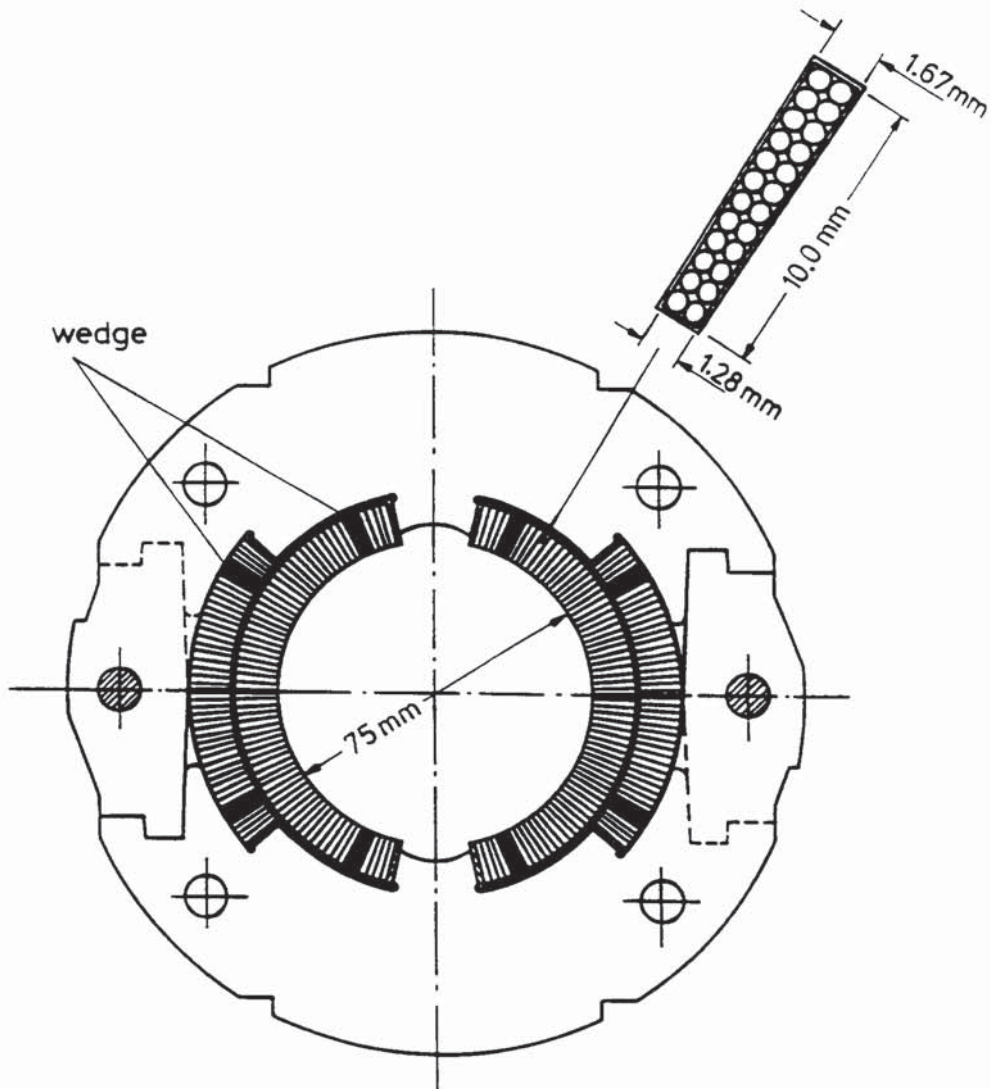


Figure 16: Cross section of the superconducting HERA dipole coil. The inner current shell has 64 windings, the outer shell 40. The limiting angles of the shells and the longitudinal wedges are chosen such that the computed higher multipole fields are less than 10^{-4} of the dipole field. The nominal field of 4.68 T is achieved with a current of 5025 A. The coil is confined by precise aluminum clamps which sustain the magnetic forces and define the exact geometry. The clamps are surrounded with a cylindrical iron yoke (not shown) contributing 22 % to the field. The cross section of the superconducting cable is shown in an enlarged view.

$$-\frac{b_3}{3r_0^2}(3x^2y - y^3) + \frac{a_4}{4r_0^3}(x^4 - 6x^2y^2 + y^4) - \frac{b_4}{r_0^3}(x^3y - xy^3) \pm \dots] \quad (2.31)$$

To get the cartesian components of the magnetic field we now have to take the gradient of $-V(x, y)$ in cartesian coordinates, see Eq. (2.16)

$$B_x(x, y) = -\frac{\partial V}{\partial x} = B_{main}[-a_1 + \frac{b_2}{r_0}y - \frac{a_2}{r_0}x - \frac{a_3}{r_0^2}(x^2 - y^2) + \frac{b_3}{r_0^2}2xy - \frac{a_4}{r_0^3}(x^3 - 3xy^2) + \frac{b_4}{r_0^3}(3x^2y - y^3) \pm \dots] \quad (2.32)$$

$$B_y(x, y) = -\frac{\partial V}{\partial y} = B_{main}[b_1 + \frac{a_2}{r_0}y + \frac{b_2}{r_0}x + \frac{a_3}{r_0^2}2xy + \frac{b_3}{r_0^2}(x^2 - y^2) + \frac{a_4}{r_0^3}(3x^2y - y^3) + \frac{b_4}{r_0^3}(x^3 - 3xy^2) \pm \dots] \quad (2.33)$$

Another useful combination of Eqs. (2.32) and (2.33) is

$$B_y + iB_x = -\frac{\partial}{\partial x}(A_s + iV) = -\sum_{n=1}^{\infty} n(\lambda_n + i\mu_n)(x + iy)^{n-1}$$

$$B_y + iB_x = B_{main} \sum_{n=1}^{\infty} (b_n - ia_n) \left(\frac{x}{r_0} + i\frac{y}{r_0}\right)^{n-1}$$

Here are two applications of the cartesian representation of multipoles:

- If the motion of particles is described in cartesian coordinates, the contribution of each individual multipole to the equation of motion is easily identified. As stated before, the coefficients b_n are called the “normal” multipole coefficients, a_n are the “skew” coefficients. In magnets containing normal coefficients only, a flat beam (i.e. no vertical extension) remains flat forever, since for $y \equiv 0$ there is $B_x \equiv 0$, i.e. no vertical force. Thus, there is no coupling of horizontal motion into the vertical.
- Equation (2.31) is useful in conventional lens design work with iron pole shoes. It describes the pole contours of dipole- ($n = 1$), quadrupole- ($n = 2$), sextupole- ($n = 3$), octupole- ($n = 4$), etc., magnets, because the pole contour is a line of constant magnetic potential. The pole contour of a normal quadrupole (b_2), for instance, is given by the hyperbola $x \cdot y = const$ (see Fig. 9 and Eq. (2.5)).

Finally, we show explicitly the field distribution of the most important multipole components:

Normal dipole ($n = 1$): $b_1 \cdot B_{main} = B_{vert}$ (horizontally bending)
$B_\varphi(r, \varphi) = B_{vert} \cdot \cos \varphi$ $B_r(r, \varphi) = B_{vert} \cdot \sin \varphi$
$B_x(x, y) = 0$ $B_y(x, y) = B_{vert}$
Skew dipole ($n = 1$): $a_1 \cdot B_{main} = B_{hor}$ (vertically bending)
$B_\varphi(r, \varphi) = B_{hor} \cdot \sin \varphi$ $B_r(r, \varphi) = -B_{hor} \cdot \cos \varphi$
$B_x(x, y) = -B_{hor}$ $B_y(x, y) = 0$
Normal quadrupole ($n = 2$): $b_2 \cdot B_{main} = -g \cdot r_0$ (where g is the gradient)
$B_\varphi(r, \varphi) = -gr \cos 2\varphi$ $B_r(r, \varphi) = -gr \sin 2\varphi$
$B_x(x, y) = -gy$ $B_y(x, y) = -gx$
Skew quadrupole ($n = 2$): $a_2 \cdot B_{main} = -g \cdot r_0$ (quadrupole rotated by 45°)
$B_\varphi(r, \varphi) = -gr \sin 2\varphi$ $B_r(r, \varphi) = gr \cos 2\varphi$
$B_x(x, y) = gx$ $B_y(x, y) = -gy$
Normal sextupole ($n = 3$): $b_3 \cdot B_{main} = \frac{1}{2}g' \cdot r_0^2$
$B_\varphi(r, \varphi) = \frac{1}{2}g'r^2 \cos 3\varphi$ $B_r(r, \varphi) = \frac{1}{2}g'r^2 \sin 3\varphi$
$B_x(x, y) = g'xy$ $B_y(x, y) = \frac{1}{2}g'(x^2 - y^2)$

3 PARTICLE MOTION IN A CIRCULAR ACCELERATOR

3.1 Trajectory equations

We consider first a machine with combined-function magnets and neglect the drift spaces between the magnets. The design orbit is then a circle. It is easy to generalize the results to machines with separated-function magnets.

The design orbit is assumed to be in the horizontal plane. We use cylindrical coordinates, r, Θ, z . The dipole field is assumed to point in the positive z direction. Then positively charged particles move in a clockwise direction, negatively charged particles counterclockwise (see Fig. 17).

Let us follow the motion of an electron. Together with the particle a system of three unit vectors $\mathbf{u}_r, \mathbf{u}_\Theta$ and \mathbf{u}_z is moved around. The radius vector of the particle is

$$\mathbf{R} = \mathbf{R}_0 + r\mathbf{u}_r + z\mathbf{u}_z \quad \mathbf{R}_0 = \text{const.}$$

Now for a small $d\Theta$

$$d\mathbf{u}_r = d\Theta\mathbf{u}_\Theta, \quad d\mathbf{u}_\Theta = -d\Theta\mathbf{u}_r, \quad d\mathbf{u}_z = 0$$

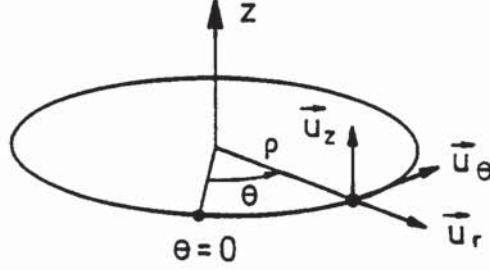


Figure 17: Coordinate system for particle motion in a circular accelerator

So

$$\begin{aligned}\dot{\mathbf{R}} &= \dot{r}\mathbf{u}_r + r\dot{\mathbf{u}}_r + \dot{z}\mathbf{u}_z \\ &= \dot{r}\mathbf{u}_r + r\dot{\Theta}\mathbf{u}_\Theta + \dot{z}\mathbf{u}_z\end{aligned}$$

The acceleration is

$$\ddot{\mathbf{R}} = (\ddot{r} - r\dot{\Theta}^2)\mathbf{u}_r + (2\dot{r}\dot{\Theta} + r\ddot{\Theta})\mathbf{u}_\Theta + \ddot{z}\mathbf{u}_z$$

Now

$$m\ddot{\mathbf{R}} = -e\mathbf{v} \times \mathbf{B} = -e \left[(r\dot{\Theta}B_z - zB_\Theta)\mathbf{u}_r + (\dot{z}B_r - \dot{r}B_z)\mathbf{u}_\Theta + (\dot{r}B_\Theta - r\dot{\Theta}B_r)\mathbf{u}_z \right] \quad (3.1)$$

In the following we assume $B_\Theta = 0$ and obtain

$$\begin{aligned}m(\ddot{r} - r\dot{\Theta}^2) &= -er\dot{\Theta}B_z(r, z, \Theta) \\ m\ddot{z} &= er\dot{\Theta}B_r(r, z, \Theta)\end{aligned} \quad (3.2)$$

In the special case of combined-function magnets the field components derived from the potential (2.10) are

$$B_z = B_0 - gx, \quad B_r = B_z = -gz \quad (3.3)$$

Inserting (3.3) into (3.2) and using $r = \rho + x$ with $\rho = \text{const}$, we get

$$\begin{aligned}m(\ddot{x} - r\dot{\Theta}^2) &= -er\dot{\Theta}(B_0 - gx) \\ m\ddot{z} &= -er\dot{\Theta}gz\end{aligned}$$

$v_\Theta = r\dot{\Theta}$ is the azimuthal component of the particle velocity. It is much larger than the transverse components v_r and v_z , so $v_\Theta = r\dot{\Theta} \approx v$. At this point it is convenient to replace the time variable t by the arc length s along the design orbit

$$s = vt, \quad \ddot{x} = v^2x'', \quad x'' = \frac{d^2x}{ds^2}$$

$$x'' = \frac{1}{r} - \frac{eB_0}{mv} + \frac{eg}{mv}x$$

$$z'' = -\frac{eg}{mv}z$$

Now $mv = p = p_0 \left(1 + \frac{\Delta p}{p_0}\right)$ where p_0 is the design momentum.

Further $\frac{1}{r} \approx \frac{1}{\rho} \left(1 - \frac{x}{\rho}\right)$ for $x \ll \rho$ and $p_0 = eB_0$, $\frac{1}{\rho} = \frac{eB_0}{p_0}$, $k = \frac{eg}{p_0}$

To first order in the small quantities x and $\frac{\Delta p}{p_0}$ we obtain

$$\boxed{\begin{aligned} x'' - \left(k - \frac{1}{\rho^2}\right)x &= \frac{1}{\rho} \frac{\Delta p}{p_0} \\ z'' + kz &= 0 \end{aligned}} \quad (3.4)$$

These are the basic equations for the particle trajectory $x(s), z(s)$ in linear approximation.

It is easy to see that the equations (3.4) are also valid for a separated-function machine, provided we define ρ as the local radius of curvature and g as the local gradient. In a dipole magnet the design orbit is part of a circle. The gradient is zero, so the equations hold with $k = 0$. In a quadrupole the central orbit is a straight line. The force on the electron is

$$m\ddot{x} = -evB_z = evgx$$

$$m\ddot{z} = evB_x = -evgz$$

$$\text{so } \begin{aligned} x'' - kx &= 0 \\ z'' + kz &= 0 \end{aligned} \quad k = \frac{eg}{p_0} \approx \frac{eg}{mv}$$

So Eqs. (3.4) are valid with $\frac{1}{\rho} = 0$.

The term $\frac{1}{\rho^2}x$ in (3.4) describes the “weak focusing” of a bending magnet. In the very large high-energy accelerators like the CERN SPS or HERA it can be neglected in comparison with the “strong focusing” term k given by the quadrupoles.

Example HERA proton ring: $k = 0.032\text{m}^{-2}$, $\frac{1}{\rho^2} = 2.9 \cdot 10^{-6}\text{m}^{-2}$.

We want to point out that even in the case of purely linear magnetic fields the equations of motion are intrinsically nonlinear due to the curved coordinate system. Especially for accelerators with small bending radius, nonlinear corrections to Eq. (3.4) have to be taken into account.

3.2 Solution of trajectory equations in terms of principal trajectories

In general, the bending strength $\frac{1}{\rho}$ and the focusing strength k are functions of the path length s along the reference orbit. The equation for the horizontal motion can be written as

$$x'' + K(s)x = \frac{1}{\rho} \cdot \frac{\Delta p}{p_0} \quad \left(K(s) = -k(s) + \frac{1}{\rho^2(s)} \right) \quad (3.5)$$

The general solution $x(s)$ is the sum of the complete solution x_h of the homogeneous equation and a particular solution x_i of the inhomogeneous equation

$$x(s) = x_h(s) + x_i(s)$$

with

$$\begin{aligned}x_h'' + K(s)x_h &= 0 \\x_i'' + K(s)x_i &= \frac{1}{\rho} \frac{\Delta p}{p_0}\end{aligned}$$

Since $\Delta p/p_0$ is assumed to be constant it is obvious that if x_i is a solution for a given $\Delta p/p_0$, $n \cdot x_i$ will be a solution for $n \cdot \Delta p/p_0$. Therefore it is useful to normalize x_i with respect to $\Delta p/p_0$:

$$D(s) = \frac{x_i}{\Delta p/p_0}$$

The general solution now reads

$$x(s) = C(s)x_0 + S(s)x'_0 + D(s)\frac{\Delta p}{p_0} \quad (3.6)$$

Here x_0 , x'_0 are the initial values of $x_h(s)$ and $x'_h(s)$ at $s = s_0$ and $C(s)$ and $S(s)$ are two independent solutions of the homogeneous equation

$$C'' + K(s)C = 0, \quad S'' + K(s)S = 0$$

For $C(s)$ and $S(s)$ to be linearly independent, the Wronski determinant W has to meet the condition

$$W = \begin{vmatrix} C & S \\ C' & S' \end{vmatrix} \neq 0$$

The derivative of the Wronskian vanishes identically

$$\frac{d}{ds}(CS' - SC') = \frac{d}{ds}W = CS'' - SC'' = -K(CS - SC) = 0$$

So the value of W is determined everywhere by the initial conditions at $s = s_0$. We choose

$$C_0 = 1, C'_0 = 0; S_0 = 0, S'_0 = 1 \quad (3.7)$$

The solutions satisfying these initial conditions are called the ‘‘Cosinelike’’ and the ‘‘Sinelike’’ trajectories and they result in $W = 1$.

$D(s)$ is the ‘‘Dispersion’’ trajectory, defined as a particular solution of the following inhomogeneous equation

$$D''(s) + K(s)D(s) = \frac{1}{\rho(s)} \quad (3.8)$$

It describes the momentum-dependent part of the motion. Here we require the initial conditions

$$D_0 = D'_0 = 0$$

because we assume (quite arbitrarily) that particles of different energy are not separated in space at the beginning.

Remark: The closed dispersion trajectory defined in chapter 5 satisfies different, namely periodic, boundary conditions.

$x(s)$ and $x'(s)$ are related to their initial values by a linear transformation

$$\begin{pmatrix} x \\ x' \end{pmatrix}_s = \begin{pmatrix} C & S \\ C' & S' \end{pmatrix} \begin{pmatrix} x \\ x' \end{pmatrix}_{s_0} + \frac{\Delta p}{p_0} \begin{pmatrix} D \\ D' \end{pmatrix} \quad (3.9)$$

Equation (3.9) can also be written as

$$\begin{pmatrix} x \\ x' \\ \frac{\Delta p}{p_0} \end{pmatrix}_s = \begin{pmatrix} C & S & D \\ C' & S' & D' \\ 0 & 0 & 1 \end{pmatrix} \begin{pmatrix} x \\ x' \\ \frac{\Delta p}{p_0} \end{pmatrix}_{s_0} \quad (3.10)$$

The dispersion trajectory can be calculated from the cosinlike and the sinlike trajectories:

$$D(s) = S(s) \int_{s_0}^s \frac{1}{\rho(t)} C(t) dt - C(s) \int_{s_0}^s \frac{1}{\rho(t)} S(t) dt \quad (3.11)$$

To prove this relation we show that $D(s)$ as given by (3.11) fulfils the equation (3.8) with the initial conditions $D_0 = D'_0 = 0$.

$$\begin{aligned} D' &= S' \int \frac{1}{\rho} C dt - C' \int \frac{1}{\rho} S dt \\ D'' &= S'' \int \frac{C}{\rho} dt - C'' \int \frac{S}{\rho} dt + \frac{1}{\rho} \underbrace{(CS' - SC')}_1 \\ D''(s) &= -K(s)D(s) + \frac{1}{\rho(s)} \end{aligned}$$

The vertical motion is of course described by an equation like (3.9) but with the last term missing.

3.3 Transformation matrices of accelerator magnets

The matrix notation of the solution of the equations of motion is particularly useful if $K(s)$ is piecewise constant, because with $K = \text{const}$ the matrix elements can be expressed analytically. The solution for the complete "lattice" of optical elements is then just the product of the individual matrices in the desired sequence, see Fig. 18. The transfer matrices of the most important magnets are discussed in the following. They may be used as building bricks to assemble the complete magnet lattice.

a) Combined-function magnet

Although not much used anymore, this magnet is treated first since dipole and quadrupole magnets can be considered as special cases of a synchrotron magnet.

We assume that the field is independent of s inside the magnet and drops abruptly to zero at the ends (hard-edge model). The principal trajectories $C(s)$, $S(s)$ solve the equation

$$y'' + Ky = 0 \quad \begin{cases} K = k \text{ for } y = z \\ K = -k + \frac{1}{\rho^2} \text{ for } y = x \end{cases}$$

With $\varphi = s\sqrt{|K|}$ the solutions are inside the magnet

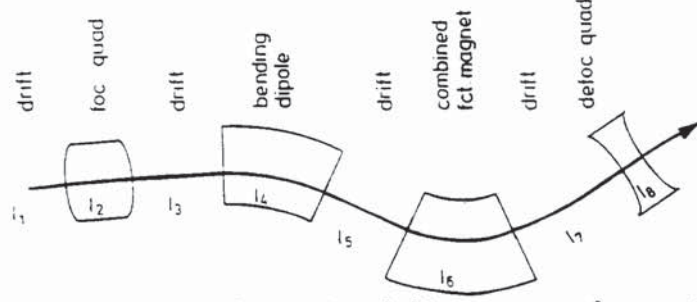


Figure 18: The complete transfer matrix of this sequence of magnetic elements is the matrix product $M_{tot} = M_8 \cdot M_7 \cdot M_6 \cdot M_5 \cdot M_4 \cdot M_3 \cdot M_2 \cdot M_1$. Each of the matrices $M_1 \dots M_8$ describes a section with $K(s) = const.$

$$\begin{pmatrix} C & S \\ C' & S' \end{pmatrix} = \begin{pmatrix} \cos \varphi & \frac{1}{\sqrt{|K|}} \sin \varphi \\ -\sqrt{|K|} \sin \varphi & \cos \varphi \end{pmatrix} \quad \begin{array}{l} \text{for } K > 0 \\ \text{(focusing)} \end{array} \quad (3.12a)$$

$$\begin{pmatrix} C & S \\ C' & S' \end{pmatrix} = \begin{pmatrix} \cosh \varphi & \frac{1}{\sqrt{|K|}} \sinh \varphi \\ \sqrt{|K|} \sinh \varphi & \cosh \varphi \end{pmatrix} \quad \begin{array}{l} \text{for } K < 0 \\ \text{(defocusing)} \end{array} \quad (3.12b)$$

$$\begin{pmatrix} C & S \\ C' & S' \end{pmatrix} = \begin{pmatrix} 1 & s \\ 0 & 1 \end{pmatrix} \quad \begin{array}{l} \text{for } K = 0 \\ \text{(drift space)} \end{array} \quad (3.12c)$$

The determinant is indeed unity: $CS' - SC' = 1$.
The dispersion is for $K > 0$

$$\begin{aligned} D(s) &= S \int_0^s \frac{C}{\rho} dt - C \int_0^s \frac{S}{\rho} dt \\ &= \frac{1}{\rho K} \sin^2 \varphi + \frac{1}{\rho K} \cos \varphi (\cos \varphi - 1) \\ D(s) &= \frac{1}{\rho K} (1 - \cos \varphi) \end{aligned}$$

For $K < 0$: $D(s) = -\frac{1}{\rho|K|} (1 - \cosh \varphi)$

$$\begin{pmatrix} D \\ D' \end{pmatrix} = \begin{pmatrix} \frac{1}{\rho K} \cdot (1 - \cos \varphi) \\ \frac{1}{\rho \sqrt{K}} \cdot \sin \varphi \end{pmatrix} \quad \text{for } K > 0 \quad (3.13a)$$

$$\begin{pmatrix} D \\ D' \end{pmatrix} = \begin{pmatrix} -\frac{1}{\rho|K|} \cdot (1 - \cosh \varphi) \\ \frac{1}{\rho \sqrt{|K|}} \cdot \sinh \varphi \end{pmatrix} \quad \text{for } K < 0 \quad (3.13b)$$

$$\begin{pmatrix} D \\ D' \end{pmatrix} = \begin{pmatrix} 0 \\ 0 \end{pmatrix} \quad \text{for } K = 0 \quad (3.13c)$$

To get the transformation matrix of the complete magnet one has to substitute the variable s by the length ℓ of the magnet.

b) Drift space

$$\frac{1}{\rho} = 0, k = 0$$

$$M_x = M_z = \begin{pmatrix} 1 & \ell & 0 \\ 0 & 1 & 0 \\ 0 & 0 & 1 \end{pmatrix} \quad (3.14)$$

c) Quadrupole Magnet

The dispersion (3.13) vanishes since $\frac{1}{\rho} = 0$. With $\varphi = \ell\sqrt{|k|}$ the transformation matrices are for $k > 0$

$$M_x = \begin{pmatrix} \cosh \varphi & \frac{1}{\sqrt{|k|}} \sinh \varphi & 0 \\ \sqrt{|k|} \sinh \varphi & \cosh \varphi & 0 \\ 0 & 0 & 1 \end{pmatrix} \quad (3.15)$$

$$M_z = \begin{pmatrix} \cos \varphi & \frac{1}{\sqrt{|k|}} \sin \varphi & 0 \\ -\sqrt{|k|} \sin \varphi & \cos \varphi & 0 \\ 0 & 0 & 1 \end{pmatrix}$$

These matrices describe horizontal defocusing, vertical focusing.

For $k < 0$, the matrices M_x and M_z are interchanged and we get horizontal focusing, vertical defocusing.

d) Thin-lens approximation

In many practical cases, the focal length f of the quadrupole magnet will be much larger than the length of the lens:

$$f = \frac{1}{k\ell} \gg \ell$$

Then the transfer matrices can be approximated by

$$M_x = \begin{pmatrix} 1 & 0 & 0 \\ \frac{1}{f} & 1 & 0 \\ 0 & 0 & 1 \end{pmatrix} \quad (3.16)$$

$$M_z = \begin{pmatrix} 1 & 0 & 0 \\ -\frac{1}{f} & 1 & 0 \\ 0 & 0 & 1 \end{pmatrix} \quad (3.17)$$

Note that these matrices describe a lens of zero length, i.e. they are derived from Eqs. (3.14) using $\ell \rightarrow 0$ while keeping $k \cdot \ell = \text{const}$. The true length l of the lens has to be recovered by two

drift spaces $\ell/2$ on either side, e.g.

$$M_x = \begin{pmatrix} 1 & \frac{\ell}{2} & 0 \\ 0 & 1 & 0 \\ 0 & 0 & 1 \end{pmatrix} \begin{pmatrix} 1 & 0 & 0 \\ -\frac{1}{f} & 1 & 0 \\ 0 & 0 & 1 \end{pmatrix} \begin{pmatrix} 1 & \frac{\ell}{2} & 0 \\ 0 & 1 & 0 \\ 0 & 0 & 1 \end{pmatrix} = \begin{pmatrix} 1 - \frac{\ell}{2f} & \ell - \frac{\ell^2}{4f} & 0 \\ -\frac{1}{f} & 1 - \frac{\ell}{2f} & 0 \\ 0 & 0 & 1 \end{pmatrix} \quad (3.18)$$

One might ask why the approximation has not been made by expanding $\sin \varphi$, $\cos \varphi$, etc. in Taylor series and neglecting higher powers of φ . However terminating the Taylor series at some power results in a transfer matrix whose determinant is not unity. For instance, in third order we obtain

$$M_x = \begin{pmatrix} 1 - \frac{\ell}{2f} & \ell - \frac{\ell^2}{6f} & 0 \\ -\frac{1}{f} & 1 - \frac{\ell}{2f} & 0 \\ 0 & 0 & 1 \end{pmatrix}$$

which **does not** fulfil $\det M = 1$. It will be shown later that this would violate Liouville's Theorem of phase-space conservation.

For accelerators in the TeV range, where $1/\rho^2 \ll |k| \ll 1/\ell^2$, the thin-lens approximation is excellent for the matrix description of the whole accelerator.

e) Dipole sector magnet

The matrices (3.12), (3.13) with $k = 0$ describe a "hard edge" dipole, i.e. the magnet ends are perpendicular to the circular trajectory (Fig. 19).

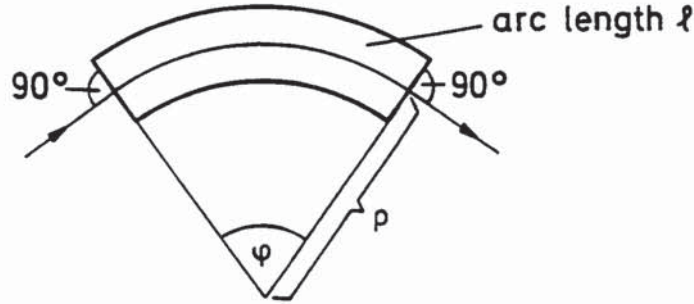


Figure 19: Dipole sector magnet

The transformation matrices are with $\varphi = \frac{\ell}{\rho}$

$$M_x = \begin{pmatrix} \cos \varphi & \rho \sin \varphi & \rho(1 - \cos \varphi) \\ -\frac{1}{\rho} \sin \varphi & \cos \varphi & \sin \varphi \\ 0 & 0 & 1 \end{pmatrix} \quad M_x = \begin{pmatrix} 1 & \ell & 0 \\ 0 & 1 & 0 \\ 0 & 0 & 1 \end{pmatrix} \quad (3.19)$$

f) Rectangular dipole magnet

In practice, dipole magnets are often built straight with the magnet end plates not perpendicular to the central trajectory. A rectangular magnet can be derived from a sector magnet

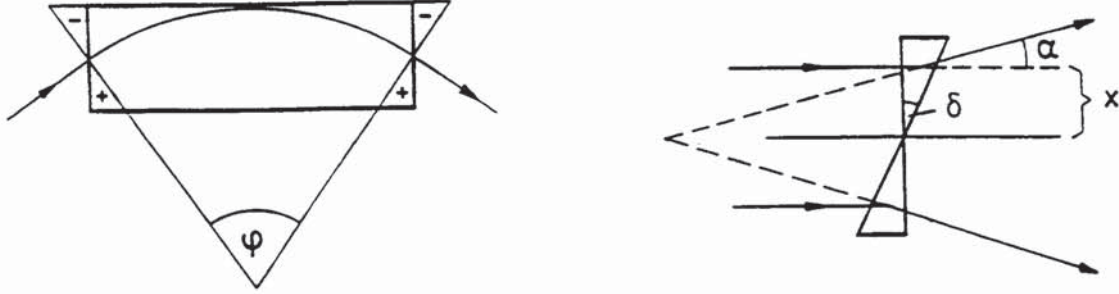


Figure 20: Rectangular dipole magnet and horizontally defocusing magnetic wedge

by superimposing at the entrance and exit a “magnetic wedge” of angle $\delta = \varphi/2$, as shown in Fig. 20.

The deflection angle in the magnetic wedge is

$$\alpha = \frac{\Delta \ell}{\rho} = \frac{x \tan \delta}{\rho} = \frac{x}{f}$$

It acts as a thin defocusing lens with $1/f = (\tan \delta)/\rho$ in the horizontal plane, as a focusing length with the same strength in the vertical plane. The horizontal transformation matrix for a rectangular magnet is

$$M_x = \begin{pmatrix} 1 & 0 & 0 \\ \frac{1}{\rho} \tan \delta & 1 & 0 \\ 0 & 0 & 1 \end{pmatrix} \begin{pmatrix} \cos \varphi & \rho \sin \varphi & \rho(1 - \cos \varphi) \\ -\frac{1}{\rho} \sin \varphi & \cos \varphi & \sin \varphi \\ 0 & 0 & 1 \end{pmatrix} \begin{pmatrix} 1 & 0 & 0 \\ \frac{1}{\rho} \tan \delta & 1 & 0 \\ 0 & 0 & 1 \end{pmatrix}$$

For $\varphi \ll 1$, $\delta = \varphi/2$:

$$M_x = \begin{pmatrix} 1 & \rho \sin \varphi & \rho(1 - \cos \varphi) \\ 0 & 1 & 2 \tan \varphi/2 \\ 0 & 0 & 1 \end{pmatrix} \quad M_z = \begin{pmatrix} \cos \varphi & \rho \sin \varphi & 0 \\ -\frac{1}{\rho} \sin \varphi & \cos \varphi & 0 \\ 0 & 0 & 1 \end{pmatrix} \quad (3.20)$$

Note that M_x is exact for $\delta = \varphi/2$ while $\varphi \ll 1$ has been used for M_z only. We conclude that in a rectangular magnet the weak horizontal focusing of a sector magnet is exactly compensated by the defocusing at the entrance and exit face. The magnet acquires, however, a weak vertical focusing of the same strength.

g) Quadrupole doublet

The transformation matrix of a system of dipoles, quadrupoles and drift spaces is obtained by multiplying the matrices of each element in the correct order. An important example is a quadrupole doublet consisting of a focusing quadrupole, a drift space and a defocusing quadrupole. Figure 21 shows two trajectories (1,2) suggesting a tendency of both horizontal and vertical focusing in this kind of arrangement.

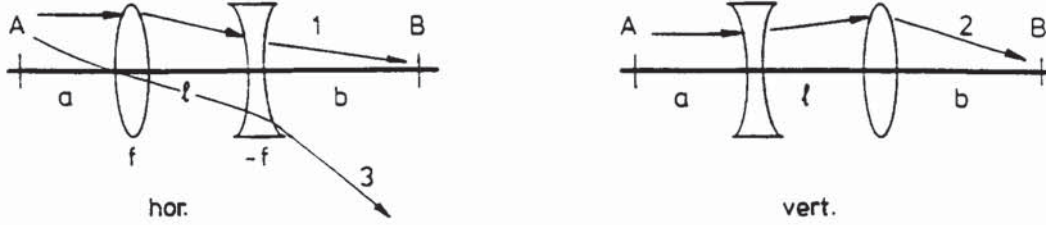


Figure 21: A quadrupole doublet consisting of a horizontally and a vertically focusing quadrupole magnet. Trajectories 1 and 2 suggest that there is a tendency of simultaneous focusing in both the horizontal and vertical directions.

The focusing action arises because trajectories entering parallel to the axis have a larger amplitude in the focusing than in the defocusing lens. Quadrupole doublets are indeed the simplest means of high energy beam focusing and imaging. We shall now derive the conditions for *simultaneous imaging in both* horizontal and vertical planes, treating the quadrupoles in the thin-lens approximation and assuming $f_{foc} = -f_{defoc} = f$ for simplicity. The horizontal transfer matrix of the doublet is (for meaning of symbols see Fig. 21)

$$M_{doub,x} = \begin{pmatrix} 1 & 0 & 0 \\ \frac{1}{f} & 1 & 0 \\ 0 & 0 & 1 \end{pmatrix} \begin{pmatrix} 1 & \ell & 0 \\ 0 & 1 & 0 \\ 0 & 0 & 1 \end{pmatrix} \begin{pmatrix} 1 & 0 & 0 \\ -\frac{1}{f} & 1 & 0 \\ 0 & 0 & 1 \end{pmatrix} = \begin{pmatrix} 1 - \frac{\ell}{f} & \ell & 0 \\ -\frac{\ell}{f^2} & 1 + \frac{\ell}{f} & 0 \\ 0 & 0 & 1 \end{pmatrix} \quad (3.21)$$

The vertical transfer matrix is obtained if f is replaced by $-f$:

$$M_{doub,z} = \begin{pmatrix} 1 + \frac{\ell}{f} & \ell & 0 \\ -\frac{\ell}{f^2} & 1 - \frac{\ell}{f} & 0 \\ 0 & 0 & 1 \end{pmatrix} \quad (3.22)$$

The matrix element $M_{21} = C' = -\ell/f^2$ is called the overall refractive power of the system and it is seen to be focusing in both planes. Somewhat sloppily one could say that a beam coming from infinity (i.e. all particles perfectly parallel to the s -axis, $x'_0 = 0$) will be focused in both planes, as indicated by trajectories 1 and 2 in Fig. 21. The effective focal length f_{doub} for these particles is

$$f_{doub} = \frac{f^2}{\ell} \quad (3.23)$$

Trajectory 3 in Fig. 21, however, illustrates that there are trajectories as well which are not at all bent towards the beam axis. For practical applications one might therefore ask: What happens to particles emerging from a point A at a finite distance a from the first lens? Optical imaging requires that there is a point B at a distance b behind the second lens where all particles emerging from A will converge. The horizontal transfer matrix from A to B is

$$M_x = \begin{pmatrix} 1 & b & 0 \\ 0 & 1 & 0 \\ 0 & 0 & 1 \end{pmatrix} M_{\text{doublet},x} \begin{pmatrix} 1 & a & 0 \\ 0 & 1 & 0 \\ 0 & 0 & 1 \end{pmatrix} = \begin{pmatrix} 1 - \frac{\ell}{f} - \frac{\ell b}{f^2} & a + b + \ell + \frac{\ell b}{f} - \frac{\ell a}{f} - \frac{\ell ab}{f^2} & 0 \\ -\frac{\ell}{f^2} & 1 + \frac{\ell}{f} - \frac{\ell a}{f^2} & 0 \\ 0 & 0 & 1 \end{pmatrix} \quad (3.24)$$

Again, M_z is obtained if f is replaced by $-f$:

$$M_z = \begin{pmatrix} 1 + \frac{\ell}{f} - \frac{\ell b}{f^2} & a + b + \ell - \frac{\ell b}{f} + \frac{\ell a}{f} - \frac{\ell ab}{f^2} & 0 \\ -\frac{\ell}{f^2} & 1 - \frac{\ell}{f} - \frac{\ell a}{f^2} & 0 \\ 0 & 0 & 1 \end{pmatrix} \quad (3.25)$$

Imaging from A to B requires $M_{12} = S \equiv 0$. Because of $\det M = 1$, the matrix can then be written in the form

$$M = \begin{pmatrix} m & 0 & 0 \\ C' & \frac{1}{m} & 0 \\ 0 & 0 & 1 \end{pmatrix} \quad (3.26)$$

m is called magnification of object A to image B . Obviously

$$x_B = m \cdot x_A \quad (\text{irrespective of } x'_A \text{ !}) \quad (3.27)$$

Remark: If also $M_{21} = C' = 0$ (i.e. zero overall refractive power), the system is called a telescopic system.

The condition $S \equiv 0$ is satisfied if

$$\frac{b}{f} = \frac{\frac{a}{f} + \frac{\ell}{f} - \frac{\ell a}{f^2}}{\frac{\ell a}{f^2} - \frac{\ell}{f} - 1} \quad \text{for } M_x \quad (3.28)$$

and

$$\frac{a}{f} = \frac{\frac{b}{f} + \frac{\ell}{f} - \frac{\ell b}{f^2}}{\frac{\ell b}{f^2} - \frac{\ell}{f} - 1} \quad \text{for } M_z \quad (3.29)$$

There are two ways to interpret Eqs. (3.27-3.29):

- If the parameter set f, ℓ, a, b is a solution in the horizontal plane, then the set f, ℓ, b, a is a solution in the vertical plane, i.e. the rôles of a and b are interchanged. This means that in general horizontal and vertical images are in different planes. This is called “astigmatic” focusing.

Example: Consider $\ell/f = 1$ and $a/f = 3$. Then $b/f = 1$ and $m_x = -1$ for imaging in the horizontal plane while $b/f = 7/3$ and $m_z = -1/3$ for imaging in the vertical plane. The vertical solution “conjugate” to the horizontal one would be $\ell/f = 1$, $a/f = 1$, $b/f = 3$, and $m_z = -1$. The latter one means, of course, that not only the horizontal and vertical images are in different distances from the doublet but also the respective objects.

- To get the horizontal and vertical images into the *same* plane (“stigmatic” focusing), $a = b$ is required. Then

$$m_x = \frac{f + a}{f - a} = \frac{1}{m_z} \quad \text{stigmatic focusing} \quad (3.30)$$

Equal horizontal and vertical magnifications $m_x = m_z$ are obviously impossible with stigmatic focusing, using quadrupole doublets. Note that, while $f_{foc} = -f_{defoc}$ has been assumed for Eqs. (3.21-3.30), this latter statement applies for all kinds of quadrupole doublets.

Example: $\ell/f = 4/3$, $a/f = b/f = 2$ yields stigmatic focusing with $m_x = -3$ and $m_z = -1/3$. Figure 22 illustrates particle trajectories in a stigmatic focusing quadrupole doublet.

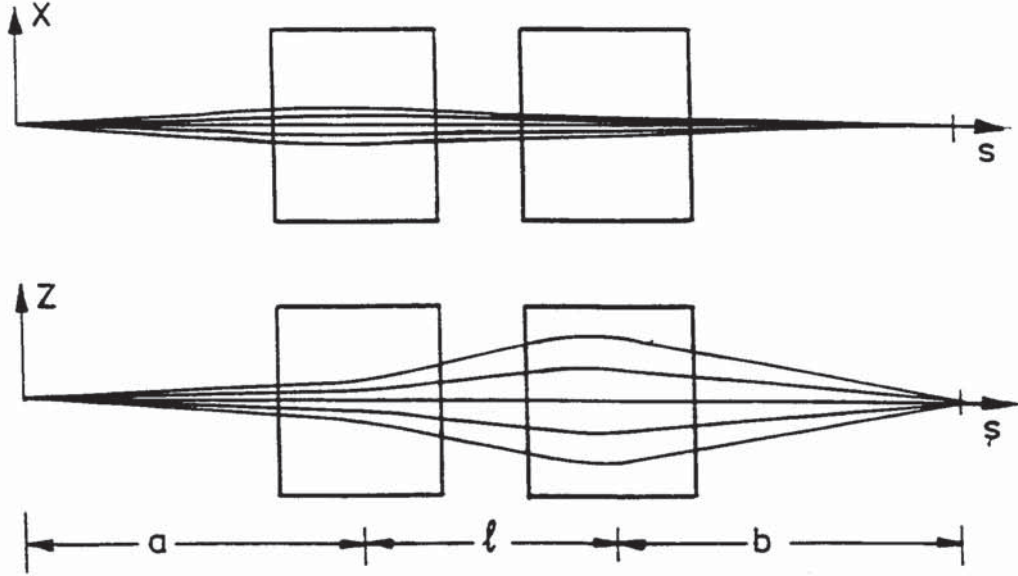


Figure 22: A stigmatic focusing quadrupole doublet showing particle trajectories that all start at the center of the object ($x_A = z_A = 0$).

In circular accelerators and for beam transport along a transfer channel we are, in general, not interested in imaging at all. Instead, we require small (or at least finite) beam envelopes for any kind of particle source, i.e. for any location of the object plane. It will be shown in section 4.7 that, to achieve focusing in an alternating series of F and D quadrupoles, the separation between two quadrupoles must not be larger than twice the focal length

$$\ell < 2|f|$$

h) Accelerating section

Acceleration in the longitudinal direction is beyond the scope of this article. However, there is also an effect on the transverse motion, which is now briefly addressed.

Consider a section of length ℓ with constant electric field E_s in the longitudinal direction. The total momentum p of an ultrarelativistic particle ($v \approx c = \text{const}$) then changes according to

$$\frac{dp}{ds} = \frac{e}{c} E_s = \text{const} \Rightarrow p(s) = p_0 + \frac{e}{c} E_s \cdot s$$

$p_0 = p(s = 0)$ is the momentum at the entrance of the section. The transverse motion of an ultrarelativistic particle is described by ($y = x$ or z)

$$\frac{d}{ds} p_y = \frac{d}{ds} \left(\frac{p(s)}{c} v_y \right) = \frac{d}{ds} \left(p(s) \frac{dy}{ds} \right) = 0 \quad (3.31)$$

which is a different type of differential equation than (3.5), because $p(s)$ is not constant any more. A first integral yields

$$p(s) \frac{dy}{ds} = \text{const} = y'_0 p_0, \text{ thus } \frac{dy}{ds} = y'(s) = \frac{y'_0 p_0}{p_0 + \frac{\epsilon}{c} E_s s} \quad (3.32)$$

Integrating once more we obtain

$$y(s) = y_0 + y'_0 \cdot \frac{c p_0}{e E_s} \ln \left(1 + \frac{e E_s}{c p_0} s \right) \quad (3.33)$$

With Eqs. (3.32,3.33) and putting $s = l$ the transfer matrix is

$$M_x = M_z = M = \begin{pmatrix} 1 & \frac{p_0 \ell \cdot \ln \left(1 + \frac{\Delta p}{p_0} \right)}{\Delta p} \\ 0 & \frac{p_0}{p_0 + \Delta p} \end{pmatrix} \quad (3.34)$$

where $\Delta p = \frac{\epsilon}{c} E_s \cdot l$ is the momentum gain in the accelerating section. The main complication with this transfer matrix is, that its determinant is not unity:

$$\det M = \frac{p_0}{p_0 + \Delta p} \quad (3.35)$$

This is due to the fact that the equation of motion contains a first-derivative term, and it reflects the effect of adiabatic damping (see end of subsection 4.4). Instead of (3.34), one often uses a normalized matrix

$$M_x^* = M_z^* = M^* = \frac{M}{\sqrt{\det M}} = \frac{1}{\sqrt{\frac{p_0}{p_0 + \Delta p}}} \begin{pmatrix} 1 & \frac{p_0 \ell \cdot \ln \left(1 + \frac{\Delta p}{p_0} \right)}{\Delta p} \\ 0 & \frac{p_0}{p_0 + \Delta p} \end{pmatrix}$$

which has $\det M^* = 1$. This trick saves much of the formalism to be derived in the following sections, but if it is used one has to keep in mind, that in this case the *normalized* emittance is a conserved quantity and not the usual emittance, see Eq. (4.34). A similar complication arises if dispersion is included in the 3×3 matrix version of (3.34).

4 BETATRON OSCILLATIONS

In this section, we shall first treat circular accelerators, because the formalism can be derived in a most stringent way for a periodic lattice. At the end (section 4.8) we will shed some light on the treatment of transfer lines or nonperiodic structures.

4.1 Stability criterion

We assume that the circular accelerator has a median plane, taken to be the horizontal plane $z = 0$, and that the magnetic guide and focusing fields are perpendicular to this plane. We further assume that there is a closed curve in this plane, called equilibrium orbit, on which a

particle with reference momentum p_0 can move for an arbitrary number of revolutions. A point P on an arbitrary particle trajectory is characterized by the coordinates s, x and z defined by Fig. 2. The differential equations for $x(s)$ and $z(s)$ in linear approximation have been derived in section 3.

$$\begin{aligned}x'' - \left(k - \frac{1}{\rho^2}\right)x &= \frac{1}{\rho} \frac{\Delta p}{p_0} \\z'' + kz &= 0\end{aligned}$$

$k(s)$ and $\rho(s)$ are periodic functions of s because the orbit is a closed curve. In the following we consider only particles of momentum $p = p_0$, i.e. $\Delta p = 0$.

Then both equations read

$$\begin{aligned}y'' + K(s)y &= 0 \\K(s+L) &= K(s)\end{aligned}\tag{4.1}$$

$K(s)$ is a periodic function. The period L may be as large as the circumference C of the accelerator, but the accelerator may be composed of N identical sections or "cells" with $C = N \cdot L$. In that case $K(s)$ has the cell length L as a period.

Remark: All large circular accelerators and storage rings possess indeed a periodic cell structure in the "regular" arcs. The straight sections usually deviate from the periodicity, for instance to accommodate interaction regions or wiggler magnets. These sections are matched to the arcs in such a way that the periodicity of the beta function (see below) is not disturbed.

The differential equation (4.1) is called Hill's equation. For the special case

$$K(s) = \text{const.} > 0$$

it describes a harmonic oscillation with two independent solutions

$$\cos(\sqrt{K}s) \quad \text{and} \quad \sin(\sqrt{K}s).$$

In the general case $K = K(s)$ we define the cosinlike and sinlike trajectories (3.7) and can express any solution $y(s)$ of Eq. (4.1) in the form

$$y(s) = y_0 C(s) + y'_0 S(s)$$

We have already shown that y and y' at the point s can be obtained from y_0, y'_0 by a matrix multiplication

$$\begin{pmatrix} y \\ y' \end{pmatrix}_s = M(s/s_0) \begin{pmatrix} y \\ y' \end{pmatrix}_{s_0}\tag{4.2}$$

with

$$M(s/s_0) = \begin{pmatrix} C(s) & S(s) \\ C'(s) & S'(s) \end{pmatrix}$$

and

$$\begin{pmatrix} C(s_0) & S(s_0) \\ C'(s_0) & S'(s_0) \end{pmatrix} = \begin{pmatrix} 1 & 0 \\ 0 & 1 \end{pmatrix}$$

The transfer matrix for two successive sections of magnets and drift spaces can be computed by matrix multiplication

$$M(s_2/s_0) = M(s_2/s_1) \cdot M(s_1/s_0) \quad (4.3)$$

Proof of Eq. (4.3):

call $C_0(s)$ and $S_0(s)$ the principal trajectories with reference point s_0

$$i.e. \begin{pmatrix} C_0(s_0) & S_0(s_0) \\ C'_0(s_0) & S'_0(s_0) \end{pmatrix} = \begin{pmatrix} 1 & 0 \\ 0 & 1 \end{pmatrix}$$

Then

$$M(s_1/s_0) = \begin{pmatrix} C_0(s_1) & S_0(s_1) \\ C'_0(s_1) & S'_0(s_1) \end{pmatrix}$$

For arbitrary $s_1 \neq s_0$, the principal trajectories $C_1(s), S_1(s)$ with reference point s_1 are in general different from $C_0(s), S_0(s)$ (see Fig. 23)

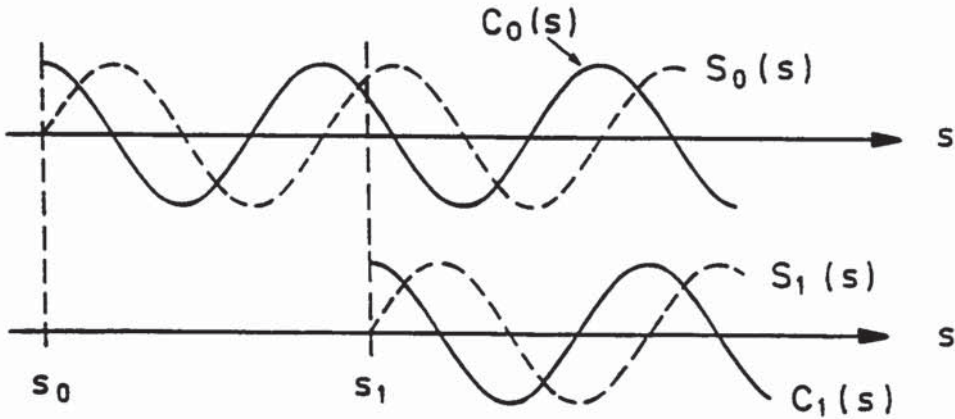


Figure 23: Cosine- and sinelike trajectories relative to different reference points s_0 and s_1

Since $C_1(s)$ and $S_1(s)$ are two linearly independent solutions, we can write

$$C_0(s) = C_0(s_1) C_1(s) + C'_0(s_1) S_1(s)$$

$$S_0(s) = S_0(s_1) C_1(s) + S'_0(s_1) S_1(s)$$

Inserting $s = s_2$ we obtain Eq. (4.3).

Of particular interest is the transfer matrix for a period L of the accelerator structure. We write it as

$$\mathbf{M}(s) \equiv M(s + L/s) \quad (4.4)$$

The transfer matrix for a full revolution is

$$M(s + NL/s) = (\mathbf{M}(s))^N$$

and for n turns

$$(\mathbf{M}(s))^{n \cdot N}$$

A necessary and sufficient condition for stable motion is that the elements of the matrix $\mathbf{M}^{n \cdot N}$ remain bounded for $n \rightarrow \infty$. To derive a condition for this we consider the eigenvalues of the matrix \mathbf{M} .

$$\mathbf{M}Y = \lambda Y \quad Y = \begin{pmatrix} y \\ y' \end{pmatrix}$$

The eigenvalues are the solutions of the determinant equation

$$\det(\mathbf{M} - \lambda I) = 0 \quad (4.5)$$

Let us write $\mathbf{M} = \begin{pmatrix} a & b \\ c & d \end{pmatrix}$, then Eq. (4.5) reads

$$\lambda^2 - \lambda(a + d) + (ad - bc) = 0 \quad (4.5a)$$

Now $\det \mathbf{M} = ad - bc = 1$ (see section 3.2). Without loss of generality we may write

$$\cos \mu = \frac{1}{2} \text{trace } \mathbf{M} = \frac{1}{2}(a + d) \quad (4.6)$$

The new quantity μ is real, if $\frac{1}{2}|a + d| < 1$ and complex or imaginary for $\frac{1}{2}|a + d| > 1$. The two solutions of (4.5a) are

$$\lambda_1 = \cos \mu + i \sin \mu = e^{i\mu}, \quad \lambda_2 = \cos \mu - i \sin \mu = e^{-i\mu} \quad (4.7)$$

Let us now assume that $|a + d| \neq 2$; then $\cos \mu \neq 1$ and $\sin \mu \neq 0$.

In that case the matrix \mathbf{M} can be expressed in a very useful form (Twiss-matrix):

$$\mathbf{M} = I \cos \mu + J \sin \mu \quad (4.8)$$

Here $I = \begin{pmatrix} 1 & 0 \\ 0 & 1 \end{pmatrix}$ is the unit matrix and $J = \begin{pmatrix} \alpha & \beta \\ -\gamma & -\alpha \end{pmatrix}$

with

$$\alpha = \frac{a - d}{2 \sin \mu}$$

$$\beta = b / \sin \mu \quad (4.9)$$

$$\gamma = -c/\sin \mu$$

From $\det M = 1$ we get the relation

$$\beta\gamma - \alpha^2 = 1 \quad (4.10)$$

The matrix J has determinant 1, trace 0 and moreover the property

$$J^2 = \begin{pmatrix} -1 & 0 \\ 0 & -1 \end{pmatrix} = -I \quad (4.11)$$

The combination $I \cos \mu + J \sin \mu$ has properties similar to the complex number $e^{i\mu} = 1 \cdot \cos \mu + i \cdot \sin \mu$; in particular for any μ_1, μ_2

$$(I \cos \mu_1 + J \sin \mu_1)(I \cos \mu_2 + J \sin \mu_2) = I \cos(\mu_1 + \mu_2) + J \sin(\mu_1 + \mu_2)$$

The n -th power of M is

$$M^n = I \cos(n\mu) + J \sin(n\mu) \quad (4.12)$$

From this relation we see immediately that the matrix elements of M^n for $n \rightarrow \infty$ remain bounded if and only if μ is real

$$\boxed{\text{Stability} \iff |\text{trace} M| < 2 \iff \mu \text{ real}} \quad (4.13)$$

For real μ , the matrix elements of M^n oscillate but remain bounded for any n . Furthermore, $\mu = \text{real}$ guarantees that α, β, γ are also real quantities. For complex or imaginary μ , on the other hand, $\cos n\mu$ and $\sin n\mu$ increase exponentially and the elements of M^n do the same so that the motion becomes unbounded.

It should be noted that the trace of M and therefore the parameter μ are independent of the reference point s . This can be seen as follows:

$$M(s_2 + L/s_1) = \underbrace{M(s_2 + L/s_2)}_{M(s_2)} M(s_2/s_1)$$

On the other hand

$$M(s_2 + L/s_1) = \underbrace{M(s_2 + L/s_1 + L)}_{M(s_2/s_1)} \underbrace{M(s_1 + L/s_1)}_{M(s_1)}$$

So $M(s_2)$ differs from $M(s_1)$ by a similarity transformation

$$M(s_2) = M(s_2/s_1) M(s_1) (M(s_2/s_1))^{-1} \quad (4.14)$$

Since the trace is not changed in such a transformation we have

$$\mu(s_2) = \mu(s_1)$$

i.e. μ is independent of s .

The transfer matrix $M(s)$ as a whole does depend on the reference point s . In particular the elements of the matrix J : α , β and γ are periodic functions of s with period L .

$$\begin{aligned}
 M(s) &= \begin{pmatrix} 1 & 0 \\ 0 & 1 \end{pmatrix} \cos \mu + \begin{pmatrix} \alpha(s) & \beta(s) \\ -\gamma(s) & -\alpha(s) \end{pmatrix} \sin \mu = \begin{pmatrix} \cos \mu + \alpha \sin \mu & \beta \sin \mu \\ -\gamma \sin \mu & \cos \mu - \alpha \sin \mu \end{pmatrix} \\
 \alpha(s+L) &= \alpha(s), \quad \beta(s+L) = \beta(s), \quad \gamma(s+L) = \gamma(s) \\
 \mu &\text{ is independent of } s.
 \end{aligned}
 \tag{4.15}$$

We have now succeeded in replacing the four matrix elements a, b, c, d fulfilling $\det M = ad - bc = 1$ by four parameters $\alpha, \beta, \gamma, \mu$ satisfying $\beta\gamma - \alpha^2 = 1$. After the transfer matrix of the whole ring has been obtained by multiplication of individual matrices as described in section 3, the quantities $\alpha, \beta, \gamma, \mu$ are easily calculated by Eqs. (4.6) and (4.9) at any reference point s . But what do we win? The advantage is that these parameters allow a simple description of the motion in terms of harmonic-oscillator language. This will be shown in the following sections.

4.2 Solution of the Hill equation

Floquet Theorem

In section 3 we have solved the homogeneous equation of motion in a piecewise manner (with $K(s) = \text{const}$ in each piece) and have combined them using matrix algebra. We shall now present a closed form solution of the transverse oscillations. From this we will gain an improved understanding of betatron oscillations. The equation

$$y'' + K(s)y = 0 \quad \text{with } K(s+L) = K(s)$$

has two independent solutions

$$y_1(s) = e^{i\mu s/L} p_1(s), \quad y_2(s) = e^{-i\mu s/L} p_2(s) \tag{4.16}$$

μ is called the characteristic coefficient of the differential equation and is given by

$$\cos \mu = \frac{1}{2} \text{trace } M(s)$$

$p_1(s)$ and $p_2(s)$ are periodic functions of s

$$p_i(s+L) = p_i(s), \quad i = 1, 2$$

The solutions are bounded if μ is real, i.e. if the trace of the transfer matrix over the magnet period of length L is less than 2.

The proof of Floquet's theorem goes in several steps.

a) We show that two special solutions y_1, y_2 exist with the property

$$y_i(s+L) = m_i \cdot y_i(s) \quad m_i = \text{const.}$$

Proof: Take two arbitrary independent solutions $g_1(s), g_2(s)$ and consider the new functions

$$h_i(s) = g_i(s + L), \quad i = 1, 2.$$

Because of the periodicity of $K(s)$ the $h_i(s)$ are also solutions. Therefore a nonsingular matrix A exists with

$$\begin{pmatrix} h_1 \\ h_2 \end{pmatrix}_s = \begin{pmatrix} g_1 \\ g_2 \end{pmatrix}_{s+L} = A \begin{pmatrix} g_1 \\ g_2 \end{pmatrix}_s$$

One can find a similarity transformation C which diagonalizes A

$$CAC^{-1} \equiv B = \begin{pmatrix} m_1 & 0 \\ 0 & m_2 \end{pmatrix}$$

and define

$$\begin{pmatrix} y_1 \\ y_2 \end{pmatrix}_s = C \begin{pmatrix} g_1 \\ g_2 \end{pmatrix}_s$$

Then

$$\begin{aligned} \begin{pmatrix} y_1 \\ y_2 \end{pmatrix}_{s+L} &= C \begin{pmatrix} g_1 \\ g_2 \end{pmatrix}_{s+L} = CA \begin{pmatrix} g_1 \\ g_2 \end{pmatrix}_s \\ &= CAC^{-1} \begin{pmatrix} y_1 \\ y_2 \end{pmatrix}_s = \begin{pmatrix} m_1 y_1 \\ m_2 y_2 \end{pmatrix}_s \end{aligned}$$

b) Now we establish a relation between A and the transfer matrix $M(s) = M(s + L/s)$. From

$$\begin{pmatrix} g_1 \\ g_2 \end{pmatrix}_{s+L} = A \begin{pmatrix} g_1 \\ g_2 \end{pmatrix}_s \quad \text{we get} \quad \begin{pmatrix} g'_1 \\ g'_2 \end{pmatrix}_{s+L} = A \begin{pmatrix} g'_1 \\ g'_2 \end{pmatrix}_s$$

Both equations can be combined in a single matrix equation

$$\begin{pmatrix} g_1 & g_2 \\ g'_1 & g'_2 \end{pmatrix}_{s+L} = \begin{pmatrix} g_1 & g_2 \\ g'_1 & g'_2 \end{pmatrix}_s \cdot A^T$$

A^T is the transposed matrix of A .

From the definition of the transfer matrix we have on the other hand

$$\begin{pmatrix} g_1 & g_2 \\ g'_1 & g'_2 \end{pmatrix}_{s+L} = \underbrace{M(s+L/s)}_{M(s)} \begin{pmatrix} g_1 & g_2 \\ g'_1 & g'_2 \end{pmatrix}_s$$

So

$$A^T = G^{-1}M(s)G \quad \text{with } G = \begin{pmatrix} g_1 & g_2 \\ g'_1 & g'_2 \end{pmatrix},$$

Since the matrices A^T and $M(s)$ are connected by a similarity transformation they have the same eigenvalues: $\lambda_1 = m_1, \lambda_2 = m_2$.

So

$$y_i(s + L) = \lambda_i y_i(s) \quad i = 1, 2.$$

Now put

$$\lambda_1 = e^{i\mu}$$

(μ may be real or complex).

From $\det M = \lambda_1 \cdot \lambda_2 = 1$ follows

$$\begin{aligned} \lambda_2 = e^{-i\mu} \quad \text{and} \quad \cos \mu &= \frac{1}{2}(\lambda_1 + \lambda_2) \\ &= \frac{1}{2} \text{trace } M \end{aligned}$$

Finally we make the ansatz

$$y_1(s) = e^{+i\mu s/L} p_1(s), \quad y_2(s) = e^{-i\mu s/L} p_2(s)$$

It is then easy to see that the functions $p_1(s), p_2(s)$ are periodic: $p_i(s + L) = p_i(s)$. This completes the proof of Floquet's theorem.

4.3 The beta function

The elements of the transfer matrix

$$M(s) \equiv M(s + L/s) = \begin{pmatrix} m_{11}(s) & m_{12}(s) \\ m_{21}(s) & m_{22}(s) \end{pmatrix}$$

are clearly periodic functions of s

$$m_{ik}(s + L) = m_{ik}(s)$$

The trace of M and therefore the characteristic coefficient μ of Hill's equation are independent of s

$$\cos \mu = \frac{1}{2} \text{trace } M = \frac{1}{2}(m_{11} + m_{22})$$

If we write $M(s)$ in the Twiss form we see that the s -dependence is in the matrix J :

$$\mathbf{M}(s) = I \cos \mu + \begin{pmatrix} \alpha(s) & \beta(s) \\ -\gamma(s) & -\alpha(s) \end{pmatrix} \sin \mu$$

We want to show that $\alpha(s)$ and $\gamma(s)$ can be related to the “beta function” $\beta(s)$. From the periodicity of $\mathbf{M}(s)$:

$$\beta(s+L) = \beta(s) \quad (4.17)$$

The condition $\det \mathbf{M}(s) = 1$ allows to eliminate $\gamma(s)$ (see Eq. (4.10)):

$$\boxed{\gamma(s) = \frac{1+\alpha^2(s)}{\beta(s)}} \quad (4.18)$$

In order to express $\alpha(s)$ through the beta function (actually its derivative) we first derive first-order differential equations for the two eigenfunctions y_1, y_2 of the Hill equation. From

$$\begin{pmatrix} y \\ y' \end{pmatrix}_{s+L} = \mathbf{M}(s) \begin{pmatrix} y \\ y' \end{pmatrix}_s = e^{\pm i\mu} \begin{pmatrix} y \\ y' \end{pmatrix}_s$$

we obtain

$$y(s) \cos \mu + (y(s)\alpha + y'(s)\beta) \sin \mu = y(s) (\cos \mu \pm i \sin \mu)$$

$$y\alpha + y'\beta = \pm iy$$

$$\frac{y'}{y} = \frac{\pm i - \alpha}{\beta} \quad (4.19)$$

This last relation is valid with the positive sign for $y_1(s)$ (Eq. (4.16)) and with negative sign for $y_2(s)$.

Let us take the equation of y_1 and differentiate it logarithmically (we write y instead of y_1).

$$\frac{y''}{y'} - \frac{y'}{y} = \frac{-\alpha'}{i-\alpha} - \frac{\beta'}{\beta}$$

$$y'' = -Ky \quad (\text{Hill equation})$$

$$\frac{y''}{y'} = -K \frac{y}{y'} = -\frac{K\beta}{i-\alpha} \quad (\text{from (4.19)}).$$

$$\frac{y''}{y'} - \frac{y'}{y} = -\frac{K\beta}{i-\alpha} - \frac{i-\alpha}{\beta} = \frac{-\alpha'}{i-\alpha} - \frac{\beta'}{\beta}$$

$$-K\beta^2 - (i-\alpha)^2 = -\alpha'\beta - \beta'(i-\alpha)$$

$$(\alpha^2 + K\beta^2 + \alpha\beta' - \alpha'\beta - 1) - i(2\alpha + \beta') = 0$$

The elements of $M(s)$ are real. Therefore we get

$$\boxed{\alpha(s) = -\frac{1}{2}\beta'(s)} \quad (4.20)$$

and

$$\alpha^2 + K\beta^2 + \alpha\beta' - \alpha'\beta - 1 = 0.$$

Using (4.20) to eliminate α and α' from the last equation we obtain the following nonlinear differential equation for the beta function

$$\frac{1}{2}\beta\beta'' - \frac{1}{4}\beta'^2 + K\beta^2 = 1 \quad (4.21)$$

We have now succeeded in expressing the elements of the transfer matrix $M(s)$ in terms of a single function $\beta(s)$, its derivative $\beta'(s)$, and a phase parameter μ . In the following we shall see that the solutions of Hill's equation can *also* be written in terms of the beta function. This illustrates the basic rôle of this function.

According to Floquet's theorem there are two linearly independent solutions y_1, y_2 of Hill's equation which can be written as a phase factor $e^{\pm i\mu s/L}$ times a periodic function $p_1(s), p_2(s)$. These solutions fulfil the first-order differential equation (4.19)

$$\frac{y'}{y} = \frac{\pm i + \frac{1}{2}\beta'}{\beta}$$

After integration we get

$$\boxed{\begin{aligned} y_{1,2}(s) &= a\sqrt{\beta(s)}e^{\pm i\Phi(s)} \\ \text{with } \Phi'(s) &= \frac{1}{\beta(s)}, \quad a = \text{const.} \end{aligned}} \quad (4.22)$$

The most general solution of the Hill equation is a pseudo-harmonic oscillation; amplitude and wavelength depend on the coordinate s and are both given in terms of the beta function:

$$\text{amplitude} \propto \sqrt{\beta(s)}; \quad \lambda(s) = 2\pi\beta(s) \quad (4.23)$$

The phase function $\Phi(s)$ is also computed from $\beta(s)$

$$\Phi(s) = \int_{s_0}^s \frac{dt}{\beta(t)} \quad (4.24)$$

Now we can also compute the characteristic coefficient μ of Hill's equation.

$$y_1(s+L) = a\sqrt{\beta(s+L)}e^{+i\Phi(s+L)}$$

$$\beta(s+L) = \beta(s) \quad (\text{see (4.17)})$$

$$\Phi(s+L) = \int_{s_0}^{s+L} \frac{dt}{\beta(t)} = \int_{s_0}^s \frac{dt}{\beta(t)} + \int_s^{s+L} \frac{dt}{\beta(t)}$$

So

$$y_1(s+L) = y_1(s) \cdot \exp\left(+i \int_s^{s+L} \frac{dt}{\beta(t)}\right)$$

Using (4.16) we find

$$\boxed{\mu = \int_s^{s+L} \frac{dt}{\beta(t)}} \quad (4.25)$$

μ is the phase advance per period (of length L).

The Q value (often denotes also as ν) is defined as the number of betatron oscillations per revolution. If the accelerator has N periods, Q is given by

$$\boxed{Q = \frac{N\mu}{2\pi} = \frac{1}{2\pi} \oint \frac{ds}{\beta(s)}} \quad (4.26)$$

In the above derivations it has been assumed that $\beta(s)$ vanishes nowhere. This is guaranteed if $|\cos \mu| < 1$ because in that case α, β, γ are real and therefore the equation $\beta\gamma - \alpha^2 = 1$ requires $\beta \neq 0$.

Remark: Note that the symbol \oint does not represent a line integral as defined in the frame of vector analysis. In accelerator physics it is, instead, frequently used to symbolize an integral over the full circumference of the circular accelerator.

Equation (4.26) means that, as a rule of thumb, the Q -value is given by the mean bending radius divided by the mean beta function.

A particle trajectory is described by a real solution of Hill's equation:

$$y(s) = a\sqrt{\beta(s)} \cos(\Phi(s) - \delta) \quad (4.27)$$

From $\Phi' = \frac{1}{\beta}$, that is $d\Phi = \frac{1}{\beta(s)} ds = \frac{2\pi}{\lambda(s)} ds$ we see again that the local wavelength of this quasi-harmonic wave is $\lambda(s) = 2\pi\beta(s)$. Since in high energy accelerators the betatron wavelength is typically of the order of several 10 m, β is of the same order of magnitude.

The derivative of $y(s)$ is

$$y'(s) = -\frac{a}{\sqrt{\beta}}(\alpha \cos(\Phi(s) - \delta) + \sin(\Phi(s) - \delta)) \quad (4.28)$$

$$\alpha = -\frac{1}{2}\beta'$$

δ is an arbitrary constant phase.

Now we consider a family of trajectories with the same amplitude a but with different phases δ . At a fixed value of s we plot the vector

$$Y(\delta) = (y(s), y'(s))$$

as a function of the phase angle δ in the (y, y') -phase space (horizontal phase space (x, x') , vertical phase space (z, z')).

The equations

$$\begin{aligned} y &= a\sqrt{\beta} \cos(\Phi - \delta) \\ y' &= -\frac{a}{\sqrt{\beta}}(\sin(\Phi - \delta) + \alpha \cos(\Phi - \delta)) \end{aligned} \quad (4.29)$$

are a parametric representation of an ellipse in the (y, y') plane. If δ varies between 0 and 2π , the point $Y = (y, y')$ moves around this ellipse (Fig. 24).

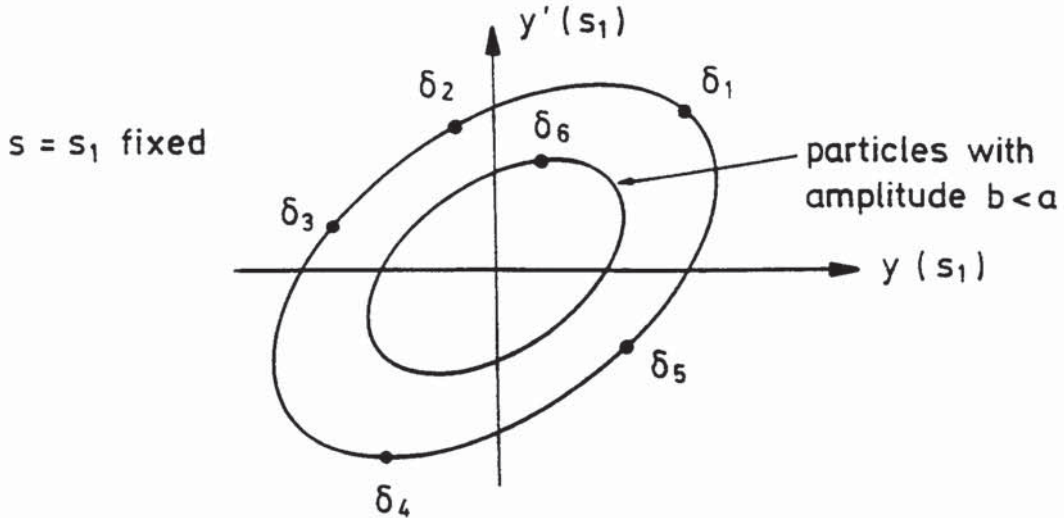


Figure 24: Phase-space ellipse for a family of particle trajectories with the same amplitude a but different phase angles $\delta_1, \delta_2, \delta_3, \dots$. For trajectories with a smaller amplitude b one obtains a correspondingly smaller ellipse.

Alternatively we can consider only one particle and follow this particle for many successive revolutions. Then its phase-space coordinates at a fixed $s = s_1$ also map out the phase-space ellipse, because for each turn in the accelerator the point (y, y') makes a noninteger number of Q turns in the phase plane (Fig. 25).

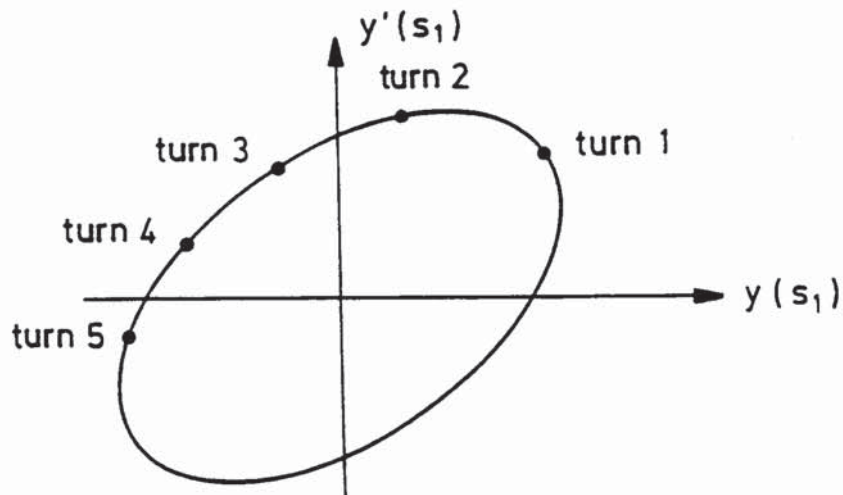


Figure 25: Phase-space ellipse for one particle after many turns in the accelerator. For each revolution of the particle, the point (y, y') makes Q turns in the phase plane (e.g. 6.2 turns in the case of the CERN PS).

4.4 Emittance and beam envelope

The area of the phase-space ellipse is an important quantity. It is given by

$$\text{area} = \pi a^2 \quad (4.30)$$

We want to show that the area remains invariant when we transform the particle trajectories through the accelerator.

The ellipse equation is, in cartesian coordinate representation,

$$\gamma y^2 + 2\alpha y y' + \beta y'^2 = a^2 \quad (4.31)$$

This can be seen by inserting y, y' from Eq. (4.29) and using $\beta\gamma - \alpha^2 = 1$.

We want to show now that both sides of Eq. (4.31) remain constant when we transform y and y' through the accelerator. This constant is called the

Courant – Snyder invariant

$$\begin{aligned} \gamma y^2 + 2\alpha y y' + \beta y'^2 &= \text{const.} \\ \text{or } \frac{1}{\beta} \left(y^2 + (\alpha y + \beta y')^2 \right) &= \text{const.} \end{aligned} \quad (4.32)$$

Proof: let $y(s)$ be an arbitrary real trajectory and $y_1(s)$ the first eigenfunction (4.16) of Hill's equation. We form the Wronskian determinant

$$\begin{aligned} W &= y y_1' - y' y_1 \\ \frac{dW}{ds} &= W' = y y_1'' - y'' y_1 = -K(y y_1 - y y_1) = 0 \end{aligned}$$

since both y, y_1 fulfil Hill's equation. So $W = \text{const.}$

y_1 fulfils the Eq. (4.19): $y_1' = \frac{i-\alpha}{\beta} y_1$. Inserting this into the expression for W yields

$$W = y_1 \left(\frac{i-\alpha}{\beta} y - y' \right) = \text{const.}$$

$$W W^* = y_1 y_1^* \left(\frac{1}{\beta^2} y^2 + \left(\frac{\alpha}{\beta} y + y' \right)^2 \right) = \text{const.}$$

Now from Eq. (4.22): $y_1 \sim \sqrt{\beta} e^{i\Phi}$, $y_1 y_1^* \sim \beta$

$$\text{So we get } \frac{1}{\beta} \left(y^2 + (\alpha y + \beta y')^2 \right) = \text{const.}$$

From the Courant-Snyder invariant we get the result that the area of the phase-space ellipse is invariant. The shape and orientation of the ellipse change when moving through the accelerator. In the center of a quadrupole of a regular FODO lattice the slope β' of the beta function is zero. Thus the main axes of the ellipse coincide with the y and y' axes (Fig. 26). (The term "FODO" lattice describes a periodic sequence of focusing and defocusing quadrupole magnets, with dipole magnets or drift spaces –denoted by "O"– between them, see Fig. 29.)

Let us now consider a particle beam centered around the reference orbit $(y, y') = (0, 0)$ and assume that the particle trajectories fill the (yy') phase space at a certain point s (e.g. the injection point) up to the phase ellipse with amplitude a . Then we know that all trajectories will remain inside or on the phase ellipse when the particles move around the accelerator. Since the area is invariant we get the important result that the phase-space density in the vicinity of any phase-space trajectory is invariant (Liouville's theorem). This is true under the condition that the particle energy is kept constant and that stochastic effects like beam-gas scattering or synchrotron radiation are neglected.

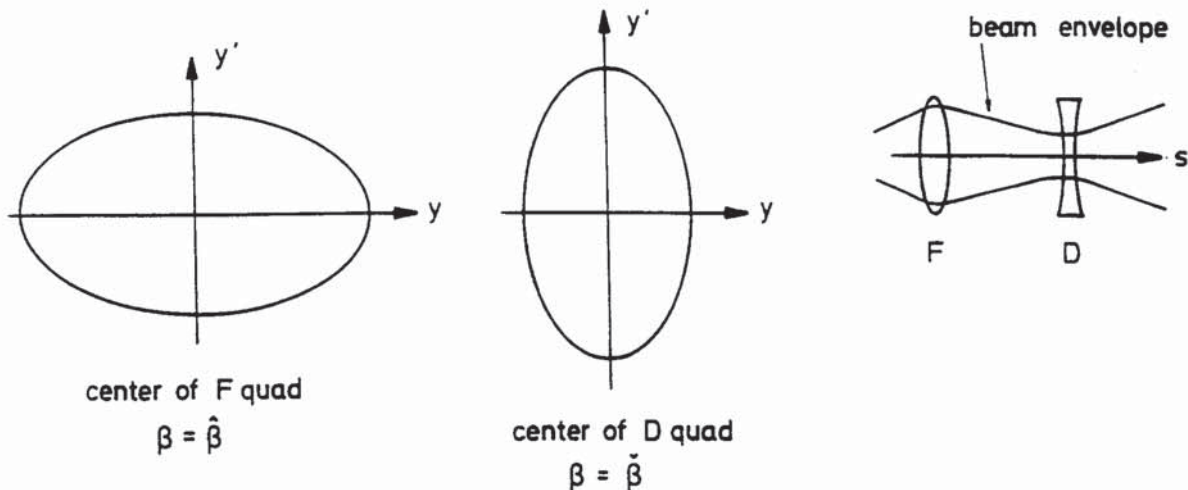


Figure 26: Phase-space ellipse in the center of a focusing or defocusing quadrupole

Since the area of the ellipse enclosing the beam in phase space is such an important quantity one introduces a new notion, the emittance ϵ

$$\text{area of ellipse} = \pi \cdot \epsilon \quad (4.33)$$

When the particles are accelerated, the emittance decreases inversely proportional to the momentum. This can be understood intuitively from the observation that only the longitudinal component of the momentum vector is increased in the accelerating cavities whereas the transverse components remain invariant, so that the beam divergence shrinks. This phenomenon is often called *adiabatic damping* which is somewhat misleading since no dissipative effect is involved. The energy dependence of the emittance can be derived in a rigorous way within the Hamiltonian formalism. The key point is that the canonically conjugate momenta of the position variables x and z are *not* the slopes $x' = dx/ds$, $z' = dz/ds$ but rather the transverse momenta p_x , p_z . The phase-space trajectory in the (x, p_x) plane, corresponding to the emittance ellipse, is of course also an ellipse since $p_x = p_0 x'$. The area is $\pi \cdot \epsilon_N \cdot (m_0 c)$. Here we have defined the *normalized emittance* by

$$\epsilon_N = \left(\frac{p_0}{m_0 c} \right) \epsilon \quad (4.34)$$

For proton and heavy-ion beams, and for electrons in linacs, the normalized emittance is the quantity that stays constant during acceleration. It remains even invariant when the beam is passed from an ion source through a whole chain of pre-accelerators into a large storage ring, provided the transitions are properly matched (see section 4.8).

In electron-positron storage rings, the (stochastic) emission of synchrotron radiation and the subsequent re-acceleration are the dominant factors determining the beam dimensions. In an ideal flat ring with complete decoupling of horizontal and vertical motion, the vertical emittance tends to zero while the horizontal emittance grows with the square of the energy. This is treated in more detail in the lectures by R. Walker, these proceedings.

Using the emittance ϵ we can write for a particle trajectory on the ellipse that encloses the beam

$$y(s) = \sqrt{\varepsilon\beta(s)} \cos(\Phi(s) - \delta) \quad (4.35)$$

The beam envelope is

$$E(s) = y_{max}(s) = \sqrt{\varepsilon}\sqrt{\beta(s)} \quad (4.36)$$

The beam divergence is

$$A(s) = y'_{max}(s) = \sqrt{\varepsilon}\sqrt{\frac{1 + \alpha^2(s)}{\beta(s)}} = \sqrt{\varepsilon}\sqrt{\gamma(s)} \quad (4.37)$$

These quantities are shown in Fig. 27.

Whenever $\alpha = 0$, the beam envelope $E(s)$ has a local minimum (“waist”) or maximum: $\frac{d}{ds}E(s) = -\sqrt{\varepsilon}\alpha/\sqrt{\beta} = 0$. At such a position, the beam divergence is $A(s) = \sqrt{\varepsilon/\beta}$. This offers another simple interpretation of the beta function at a beam waist: The beta function is just the ratio of beam size to beam divergence:

$$\beta(\text{beam waist}) = \frac{E(s)}{A(s)} = \frac{\sqrt{\varepsilon \cdot \beta}}{\sqrt{\varepsilon/\beta}} \quad (4.38)$$

Since β is typically of the order of meters, a beam of a few mm diameter will typically have a divergence of a milliradian.

Finally the equation of the ellipse enclosing the beam is

$$\gamma y^2 + 2\alpha y y' + \beta y'^2 = \varepsilon \quad (4.39)$$

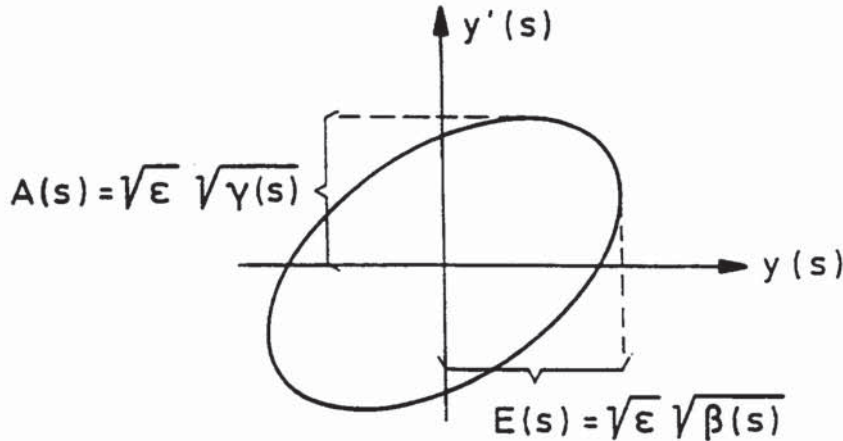


Figure 27: Beam envelope and divergence

Remark: There is a possible confusion here, since ε is often defined as the area rather than the (area)/ π . To avoid such confusion, one often quotes numbers like $(10\pi)mm \cdot mrad$. With our definition of the emittance this implies $\varepsilon = 10 mm \cdot mrad$. In the alternative definition one would have $\varepsilon = 31.4 mm \cdot mrad$. Moreover, there are different conventions in the definition of the emittance for electron or proton beams, respectively. Traditionally, the electron emittance is defined for *one* standard deviation of the phase-space distribution function while for protons *two* standard deviations are used.

4.5 Transformation of α, β, γ

The phase ellipse at a point s is characterized by the parameters $\alpha(s)$, $\beta(s)$, $\gamma(s)$ and the emittance ε . It is important to know the beam envelope and divergence at each location of the accelerator. Therefore it is of great interest to know how to transform α, β, γ through the optical system.

We evaluate the invariant ε at a reference point s_0 and an arbitrary other point s .

$$\varepsilon = \gamma y^2 + 2\alpha y y' + \beta y'^2 = \gamma_0 y_0^2 + 2\alpha_0 y_0 y'_0 + \beta_0 y_0'^2$$

Using the principal trajectories we can relate $y(s)$, $y'(s)$ to $y_0 = y(s_0)$, $y'_0 = y'(s_0)$

$$\begin{pmatrix} y \\ y' \end{pmatrix} = \begin{pmatrix} C & S \\ C' & S' \end{pmatrix} \begin{pmatrix} y_0 \\ y'_0 \end{pmatrix}$$

The inverse transformation matrix is

$$\begin{pmatrix} S' & -S \\ -C' & C \end{pmatrix} \text{ because of } \begin{vmatrix} C & S \\ C' & S' \end{vmatrix} = 1.$$

So

$$\begin{aligned} y_0 &= S'y - Sy' \\ y'_0 &= -C'y + Cy' \end{aligned}$$

$$\begin{aligned} \varepsilon &= \gamma_0 (S'y - Sy')^2 + 2\alpha_0 (S'y - Sy')(-C'y + Cy') \\ &\quad + \beta_0 (-C'y + Cy')^2 = \gamma y^2 + 2\alpha y y' + \beta y'^2 \end{aligned}$$

Comparing the coefficients yields:

$$\begin{aligned} \beta(s) &= C^2 \beta_0 - 2SC\alpha_0 + S^2 \gamma_0 \\ \alpha(s) &= -CC'\beta_0 + (SC' + S'C)\alpha_0 - SS'\gamma_0 \\ \gamma(s) &= C'^2 \beta_0 - 2S'C'\alpha_0 + S'^2 \gamma_0 \end{aligned}$$

In matrix notation

$$\begin{pmatrix} \beta \\ \alpha \\ \gamma \end{pmatrix} = \begin{pmatrix} C^2 & -2SC & S^2 \\ -CC' & SC' + S'C & -SS' \\ C'^2 & -2S'C' & S'^2 \end{pmatrix} \begin{pmatrix} \beta_0 \\ \alpha_0 \\ \gamma_0 \end{pmatrix} \quad (4.40)$$

By means of this matrix equation one can transform the beta function piecewise through the magnets and drift spaces. It is useful to start at a symmetry point s_0 of the machine where the derivative of β vanishes.

$$\begin{pmatrix} \beta_0 \\ \alpha_0 \\ \gamma_0 \end{pmatrix} = \begin{pmatrix} \beta_0 \\ 0 \\ \frac{1}{\beta_0} \end{pmatrix} \quad \alpha_0 = -\frac{1}{2}\beta_0' = 0$$

In a drift space we get

$$\beta(s) = \beta_0 - 2\alpha_0 s + \gamma_0 s^2, \quad \alpha(s) = \alpha_0 - \gamma_0 s, \quad \gamma(s) = \gamma_0$$

If now s_0 is a symmetry point like the interaction point of a colliding-beam storage ring we have

$$\beta(s) = \beta_0 + \frac{s^2}{\beta_0} \quad (4.41)$$

In order to get high luminosity one needs a small beam size at the interaction point (IP) and thus β_0 as small as possible. Due to Eq. (4.41) then β becomes large in the quadrupoles next to the IP. Therefore one needs large aperture quadrupoles, located as close to the IP as possible. This in turn means that the focusing strength must be large. The limiting factor in these so called “mini-beta schemes” turns out to be, in most cases, the large chromatic errors of the quadrupole magnets involved, see section 5.3 [9].

We have already seen that the beta function has the same periodicity as Hill’s equation:

$$y'' + K(s)y = 0$$

$$K(s + L) = K(s) \quad , \quad \beta(s + L) = \beta(s)$$

The solutions (4.27), i.e. the particle trajectories, however, are in general not periodic (Fig. 28). On the contrary, an integer Q value, i.e. an integer number of betatron oscillations per revolution, has to be carefully avoided because otherwise a small perturbation at a certain point $s = s_1$ would be seen by the particle at every passage with the same betatron phase angle. This would lead to a resonance-like increase in the betatron amplitude and finally to a loss of the particle.

4.6 Principal trajectories in terms of amplitude and phase function

We denote with $C(s)$ and $S(s)$ the cosinlike and sinlike trajectories relative to the start point $s = s_0$

$$C(s_0) = 1 \quad S(s_0) = 0$$

$$C'(s_0) = 0 \quad S'(s_0) = 1$$

Both can be represented by the form (4.27) of a real trajectory

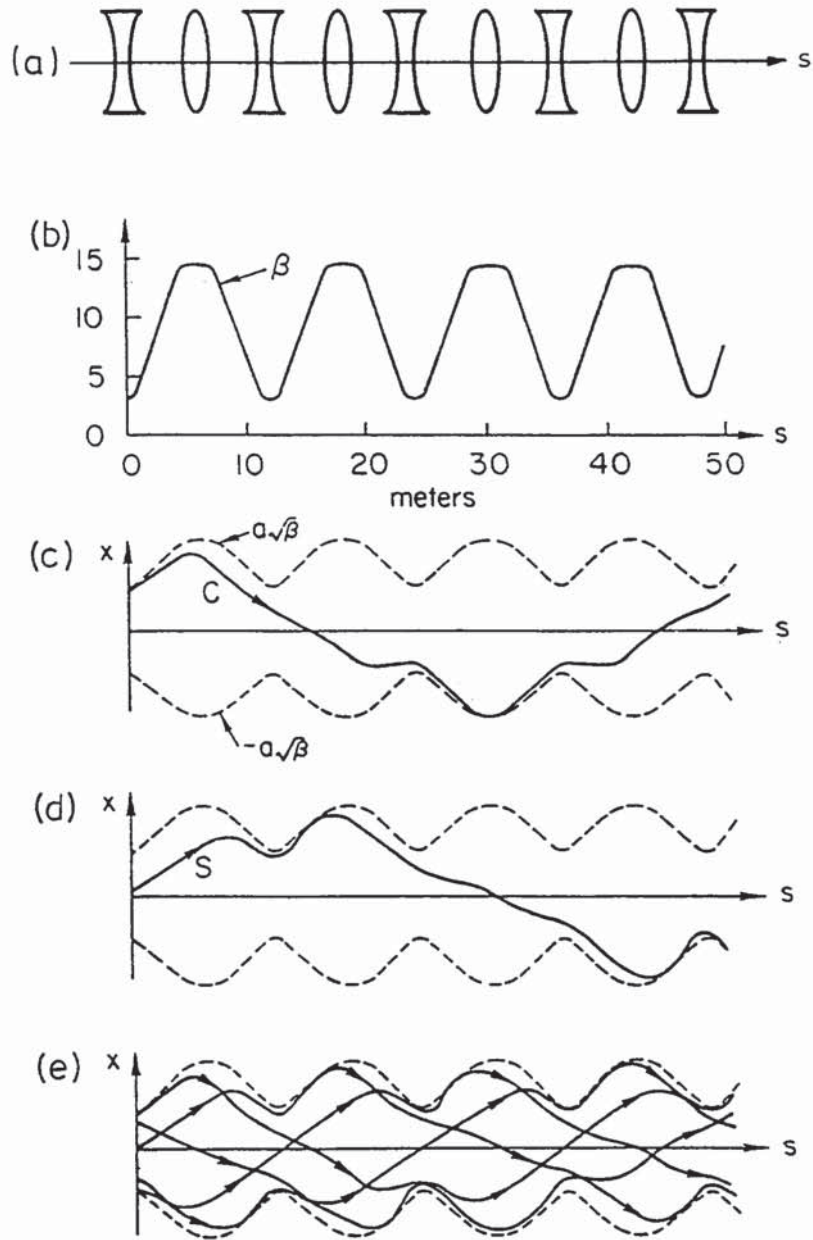


Figure 28: a) A regular FODO lattice of focusing and defocusing lenses b) Beta-function. c) Cosine-like trajectory for $s = 0$. d) Sine-like trajectory for $s = 0$. e) One trajectory on several successive revolutions. (According to M. Sands, *The Physics of Electron Storage Rings*, SLAC-121).

$$\begin{aligned}
C(s) &= \sqrt{\beta(s)}(a \cos(\Phi(s) - \Phi_0) + b \sin(\Phi(s) - \Phi_0)) \\
&\text{with } \Phi_0 = \Phi(s_0) \\
C' &= \frac{1}{2}\beta^{-\frac{1}{2}}\beta'(a \cos(\Phi - \Phi_0) + b \sin(\Phi - \Phi_0)) \\
&\quad + \sqrt{\beta}(-a \sin(\Phi - \Phi_0) + b \cos(\Phi - \Phi_0))\Phi'
\end{aligned}$$

From $C(s_0) = 1$, $C'(s_0) = 0$ we get

$$a = \frac{1}{\sqrt{\beta_0}} \quad b = \alpha_0 a = \frac{\alpha_0}{\sqrt{\beta_0}}$$

$S(s)$ can be computed similarly. The transformation matrix becomes

$$\begin{pmatrix} C(s) & S(s) \\ C'(s) & S'(s) \end{pmatrix} = \begin{pmatrix} \sqrt{\frac{\beta}{\beta_0}}(\cos \Delta\Phi + \alpha_0 \sin \Delta\Phi) & \sqrt{\beta\beta_0} \sin \Delta\Phi \\ \frac{1}{\sqrt{\beta\beta_0}}((\alpha_0 - \alpha) \cos \Delta\Phi - (1 + \alpha\alpha_0) \sin \Delta\Phi) & \sqrt{\frac{\beta_0}{\beta}}(\cos \Delta\Phi - \alpha \sin \Delta\Phi) \end{pmatrix} \quad (4.42)$$

$$\text{with } \Delta\Phi = \Phi(s) - \Phi(s_0)$$

An interesting special case is the transformation matrix for one revolution. For simplicity we start at a symmetry point

$$s = s_0 : \beta'_0 = 0, \quad \alpha_0 = 0$$

Then

$$\begin{pmatrix} C & S \\ C' & S' \end{pmatrix} = \begin{pmatrix} \cos 2\pi Q & \beta_0 \sin 2\pi Q \\ -\frac{1}{\beta_0} \sin 2\pi Q & \cos 2\pi Q \end{pmatrix} \quad (4.42a)$$

4.7 Transformation through a FODO cell

Most high energy accelerators or storage rings have a periodic sequence of quadrupole magnets of alternating polarity in the arcs, see Fig. 29. The dipole magnets are put in between. Here we want to discuss the optical properties of a ‘‘FODO’’ cell disregarding the bending magnets (they are treated as drift spaces). The more general case will be considered in section 6.

We work in the ‘‘thin-lens’’ approximation, see section 3.3d.

$$M_F = \begin{pmatrix} 1 & 0 \\ -\frac{1}{f} & 1 \end{pmatrix} \quad M_0 = \begin{pmatrix} 1 & L/2 \\ 0 & 1 \end{pmatrix} \quad M_D = \begin{pmatrix} 1 & 0 \\ +\frac{1}{f} & 1 \end{pmatrix}$$

The transformation matrix of the cell is

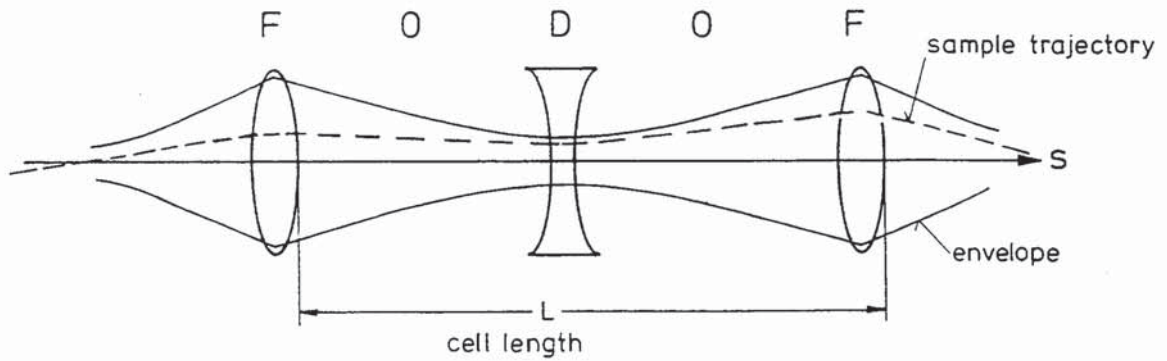


Figure 29: FODO cell

$$\begin{aligned}
 M &= M_F \cdot M_O \cdot M_D \cdot M_O \\
 M &= \begin{pmatrix} 1 + \frac{L}{2f} & L + \frac{L^2}{4f} \\ -\frac{L}{2f^2} & 1 - \frac{L}{2f} - \frac{L^2}{4f^2} \end{pmatrix} \quad (4.43)
 \end{aligned}$$

If we compare this to the Twiss representation (4.15) of the transformation matrix over one period we obtain

$$\begin{aligned}
 \cos \mu &= \frac{1}{2} \text{trace } M = 1 - \frac{L^2}{8f^2} \\
 \cos \mu &= 1 - 2 \sin^2 \frac{\mu}{2} \\
 |\sin \frac{\mu}{2}| &= \frac{L}{4f} \quad (4.44)
 \end{aligned}$$

This equation allows one to compute the phase advance per cell from the cell length and the focal length of the quadrupoles.

Stability requires (see (4.13)): $|\cos \mu| < 1$

$$\text{i.e.} \quad L/4f < 1 \quad (4.45)$$

Stability: $f > L/4$

For a phase advance of 90° per cell

$$f = \frac{1}{\sqrt{2}} \cdot \frac{L}{2}$$

Example: HERA proton ring

$$\begin{aligned}
 L &= 47 \text{ m}, \quad k \simeq 0.032 \text{ m}^{-2}, \quad \ell_{quad} \simeq 1.9 \text{ m} \\
 f &\simeq 16.4 \text{ m} \quad \mu \simeq 90^\circ \quad \beta = \left(L + \frac{L^2}{4f} \right) / \sin \mu \simeq 80.7 \text{ m (in focusing quadrupole)}
 \end{aligned}$$

The limiting case $L = 4f$ of (4.45) has a simple interpretation. It is well known from optics that an object at a distance $a = 2f$ from a focusing lens has its image at $b = 2f$. A regular arrangement of focusing lenses with gaps $L = 4f$ in between provides thus a sequence of point-to-point imaging (Fig. 30). Defocusing lenses that are inserted at these image points have no

effect at all because they are traversed on the axis. If however the lens system is moved further apart ($L > 4f$), this is no more true and the divergence of the light or particle beam is increased by every defocusing lens.

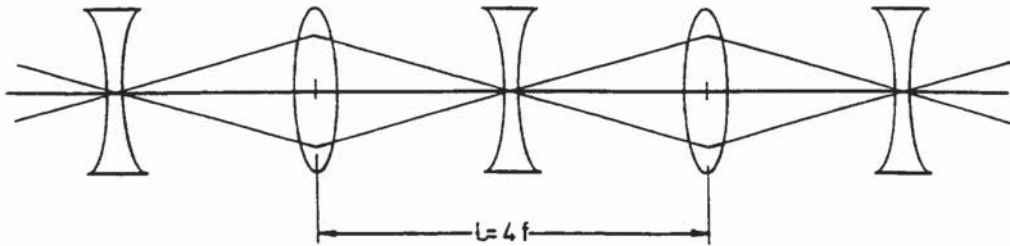


Figure 30: Point-to-point imaging in an arrangement of focusing lenses with distances $L = 4f$. The defocusing lenses have no effect if a point-like object is located exactly on the axis at distance $2f$ from a focusing lens.

As another example of the application of FODO cells, Fig. 31 illustrates the evolution of the phase space ellipse in a very simple circular accelerator consisting of just one FODO cell.

4.8 Non-periodic beam optics

In the previous sections, the Twiss parameters $\alpha, \beta, \gamma, \mu$ have been derived for a periodic, circular accelerator. The condition of periodicity was essential for the definition of the beta function, see Eq. (4.17). Quite often, however, a particle beam moves only once along a beam transfer line, but one is nonetheless interested in quantities like beam envelopes and beam divergence. We will now show that the quantities $\alpha, \beta, \gamma, \mu$ are useful in beam transfer lines as well. It will turn out that the main difference is that in transfer lines the beta function is no longer uniquely determined by the transfer matrix, but also depends on initial conditions which have to be specified in an adequate way.

There is a very simple Gedankenexperiment to show that the Twiss parameters are useful in transfer lines as well: consider a circular accelerator which contains the transfer line as a part of its lattice. Then it is obvious that the optics in the transfer section can be described in terms of Twiss parameters. Now one has to realize that the Twiss parameters in the transfer section will depend on the *complete* revolution matrix. Thus, since there is large arbitrariness in how the transfer line is complemented, the Twiss parameters in the transfer line are not at all well defined. On the other hand Eq. (4.40) shows, that the Twiss parameters are perfectly known in the whole transfer line if only α and β are determined somehow at the entrance of the line. How can this be done reasonably?

Since α and β are related to the beam divergence and beam envelope, a sensible approach is to derive the initial conditions of α and β from the actual phase space distribution of the beam entering the transfer line. In Fig. 32 we have sketched such a distribution.

The lines of constant phase space density are often well fitted by properly parametrized ellipses. (An ellipse is indeed one of the most simple parametrizations one can think of; the main reason for choosing an ellipse, however, will readily be seen.) $1/\pi$ times the area of the ellipse which contains a certain fraction of the particles (say 90 %) is called the beam emittance. The most general

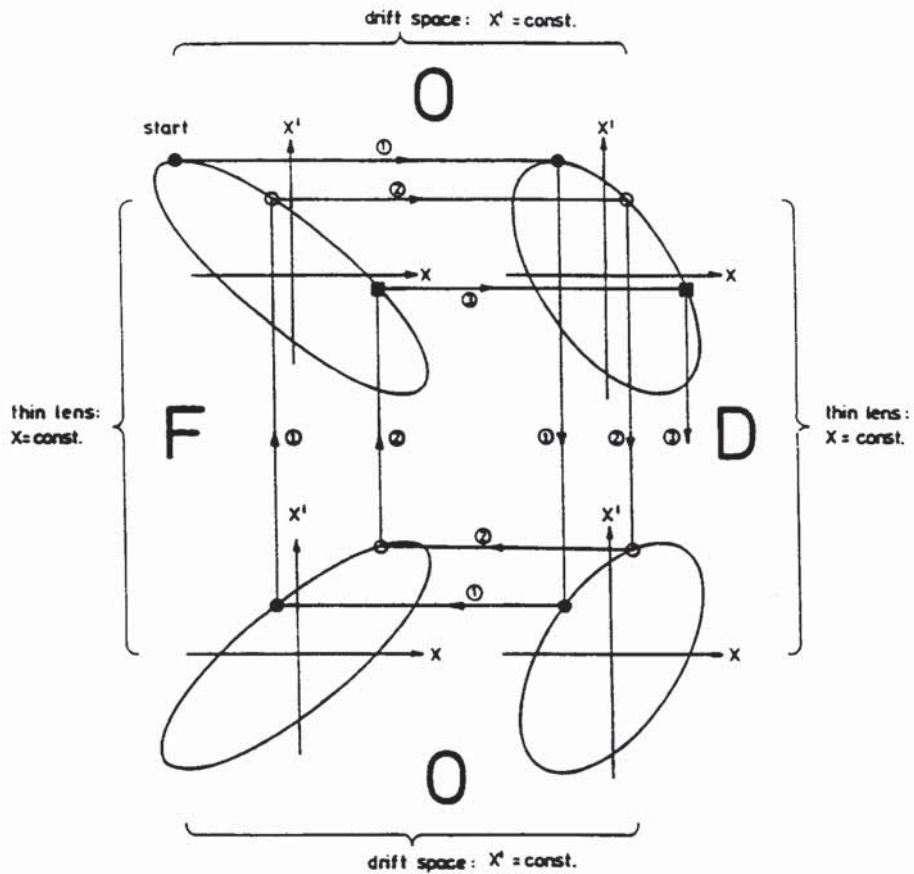


Figure 31: Phase-space dynamics in a simple circular accelerator consisting of one FODO cell. The two 180° bending magnets are assumed to be located in the drift spaces. Their weak focusing contribution is neglected. The periodicity of α, β, γ is reflected by the fact that the phase-space ellipse is transformed into itself after each turn. An individual particle trajectory, however, which starts, for instance, somewhere on the ellipse at the exit of the focusing quadrupole (small circle), is seen to move on the ellipse from turn to turn as determined by the phase angle μ . Thus, an individual particle trajectory is not periodic, while the envelope of a whole beam is.

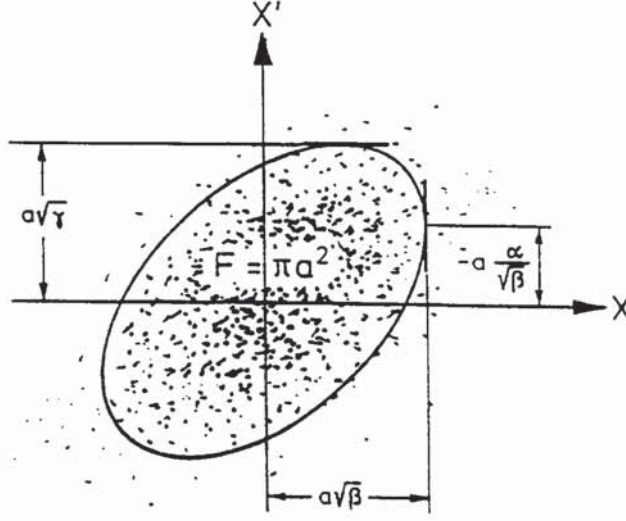


Figure 32: A particle beam is often reasonably well described by a two dimensional Gaussian distribution in phase space. The lines of constant phase-space density are then ellipses. Since the phase-space density decreases only slowly with amplitude, the phase-space area containing *all* particles might be hard to determine (experimentally as well as theoretically). Also, it is not the quantity relevant for most of the applications. Therefore, the emittance is defined as $1/\pi$ times the phase-space area containing a certain fraction of the particles (e.g. 90 %).

ellipse parametrization in phase space is given by ($y = x$ or z)

$$\gamma y^2 + 2\alpha y y' + \beta y'^2 = a^2 \quad (4.46)$$

Since only three free parameters are needed, we can impose another condition:

$$\beta\gamma - \alpha^2 = 1 \quad (4.47)$$

With this normalization of the parameters α , β , γ , the parameter a has the simple meaning that πa^2 is the ellipse area, thus

$$a^2 = \varepsilon = \text{emittance} \quad (4.48)$$

It is obvious from Eqs. (4.46-4.48) that our beam ellipse parameters α , β , γ , a satisfy the same equations as the Twiss parameters defined for a circular accelerator, see Eqs. (4.18, 4.30, 4.31). In a circular accelerator, however, α , β , γ are completely determined by the magnet optics and the condition of periodicity while beam properties are not at all involved (only ε is chosen to fit the actual beam size). In a transfer line optics, on the other hand, we can choose β , β' , ε at the entrance to fit best the incoming beam.

From then on the optics calculation proceeds the same way as in the circular accelerator:

Linear optics performs a linear transformation of phase-space coordinates,

$$\begin{pmatrix} y \\ y' \end{pmatrix}_1 = M(s_1/s_0) \begin{pmatrix} y \\ y' \end{pmatrix}_0 = \begin{pmatrix} C & S \\ C' & S' \end{pmatrix} \begin{pmatrix} y \\ y' \end{pmatrix}_0 \quad (4.49)$$

The beam ellipse at the entrance s_0 is therefore transformed into another ellipse at s_1 :

$$\gamma_1 y_1^2 + 2\alpha_1 y_1 y_1' + \beta_1 y_1'^2 = a_1^2 = \gamma_0 y_0^2 + 2\alpha_0 y_0 y_0' + \beta_0 y_0'^2 = a_0^2 \quad (4.50)$$

Using Eq. (4.49) this can be written in the well known form (see Eq. (4.40))

$$\begin{pmatrix} \beta_1 \\ \alpha_1 \\ \gamma_1 \end{pmatrix} = \begin{pmatrix} C^2 & -2SC & S^2 \\ -CC' & SC' + S'C & -SS' \\ C'^2 & -2S'C' & S'^2 \end{pmatrix} \begin{pmatrix} \beta_0 \\ \alpha_0 \\ \gamma_0 \end{pmatrix} \quad (4.51)$$

Using $\det M = 1$ it is easy to prove that

$$\beta_1 \gamma_1 - \alpha_1^2 = 1$$

i.e. πa_1^2 still means the phase-space area. By virtue of Eq. (4.50)

$$a_0^2 = \varepsilon_0 = a_1^2 = \varepsilon_1$$

i.e. beam emittance is preserved.

Compared to the previous sections, there is nothing new with Eqs. (4.46-4.51). It is just the interpretation of the Twiss parameters which makes a difference.

5 MOTION OF PARTICLES WITH MOMENTUM DEVIATION

The central design orbit of a circular accelerator is a closed curve that goes through the center of all quadrupoles (assuming that the magnets are well aligned). This orbit is a possible particle trajectory: particles with nominal momentum p_0 which start at some point with zero displacement and zero slope will move on the design orbit for an arbitrary number of revolutions. However, particles with $p = p_0$ which start with non-vanishing initial conditions will conduct betatron oscillations about the orbit. Their path around the ring does not close onto itself since the Q-value is non-integer.

Now we consider a particle with a larger momentum $p > p_0$. The design orbit is no more a possible trajectory for this particle. This is easy to understand for a weakly focusing machine (or in a homogeneous field): particles with larger momentum need a circle of larger radius on which they can move indefinitely (see Fig. 33).

If they do not start on exactly that circle, they will perform betatron oscillations about this new, larger circle which therefore is the reference orbit for the particles with the given momentum deviation $dp = p - p_0$. Since its radial distance $x(s, dp/p_0)$ from the design orbit is proportional to dp/p_0 , it is practical to divide by the momentum deviation and define the closed dispersion orbit $D(s)$ by the equation

$$x\left(s, \frac{dp}{p_0}\right) = D(s) \cdot \frac{dp}{p_0}$$

In a machine with weak focusing, $D(s)$ is of course a constant. In strongly focusing machines such an orbit exists, too, but it looks a lot more complicated. The focusing quadrupoles do not permit the particles to deviate too much from the central orbit and bend the trajectory towards the central orbit whereas the defocusing quadrupoles bend it away. It is then easy to understand that the closed dispersion orbit has its maximum deviation from the design orbit in the center

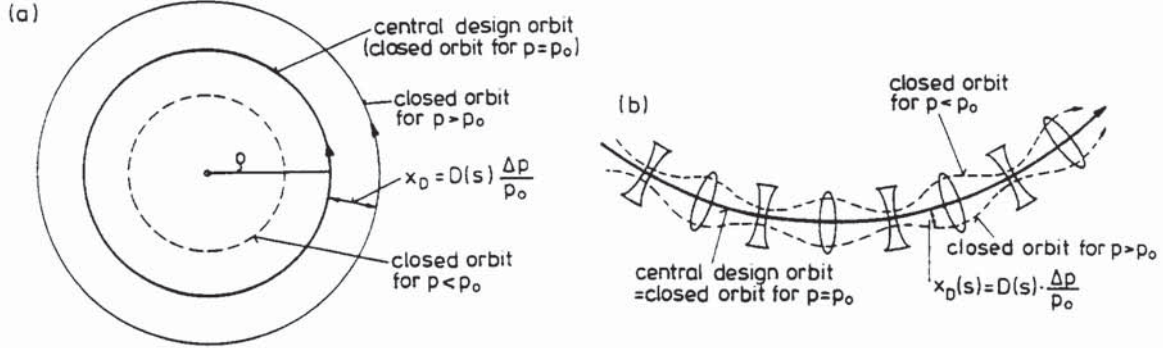


Figure 33: Closed orbit for particles with momentum $p \neq p_0$ in a weakly (a) and strongly (b) focusing circular accelerator.

of the focusing quadrupoles and its minimum deviation in the defocusing quadrupoles. This is sketched in Fig. 33 b.

In the following we want to derive the mathematical expression for the closed dispersion orbit.

5.1 Closed orbit for $\Delta p \neq 0$

A particle with $\Delta p = p - p_0 \neq 0$ satisfies the inhomogeneous Hill equation for the horizontal motion

$$x'' + K(s)x = \frac{1}{\rho} \frac{\Delta p}{p_0} \quad (5.1)$$

The total deviation of the particle from the reference orbit of the machine can be written as

$$x(s) = x_D(s) + x_\beta(s) \quad (5.2)$$

Here $x_D(s) = D(s) \cdot \frac{\Delta p}{p_0}$ describes the deviation of the closed orbit for off-momentum particles with a fixed Δp from the reference orbit; $x_\beta(s)$ describes the betatron oscillation around this closed dispersion orbit.

$D(s)$ is the “periodic dispersion”. It satisfies just the same differential equation as the dispersion trajectory in section 3.2:

$$D'' + K(s)D = \frac{1}{\rho(s)} \quad (5.3)$$

But now we impose *periodic* boundary conditions

$$D(s+C) = D(s), \quad D'(s+C) = D'(s) \quad (5.4)$$

$C = NL$ is the circumference of the machine.

The periodic dispersion is often denoted as $\eta(s)$.

In general, also the equation for the vertical coordinate z contains a nonvanishing right hand side, e.g. due to field and alignment errors in the magnets. We therefore consider more generally the equation

$$y'' + K(s)y = F(s) \quad (5.5)$$

$K(s)$ and $1/\rho(s)$ have the period L but in general $F(s)$ has only the period $C = NL$, e.g. if we have one magnet error.

We look for a periodic solution of the inhomogeneous equation (5.5). The general solution is

$$y(s) = aC(s) + bS(s) + u(s) \quad (5.6)$$

$u(s)$ is a special solution of the inhomogeneous equation. It is given by (cf. (3.11))

$$u(s) = S(s) \int_{s_0}^s F(t)C(t)dt - C(s) \int_{s_0}^s F(t)S(t)dt \quad (5.7)$$

The reference point $s = s_0$ is arbitrary; $C(s)$ and $S(s)$ are the cosinelike and sinelike trajectories referred to this point s_0 .

Our goal is to find a periodic solution of the type (5.6)

$$Y(s+C) = Y(s), \quad Y'(s+C) = Y'(s) \quad (5.8)$$

Since s_0 is arbitrary we can evaluate the conditions (5.8) at $s = s_0$ to compute the unknown constants a and b .

$$\begin{aligned} ac_1 + bs_1 + u_1 &= ac_0 + bs_0 + u_0 \\ ac'_1 + bs'_1 + u'_1 &= ac'_0 + bs'_0 + u'_0 \end{aligned}$$

Here

$$\begin{aligned} c_0 &= C(s_0) = 1, & c'_0 &= C'(s_0) = 0 \\ c_1 &= C(s_0 + C), & c'_1 &= C'(s_0 + C) \\ u_0 &= 0, & u'_0 &= 0, & u_1 &= u(s_0 + C) \text{ etc.} \end{aligned}$$

We obtain

$$a = \frac{s_1 u'_1 - (s'_1 - 1)u_1}{(c_1 - 1)(s'_1 - 1) - c'_1 s_1}$$

The denominator is

$$\begin{aligned} &1 + (c_1 s'_1 - s_1 c'_1) - (c_1 + s'_1) \\ &= 1 + \underbrace{\det \mathbf{M}}_1 - \underbrace{\text{trace } \mathbf{M}}_{2 \cos 2\pi Q} = 4 \sin^2(\pi Q) \end{aligned}$$

$$\text{Here } \mathbf{M} = \begin{pmatrix} C(s_0 + C) & S(s_0 + C) \\ C'(s_0 + C) & S'(s_0 + C) \end{pmatrix} \text{ is the transformation matrix for one revolution.}$$

The numerator is

$$s_1 \left(s'_1 \int FC - c'_1 \int FS \right) - (s'_1 - 1) \left(s_1 \int FC - c_1 \int FS \right)$$

$$\left(\text{abbreviation : } \int FS = \int_{s_0}^{s_0+C} F(t)S(t)dt \right)$$

$$\text{Num.} = \underbrace{(c_1 s'_1 - c'_1 s_1)}_{\det M = 1} \int FS - c_1 \int FS + s_1 \int FC$$

$$c_1 = C(s_0 + C) = \cos 2\pi Q + \alpha_0 \sin 2\pi Q \quad (\text{see Eq.(4.42)})$$

$$s_1 = \beta_0 \sin 2\pi Q$$

$$\text{Num.} = (1 - \cos 2\pi Q - \alpha_0 \sin 2\pi Q) \sqrt{\beta_0} \int_{s_0}^{s_0+C} \sqrt{\beta(t)} F(t) \sin \Delta\Phi(t) dt$$

$$+ \sqrt{\beta_0} \sin 2\pi Q \int_{s_0}^{s_0+C} \sqrt{\beta(t)} F(t) (\cos \Delta\Phi(t) + \alpha_0 \sin \Delta\Phi(t)) dt$$

$$= \sqrt{\beta_0} 2 \sin \pi Q \int_{s_0}^{s_0+C} \sqrt{\beta(t)} F(t) \cos(\Phi(t) - \Phi_0 - \pi Q) dt$$

Now $a = Y(s_0)$. The point s_0 was chosen arbitrarily. Therefore we get for the closed trajectory

$$Y(s) = \frac{\sqrt{\beta(s)}}{2 \sin \pi Q} \int_s^{s+C} \sqrt{\beta(t)} F(t) \cos(\Phi(t) - \Phi(s) - \pi Q) dt$$

$$= \frac{\sqrt{\beta(s)}}{2 \sin \pi Q} \oint \sqrt{\beta(t)} F(t) \cos(|\Phi(t) - \Phi(s)| - \pi Q) dt \quad (5.9)$$

Note that in the first equation $t > s$ is required, i.e. the integration has to start at s , while in the second one this restriction does not apply.

The closed periodic dispersion function is obtained for $F(t) = \frac{1}{\rho(t)} \cdot \frac{\Delta p}{p_0}$:

$$D(s) \equiv \eta(s) = \frac{\sqrt{\beta(s)}}{2 \sin \pi Q} \oint \frac{\sqrt{\beta(t)}}{\rho(t)} \cos(|\Phi(t) - \Phi(s)| - \pi Q) dt \quad (5.10)$$

These equations exhibit an essential instability of a circular accelerator: a finite dispersion exists only if the number of betatron oscillations per revolution Q is different from an integer. Consider an integer Q and look at a certain dipole. A particle with Δp will receive a different kick angle than the reference particle with $p = p_0$. Since Q is integer, these angular deviations add up coherently from turn to turn, and soon the particle hits the vacuum chamber.

While Eqs. (5.9) and (5.10) are very useful for understanding the overall oscillatory behaviour of closed orbits in the presence of dipole errors or momentum errors, numerical calculations will be easier if matrix formalism is applied. This is provided by Eq. (3.10), since $x_D(s) = \eta(s) \cdot \frac{\Delta p}{p_0}$ is a possible particle trajectory (we use now D, D' for the dispersion trajectory part of the transfer matrix and η, η' for the periodic dispersion).

$$\begin{pmatrix} \eta \frac{\Delta p}{p_0} \\ \eta' \frac{\Delta p}{p_0} \\ \frac{\Delta p}{p_0} \end{pmatrix} = \begin{pmatrix} C & S & D \\ C' & S' & D' \\ 0 & 0 & 1 \end{pmatrix} \begin{pmatrix} \eta \frac{\Delta p}{p_0} \\ \eta' \frac{\Delta p}{p_0} \\ \frac{\Delta p}{p_0} \end{pmatrix}$$

or

$$\begin{pmatrix} \eta \\ \eta' \\ 1 \end{pmatrix} = \begin{pmatrix} C & S & D \\ C' & S' & D' \\ 0 & 0 & 1 \end{pmatrix} \begin{pmatrix} \eta \\ \eta' \\ 1 \end{pmatrix}$$

This means: η and η' are eigenvector components of the revolution matrix M for the eigenvalue 1. (We leave the proof that the 3×3 matrix M always has an eigenvalue 1 as an exercise.)

Explicitly, the last equation implies

$$\eta = \frac{(1 - S')D + SD'}{2 - C - S'} = \frac{(1 - S')D + SD'}{4 \sin^2 \pi Q}$$

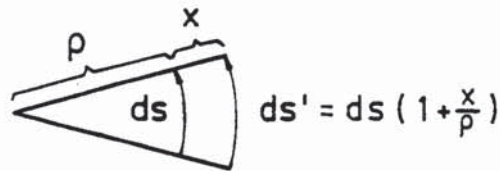
$$\eta' = \frac{C'D + (1 - C)D'}{4 \sin^2 \pi Q}$$

Again it is seen that integer Q values are to be avoided. Once η and η' have been determined at one point s_0 , the values at any other point s are calculated by a simple matrix multiplication:

$$\begin{pmatrix} \eta \\ \eta' \\ 1 \end{pmatrix}_s = M(s/s_0) \begin{pmatrix} \eta \\ \eta' \\ 1 \end{pmatrix}_{s_0}$$

Momentum compaction

A particle with $\Delta p/p_0 > 0$ travels on a revolution a longer distance than the reference particle ($\Delta p = 0$).



Consider a particle moving on the closed dispersion trajectory.

$$x_D(s) = D(s) \frac{\Delta p}{p_0}$$

The circumference for this particle is

$$C' = \oint \left(1 + \frac{x_D(s)}{\rho} ds \right) = C + \Delta C$$

$$\frac{\Delta C}{C} = \alpha \frac{\Delta p}{p_0} \quad (5.11)$$

$$\boxed{\alpha = \frac{1}{C} \oint \frac{D(s)}{\rho(s)} ds} \quad (5.12)$$

The quantity α is the relative change in orbit length divided by the relative momentum deviation. It is called “momentum compaction factor”, which is a rather misleading notion. A rough estimate in terms of the horizontal Q -value is given by

$$\alpha \approx \frac{1}{Q_x^2}$$

5.2 Dispersion in transfer lines

In transfer lines, the dispersion function is also derived from Eqs. (5.6) and (5.7), but periodicity cannot be assumed anymore. Instead, initial conditions are derived from the beam properties at the entrance of the transfer lines. If here a significant correlation exists between the phase space coordinates of the particles and their respective momenta, appropriate initial conditions are

$$D_o \left\langle \left(\frac{\delta p_i}{p} \right)^2 \right\rangle_i = \left\langle x_i \frac{\delta p_i}{p} \right\rangle_i; \quad D'_o \left\langle \left(\frac{\delta p_i}{p} \right)^2 \right\rangle_i = \left\langle x'_i \frac{\delta p_i}{p} \right\rangle_i;$$

where $\langle \rangle_i$ denotes averaging over the whole ensemble of particles at the entrance.

The dispersion as a function of the position s is then

$$D(s) = D_o C(s) + D'_o S(s) + S(s) \int_{s_o}^s \frac{1}{\rho(t)} C(t) dt - C(s) \int_{s_o}^s \frac{1}{\rho(t)} S(t) dt \quad (5.13)$$

If no such correlation is known at the entrance, one usually chooses $D_o = D'_o = 0$, see Eq. (3.11). A transfer line is called *non-dispersive* if

$$D_o = D'_o = 0, \quad \int_{s_o}^s \frac{C(t)}{\rho(t)} dt = 0 \quad \int_{s_o}^s \frac{S(t)}{\rho(t)} dt = 0$$

It is instructive to consider also the generalization of the momentum compaction factor. The relative change in orbit length per relative momentum deviation is given by

$$\alpha(s, s_o) = \frac{\Delta L / L_o}{\Delta p / p_o} = \frac{1}{L_o} \int_{s_o}^s \frac{D(t)}{\rho(t)} dt \quad \text{with} \quad L_o = \int_{s_o}^s dt$$

Finally we consider the relative change in time of flight per relative momentum deviation:

$$\frac{\Delta t / t_o}{\Delta p / p_o} = \frac{p_o}{t_o} \frac{\Delta(\frac{L}{v})}{\Delta p} = \alpha(s, s_o) - 1 + \frac{v^2}{c^2}$$

This quantity is sometimes denoted by $\eta(s, s_o)$. If $\eta(s, s_o) = 0$, the transfer line is called *isochronous*, because then the time of flight does not depend on momentum. For ultrarelativistic particles ($(1 - \frac{v^2}{c^2}) \rightarrow 0$), there is no difference between α and η .

5.3 Influence of field errors

In this section we want to touch very briefly the effect of a dipole or quadrupole error.

a) Dipole error

If $B_z = B_o + \Delta B$ or $B_x = \Delta B$, we have an additional, s -dependent Lorentz force. This leads again to an equation of the type (5.5). The periodic closed orbit is given by (5.9) with $F(t) = \frac{e}{p_o} \Delta B(t)$. In order to have bounded motion the Q value must be non integer, $Q \neq n$.

We see that even for particles with reference momentum p_0 an integer Q value is forbidden, since small field errors are always present.

The main source of orbit errors in accelerators is the displacement of quadrupoles from the design orbit. Correction dipoles are needed to correct the orbit. Eq. (5.9) tells us that their effect is largest if they are placed at points with a large beta function. So a horizontally deflecting correction dipole should be placed close to a horizontally focusing quadrupole and a vertically deflecting correction dipole close to a vertically focusing quadrupole.

b) Quadrupole errors

Let $K_0(s)$ be the design quadrupole strength, $\Delta K(s)$ the error. For a particle with $\Delta p = 0$ we have

$$y'' + (K_0(s) + \Delta K(s))y = 0$$

Call M_0 the transformation matrix for a revolution in the undisturbed machine

$$M_0 = I \cos \mu_0 + J \sin \mu_0$$

$$\mu_0 = 2\pi Q$$

Suppose the error occurs only at $s = s_1$ over a short length ds_1 and let M denote the transformation matrix for the disturbed machine.

We get

$$M = m m_0^{-1} M_0$$

Here m_0 is the matrix of the section of length ds_1 in the undisturbed case, m the matrix in the disturbed case

$$m_0 = \begin{pmatrix} 1 & 0 \\ -K_0(s_1)ds_1 & 1 \end{pmatrix} \quad m = \begin{pmatrix} 1 & 0 \\ (-K_0(s_1) + \Delta K(s_1))ds_1 & 1 \end{pmatrix}$$

To first order in ds_1 :

$$M = \begin{pmatrix} 1 & 0 \\ -\Delta K ds_1 & 1 \end{pmatrix} \cos \mu_0 + \begin{pmatrix} \alpha & \beta \\ -\alpha \Delta K ds_1 - \gamma & -\beta \Delta K ds_1 - \alpha \end{pmatrix} \sin \mu_0$$

$$\cos \mu = \frac{1}{2} \text{trace } M = \cos \mu_0 - \frac{1}{2} \beta \Delta K ds_1 \sin \mu_0$$

If the perturbation is distributed around the ring, we get

$$\Delta(\cos \mu) = \cos \mu - \cos \mu_0 = -\frac{\sin \mu_0}{2} \oint \beta(s) \Delta K(s) ds$$

Now

$$\Delta Q = \frac{\Delta \mu}{2\pi} = -\frac{\Delta(\cos \mu)}{2\pi \sin \mu_0}$$

A gradient error therefore leads to a shift in the Q value

$$\Delta Q = \frac{1}{4\pi} \oint \beta(s) \Delta K(s) ds \quad (5.14)$$

The Q shift is proportional to both the magnitude of the gradient error and the beta function at the location of the error.

A gradient error changes the beta function itself. Without proof we state the result

$$\Delta\beta(s) = \frac{\beta(s)}{2 \sin(2\pi Q)} \oint \beta(t) \Delta K(t) \cos(2|\Phi(t) - \Phi(s)| - 2\pi Q) dt \quad (5.15)$$

Again the change of the beta function is proportional to the magnitude of the perturbation and the amplitude of the beta function itself at the point of the perturbation.

Gradient errors in the interaction region quadrupoles are therefore most dangerous. The second important result is that $\Delta\beta$ remains only finite if Q is different from a half-integer number ($\sin(2\pi Q)$ in the denominator).

The observation that dipole errors lead to integer resonances, quadrupole errors to resonances at half-integer Q values indicates that sextupole fields excite resonances at third-integer Q values. This is in fact the case but not the subject of the present introductory course.² Moreover, one has in general a coupling between horizontal and vertical betatron oscillations due to sextupoles or misalignment of magnets (skew quadrupole fields, see the table at the end of section 2f) etc. This leads to a more general condition

$$mQ_x + nQ_z \neq \ell \quad (5.16)$$

(m, n, ℓ integer numbers; m, n small)

The working point (Q_x, Q_z) has to be chosen in a reasonable distance from the resonance lines (Fig. 34)

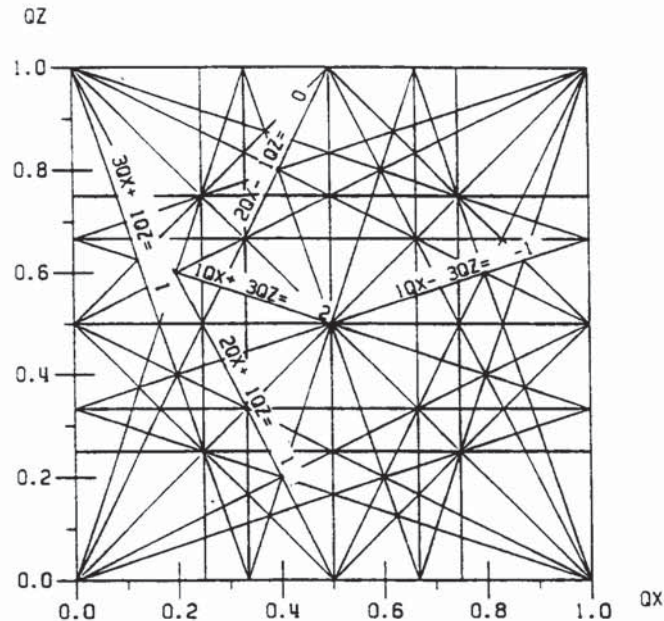


Figure 34: Resonance diagram up to fourth order. Some of the resonance lines have been identified explicitly.

²Resonances are discussed in detail in E. Wilson's lectures at this and the previous accelerator schools (see e.g. the proceedings of the 1984 accelerator school, CERN 85-19).

5.4 Chromaticity

Particles with $\Delta p \neq 0$ are focused differently in the quadrupoles. This leads to a shift of the Q value.

From

$$K = \frac{eg}{p}$$

we get

$$\Delta K = \frac{dK}{dp} \Delta p = -\frac{eg}{p_0} \cdot \frac{\Delta p}{p_0} = -K_0 \frac{\Delta p}{p_0}$$

Formally this is the same as a gradient error. We can therefore use (5.14) to calculate the Q shift

$$\Delta Q = -\frac{1}{4\pi} \oint \beta(s) K(s) ds \frac{\Delta p}{p_0} = \xi \frac{\Delta p}{p_0}$$

$$\boxed{\xi = -\frac{1}{4\pi} \oint \beta(s) K(s) ds} \quad (5.17)$$

ξ is called the chromaticity of the machine. For a linear magnet lattice it is always negative. The main contribution to the chromaticity comes from quadrupoles which are strongly excited and where the β function is large (e.g. interaction region quadrupoles).

In big accelerators the chromaticity arising from the linear lattice (also called the “linear” or “natural” chromaticity) is a large quantity (e.g. $\xi \approx -60$ in the HERA storage rings). Then, the “tune” spread due to the finite momentum band becomes so large that some part of the beam unavoidably hits dangerous resonance lines. In the HERA case, for instance, a beam with a relative momentum spread of only $\pm 10^{-3}$ would cover a tune range of 0.12! For this reason, and in order to avoid the so-called “head-tail” instability, one has to compensate the chromaticity. This can be achieved with sextupoles. The sextupole magnets have to be placed at locations where the closed dispersion orbit $D(s)$ is nonzero, (Fig. 35).

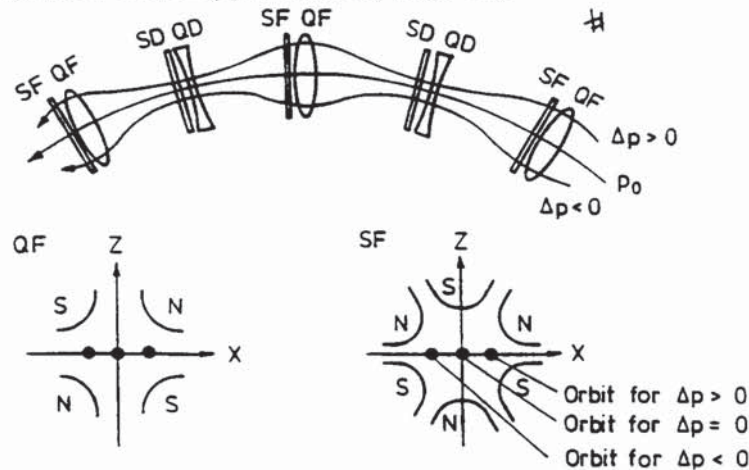


Figure 35: Dispersion trajectory in a sextupole magnet

Consider a particle with $\Delta p \neq 0$ moving without betatron oscillation on the closed dispersion trajectory.

$$x_D(s) = D(s) \frac{\Delta p}{p_0}$$

Now put a sextupole magnet at a place with $D(s) \neq 0$.

The sextupole field at $x = x_D$ in the horizontal plane $z = 0$ is

$$B_z = \frac{1}{2} g' x^2 \quad (5.18)$$

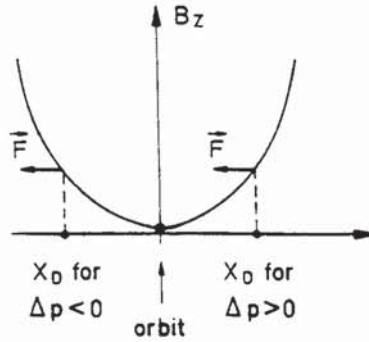


Figure 36: Force on electrons in a sextupole magnet

Particles which move with $\Delta p = 0$ on the reference orbit are not influenced. With the polarity shown in Fig. 35, the sextupole deflects electrons with $\Delta p > 0$ towards the central orbit and electrons with $\Delta p < 0$ away from it (Fig. 36). It is therefore clear that the closed dispersion orbit (5.10), which was computed for a “linear” machine with only dipole and quadrupole magnets, will change when sextupoles are switched on. The dispersion orbit of the “nonlinear” machine can be determined by an iterative procedure.

Now consider a particle that conducts betatron oscillations around that orbit. We want to show that the sextupole acts like a position-dependent quadrupole and influences both horizontal and vertical motion.

Let $\Delta p > 0$ and consider small deviations \bar{x}, \bar{z} from the closed dispersion trajectory

$$\begin{aligned} x &= x_D + \bar{x} \\ z &= 0 + \bar{z} \end{aligned}$$

To first order in the small quantities \bar{x}, \bar{z} :

$$\begin{aligned} B_x &\approx g' x_D \bar{z} = \left(g' D(s) \frac{\Delta p}{p_0} \right) \bar{z} \\ B_z &\approx \underbrace{\frac{1}{2} g' x_D^2}_{\text{causes deflection of closed dispersion orbit}} + \left(g' D(s) \frac{\Delta p}{p_0} \right) \bar{x} \end{aligned} \quad (5.19)$$

Thus the sextupole acts like a quadrupole whose strength increases linearly with Δp . The equivalent quadrupole strength is

$$\frac{eg'x_D}{p_0} = m \cdot D(s) \frac{\Delta p}{p_0} \quad (5.20)$$

$$m = \frac{eg'}{p_0} \quad (\text{Eq. (2.13)})$$

In a regular FODO lattice, two families of sextupoles are needed, (horizontally) focusing ones near the F quadrupoles and defocusing ones near the D quadrupoles. By a proper choice of their strengths one can achieve simultaneous compensation of the horizontal and vertical chromaticities.

$$\xi_{comp} = -\frac{1}{4\pi} \oint [K(s) - m(s)D(s)] \beta(s) ds \quad (5.21)$$

The sextupole compensation of the chromaticity is unavoidable in large rings but has unfortunate consequences: one introduces non-linear fields and a coupling between horizontal and vertical motion (see (2.12)). These adverse effects can be minimized by using a large number of sextupoles with moderate strength, distributed around the ring, rather than a few very strong sextupoles.

6 COMPARISON OF STRONG AND WEAK FOCUSING

6.1 Simplified model of strong focusing

In this chapter we follow closely K. Steffen's lectures at the Orsay accelerator school. We consider a FODO channel and make the following simplifying assumptions

- The weak focusing of the bending magnets is neglected since the radius of curvature is much larger than the focal length of the quadrupoles. (HERA p-ring: $\rho = 584 \text{ m}$, $f = 16.4 \text{ m}$)
- we neglect the short drift spaces between dipoles and quadrupoles
- F and D quadrupoles have the same strength $1/f$ and are treated as thin lenses ($\ell_q \rightarrow 0$).

The simplified model depends only on three parameters

$\ell = L/2$ half cell length \simeq dipole length

$\frac{1}{\rho}$ bending strength; $\varphi = \frac{\ell}{\rho}$.

$\pm \frac{1}{f}$ = $\pm \frac{1}{2f}$ strength of half quadrupole

Its periodic solution and individual particle trajectories have been illustrated in Figs. 28, 30, 31. We now want to explicitly calculate the Twiss parameters as a function of ℓ, ρ, f . We compute the transformation through a half cell from the middle of the F quadrupole to the middle of the D quadrupole (Fig. 37)

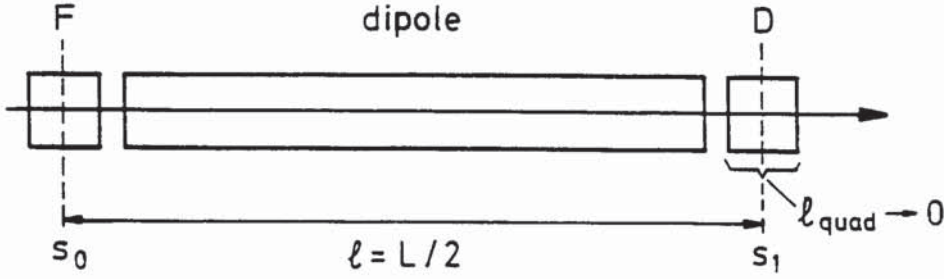


Figure 37: Half cell

$$M(s_1/s_0) = \begin{pmatrix} 1 & 0 \\ \frac{1}{f'} & 1 \end{pmatrix} \begin{pmatrix} 1 & \rho \sin \varphi \\ 0 & 1 \end{pmatrix} \begin{pmatrix} 1 & 0 \\ -\frac{1}{f'} & 1 \end{pmatrix}$$

$\frac{1}{2}$ D-quad. rectangular dipole $\frac{1}{2}$ F-quad.

$$M(s_1/s_0) = \begin{pmatrix} 1 - \frac{\rho}{f'} \sin \varphi & \rho \sin \varphi \\ -\frac{\rho}{f'^2} \sin \varphi & 1 + \frac{\rho}{f'} \sin \varphi \end{pmatrix} \quad (6.1)$$

The transformation through the next half cell to the middle of the next F quadrupole at $s_2 = s_1 + \ell$ is simply obtained by replacing f' by $-f'$ in (6.1).

So the transfer matrix for the whole cell is

$$\begin{aligned} \mathbf{M}(s_0) &= M(s_0 + L/s_0) = M(s_2/s_1) \cdot M(s_1/s_0) \\ \mathbf{M}(s_0) &= \begin{pmatrix} 1 - 2\frac{\rho^2}{f'^2} \sin^2 \varphi & 2\rho \sin \varphi + 2\frac{\rho^2}{f'} \sin^2 \varphi \\ -2\frac{\rho}{f'^2} \sin \varphi + 2\frac{\rho^2}{f'^3} \sin^2 \varphi & 1 - 2\frac{\rho^2}{f'^2} \sin^2 \varphi \end{pmatrix} \\ \cos \mu &= \frac{1}{2} \text{trace } \mathbf{M} = 1 - 2\frac{\rho^2}{f'^2} \sin^2 \varphi \end{aligned} \quad (6.2)$$

Now

$$\begin{aligned} \varphi = \frac{\ell}{\rho} \ll 1, \quad \text{so } \sin \varphi &\approx \frac{\ell}{\rho}; \quad \frac{1}{f'} = \frac{1}{2f} \\ \cos \mu &= 1 - \frac{1}{2} \frac{\ell^2}{f^2} = 1 - \frac{1}{8} \frac{L^2}{f^2} \end{aligned}$$

So in the approximation $\sin \varphi \approx \varphi$ we get the same result for the phase advance in a FODO cell as in section 4.7 where we treated the bending magnets as drift spaces. The present treatment offers additional information. In the middle of an F quadrupole the beta function assumes its maximum value $\hat{\beta}$, in the middle of a D quadrupole its minimum value $\hat{\beta}$. The slope β' is zero here, so $\alpha = 0$ and $\gamma = 1/\beta$. The matrix (4.42), applied to the transformation $s_0 \rightarrow s_1$, is therefore (with $\Delta\Phi = \mu/2$)

$$\begin{pmatrix} C & S \\ C' & S' \end{pmatrix} = \begin{pmatrix} \sqrt{\hat{\beta}/\check{\beta}} \cos \Delta\Phi & \sqrt{\hat{\beta}\check{\beta}} \sin \Delta\Phi \\ -\frac{1}{\sqrt{\hat{\beta}\check{\beta}}} \sin \Delta\Phi & \sqrt{\hat{\beta}/\check{\beta}} \cos \Delta\Phi \end{pmatrix} \quad \Delta\Phi = \frac{\mu}{2} \quad (6.3)$$

From the equality of the matrices (6.1) and (6.3) it follows

$$\begin{aligned} \frac{S'}{C} &= \hat{\beta}/\check{\beta} = \frac{1 + \frac{\rho}{f'} \sin \varphi}{1 - \frac{\rho}{f'} \sin \varphi} \\ -\frac{S}{C'} &= \hat{\beta}\check{\beta} = f'^2 \end{aligned}$$

Now $f' = 2f$ and from (6.2) $\frac{\rho}{f'} \sin \varphi = \sin \frac{\mu}{2} \approx \frac{L}{4f} = \frac{\mu}{4f}$. This allows to compute $\hat{\beta}$ and $\check{\beta}$ as functions of μ

$$\begin{aligned} \hat{\beta} &= L \frac{1 + \sin \frac{\mu}{2}}{\sin \mu} \\ \check{\beta} &= L \frac{1 - \sin \frac{\mu}{2}}{\sin \mu} \end{aligned} \quad (6.4)$$

We see that our basic assumption $|\cos \mu| < 1$, that is $\sin \mu \neq 0$, is necessary to get a finite value for $\hat{\beta}$.

For $0 < \mu < \pi$: $\sin \frac{\mu}{2} < 1$, $\frac{L}{4f} < 1$ (see (4.45)). For a given cell length L , the phase advance with the smallest $\hat{\beta}$ requires the least beam aperture. We obtain it by differentiating (6.4):

$$\begin{aligned} \text{From } \frac{d\hat{\beta}}{d\mu} = 0 \quad \text{it follows} \quad \sin^2 \frac{\mu}{2} \left(2 + \sin \frac{\mu}{2} \right) &= 1 \\ \mu &= 76.35^\circ \end{aligned}$$

In practice, phase advances per cell are typically 60° to 90° .

To transform the dispersion through the half cell we have to compute the 3×3 transfer matrix.

$$\begin{pmatrix} C & S & D \\ C' & S' & D' \\ 0 & 0 & 1 \end{pmatrix}_{\text{half cell}} = \begin{pmatrix} 1 & 0 & 0 \\ \frac{1}{f'} & 1 & 0 \\ 0 & 0 & 1 \end{pmatrix}_{\frac{1}{2} \text{ D quad.}} \begin{pmatrix} 1 & \rho \sin \varphi & \rho(1 - \cos \varphi) \\ 0 & 1 & 2 \tan \frac{\varphi}{2} \\ 0 & 0 & 1 \end{pmatrix}_{\text{dipole}} \begin{pmatrix} 1 & 0 & 0 \\ -\frac{1}{f'} & 1 & 0 \\ 0 & 0 & 1 \end{pmatrix}_{\frac{1}{2} \text{ F quad.}}$$

$$\begin{pmatrix} C & S & D \\ C' & S' & D' \\ 0 & 0 & 1 \end{pmatrix}_{\text{half cell}} = \begin{pmatrix} 1 - \frac{\rho}{f'} \sin \varphi & \rho \sin \varphi & \rho(1 - \cos \varphi) \\ -\frac{\rho}{f'^2} \sin \varphi & 1 + \frac{\rho}{f'} \sin \varphi & \frac{\rho}{f'}(1 - \cos \varphi) + 2 \tan \frac{\varphi}{2} \\ 0 & 0 & 1 \end{pmatrix}$$

Now in the center of the F -quad: $D(s_0) = \hat{D}$, $D'(s_0) = 0$ and in the center of the D -quad: $D(s_1) = \check{D}$, $D'(s_1) = 0$

So

$$\begin{pmatrix} C_1 & S_1 & \check{D} \\ C'_1 & S'_1 & 0 \\ 0 & 0 & 1 \end{pmatrix} = \begin{pmatrix} C & S & D \\ C' & S' & D' \\ 0 & 0 & 1 \end{pmatrix}_{\text{half cell}} \begin{pmatrix} C_0 & S_0 & \hat{D} \\ C'_0 & S'_0 & 0 \\ 0 & 0 & 1 \end{pmatrix}$$

This yields two equations for \hat{D} and \check{D} . The result is

$$\begin{aligned} \hat{D} &= \frac{\ell^2}{\rho} \frac{1 + \frac{1}{2} \sin \frac{\mu}{2}}{\sin^2 \frac{\mu}{2}} \\ \check{D} &= \frac{\ell^2}{\rho} \frac{1 - \frac{1}{2} \sin \frac{\mu}{2}}{\sin^2 \frac{\mu}{2}} \end{aligned} \quad (6.5)$$

The highest and lowest values of the beta function and the dispersion are plotted in Fig. 38 as a function of the phase advance μ .

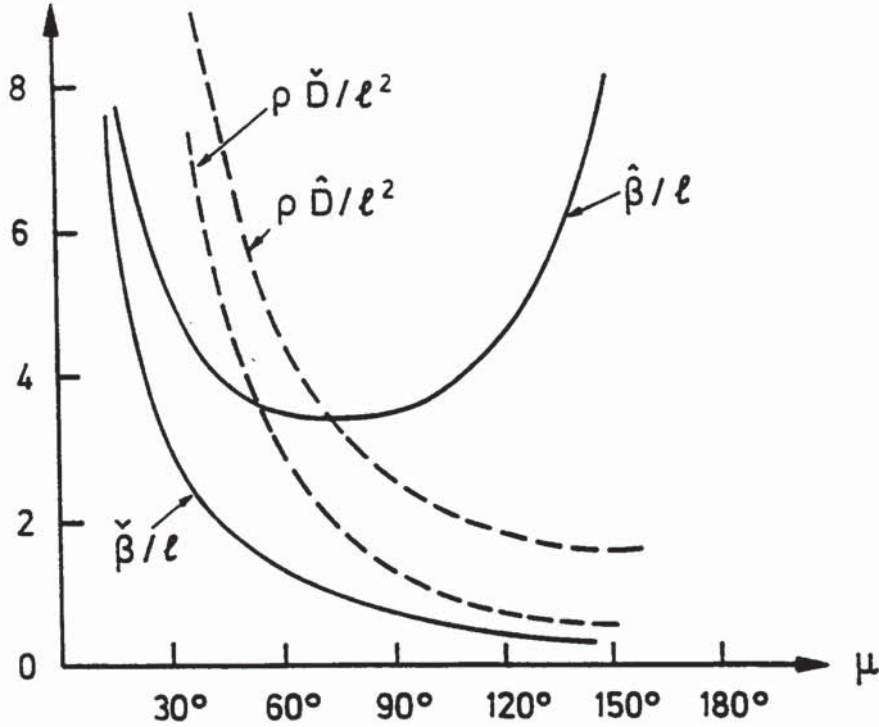


Figure 38: The extreme values of β and D as functions of the phase advance μ in the cell.

It is instructive to compute β and D as functions of s within the half cell. For simplicity we set $s_0 = 0$. Starting from the center of the F -quad at $s_0 = 0$ we first have to apply the matrix equation (4.40) for a half quadrupole to compute α, β, γ at the exit of the F -quad and then the same equation for a bending magnet of length s with $0 < s < \ell$.

$$\begin{pmatrix} \beta \\ \alpha \\ \gamma \end{pmatrix}_{\text{exit F-quad}} = \begin{pmatrix} 1 & 0 & 0 \\ \frac{1}{f'} & 1 & 0 \\ \frac{1}{f'^2} & \frac{2}{f'} & 1 \end{pmatrix} \begin{pmatrix} \hat{\beta} \\ 0 \\ 1/\hat{\beta} \end{pmatrix} = \begin{pmatrix} \hat{\beta} \\ \frac{\hat{\beta}}{f'} \\ \frac{\hat{\beta}}{f'^2} + \frac{1}{\hat{\beta}} \end{pmatrix}$$

matrix (4.40) center of
for 1/2 quad F-quad

Now for a bending magnet of length s

$$\begin{pmatrix} C & S \\ C' & S' \end{pmatrix} = \begin{pmatrix} 1 & \rho \sin \varphi \\ 0 & 1 \end{pmatrix} \approx \begin{pmatrix} 1 & s \\ 0 & 1 \end{pmatrix} \quad (\text{for } \varphi = \frac{s}{\rho} \ll 1)$$

so

$$\begin{pmatrix} \beta(s) \\ \alpha(s) \\ \gamma(s) \end{pmatrix} = \begin{pmatrix} 1 & -2s & s^2 \\ 0 & 1 & -s \\ 0 & 0 & 1 \end{pmatrix} \begin{pmatrix} \hat{\beta} \\ \frac{\hat{\beta}}{f'} \\ \frac{\hat{\beta}}{f'^2} + \frac{1}{\hat{\beta}} \end{pmatrix}$$

matrix (4.40)
for dipole

We get

$$\beta(s) = \hat{\beta} - 2\frac{\hat{\beta}}{f'}s + \left(\frac{\hat{\beta}}{f'^2} + \frac{1}{\hat{\beta}}\right)s^2 \quad (6.6)$$

$$\rightarrow \beta(s) = \hat{\beta} \text{ for } s = 0, \quad \beta(s) = \check{\beta} \text{ for } s = \ell.$$

The dispersion $D(s)$ is obtained using the transformation matrices (3.15) and (3.20).

$$\begin{pmatrix} C & S & D \\ C' & S' & D' \\ 0 & 0 & 1 \end{pmatrix}_{\text{exit F-quad}} = \begin{pmatrix} 1 & 0 & 0 \\ -\frac{1}{f'} & 1 & 0 \\ 0 & 0 & 1 \end{pmatrix} \begin{pmatrix} C_0 & S_0 & \hat{D} \\ C'_0 & S'_0 & 0 \\ 0 & 0 & 1 \end{pmatrix}$$

1/2 F-quad values in center
of F-quad

$$\begin{pmatrix} C(s) & S(s) & D(s) \\ C'(s) & S'(s) & D'(s) \\ 0 & 0 & 1 \end{pmatrix} = \begin{pmatrix} 1 & s & \frac{1}{2}\frac{s^2}{\rho} \\ 0 & 1 & s/\rho \\ 0 & 0 & 1 \end{pmatrix} \begin{pmatrix} C & S & D \\ C' & S' & D' \\ 0 & 0 & 1 \end{pmatrix}_{\text{exit F-quad}}$$

matrix (3.20)
for $\varphi = \frac{s}{\rho} \ll 1$

The result is

$$D(s) = \hat{D} \left(1 - \frac{s}{f'} \right) + \frac{1}{2} \frac{s^2}{\rho} \quad (6.7)$$

$$\Rightarrow D(s_0 = 0) = \hat{D}, \quad D(s = \ell) = \check{D}$$

In an accelerator, where the arcs consist of identical FODO cells, the momentum compaction factor is

$$\alpha = \frac{1}{2\pi R} \oint \frac{D(s)}{\rho(s)} ds \approx \frac{1}{\rho} \cdot \frac{2\pi\rho}{2\pi R} \cdot \frac{1}{2} (\hat{D} + \check{D}) = \frac{\hat{D} + \check{D}}{2R} = \frac{\ell^2}{\rho R \sin^2 \frac{\mu}{2}} = \frac{f'^2}{\rho R}$$

$$R = \frac{C}{2\pi} \text{ is the average machine radius including the straight sections.}$$

For example

$$\alpha = \frac{f'^2}{R\rho} = \frac{4f^2}{R\rho} \approx 1.4 \cdot 10^{-3} \quad \text{for the HERA proton ring} \quad (6.8)$$

The chromaticity can be estimated as follows (cf. Eq. (5.17)):

$$\xi = -\frac{1}{4\pi} \oint \beta(s) K(s) ds$$

In a focusing quadrupole:

$$\beta \approx \hat{\beta}, \quad K(s)\Delta s = \frac{1}{f} \quad (\Delta s \text{ denotes the length of the quad});$$

in a defocusing quadrupole:

$$\beta \approx \check{\beta}, \quad K\Delta s = -\frac{1}{f}$$

Therefore, the chromaticity caused by the regular cell structure of the accelerator is

$$\xi \approx -\frac{1}{4\pi} N \frac{1}{f} (\hat{\beta} - \check{\beta}) = -\frac{N}{\pi} \tan \frac{\mu}{2} \quad N = \text{number of cells} \quad (6.9)$$

Each FODO cell contributes $-\frac{1}{\pi} \tan \frac{\mu}{2}$.

In the HERA proton ring, the contribution of the arcs is $N = 104$, $\hat{\beta} \approx 80m$, $\check{\beta} \approx 20m$, $f \simeq 16m$; so $\xi_{arcs} \approx -30$.

The interaction region quadrupoles contribute a large amount to the total chromaticity since there $\beta(s)$ and $K(s)$ are both large. The chromaticity of the straight sections in the HERA proton ring (including the interaction regions) amounts to $\xi_{straight\ sections} \approx -30$. Thus the total linear chromaticity of the HERA proton ring is $\xi_{HERA} \approx -60$.

For a particle with a momentum error of $\Delta p/p_0 = 5 \cdot 10^{-4}$ this would imply a tune shift of $\Delta Q = -0.03$ if no sextupoles were present.

6.2 Stability diagram

In principle one can choose different strengths for the focusing and the defocusing quadrupoles. Call

$$\frac{\ell}{f'_1} = F > 0, \quad \text{and} \quad -\frac{\ell}{f'_2} = D > 0$$

Then for the horizontal motion, we have(cf. Eq. (3.21))

$$\begin{pmatrix} C & S \\ C' & S' \end{pmatrix}_{\text{half cell}} = \begin{pmatrix} 1 - F & \ell \\ -\frac{1}{\ell}(F - D + FD) & 1 + D \end{pmatrix} \quad (6.10)$$

This matrix has to be equal to the matrix (6.3). In particular

$$-C'S = F - D + FD = \sin^2 \frac{\mu_x}{2}$$

For the vertical motion, one simply has to interchange F and D in (6.10)

$$D - F + FD = \sin^2 \frac{\mu_z}{2}$$

Now $0 \leq \sin^2 \frac{\mu}{2} \leq 1$ has to hold in both cases. The criterion for stability in both planes is therefore

$$0 \leq F - D + FD \leq 1$$

$$0 \leq D - F + FD \leq 1$$

The limits of the stable region are

$$\begin{aligned} \sin \frac{\mu_x}{2} = 0 &\Rightarrow F = \frac{D}{1+D} & \sin \frac{\mu_z}{2} = 0 &\Rightarrow D = \frac{F}{1+F} \\ \sin \frac{\mu_x}{2} = 1 &\Rightarrow F = 1 & \sin \frac{\mu_z}{2} = 1 &\Rightarrow D = 1 \end{aligned}$$

The stable region has the appearance of a necktie (Fig. 39).

6.3 Weak focusing with constant gradient

Let us assume a continuous ring magnet with the magnetic field independent of s . The focusing strengths

$$\begin{aligned} K_z &= k \\ K_x &= \left(\frac{1}{\rho^2} - k \right) \end{aligned} \quad (6.11)$$

can be made both positive, if k is smaller than the "weak focusing term" $\frac{1}{\rho^2}$.

We choose a small gradient g

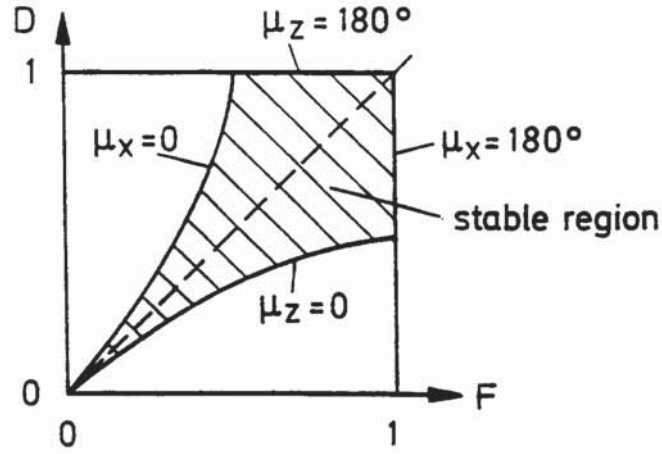


Figure 39: Stability diagram for different strengths of focusing and defocusing quadrupoles

$$B_z(x) = B_0 - gx \quad (6.12)$$

Then the field index n , defined in Eq. (1.5), is

$$n = -\frac{\rho}{B_0} \frac{\partial B_z}{\partial x} = \frac{\rho g}{B_0} = \frac{p_0 \rho}{e B_0} k = \rho^2 k \quad (6.13)$$

$$K_x = \frac{1-n}{\rho^2}, \quad K_z = \frac{n}{\rho^2} \quad (6.14)$$

From the conditions $K_x > 0$, $K_z > 0$ for focusing in both planes we recover our old result Eq. (1.6): $0 < n < 1$.

The transfer matrix for one revolution is for the horizontal motion

$$\begin{pmatrix} C & S & D \\ C' & S' & D' \\ 0 & 0 & 1 \end{pmatrix} = \begin{pmatrix} \cos \varphi & \frac{\rho}{\sqrt{1-n}} \sin \varphi & \frac{\rho}{1-n} (1 - \cos \varphi) \\ -\frac{\sqrt{1-n}}{\rho} \sin \varphi & \cos \varphi & \frac{1}{\sqrt{1-n}} \sin \varphi \\ 0 & 0 & 1 \end{pmatrix} \quad (6.15)$$

The matrix (6.15) does not depend on the start point s . If we equate it to the (3×3) -extension of the matrix (4.42), we see that β does not depend on s and therefore $\alpha = -\frac{1}{2}\beta' = 0$.

We get

$$\begin{aligned} \beta_x &= \frac{\rho}{\sqrt{1-n}} = \text{const} \\ Q_x &= \sqrt{1-n} \end{aligned} \quad (6.16)$$

The number of betatron oscillations per turn is less than 1.
The dispersion is

$$D = \frac{\rho}{1-n} = \text{const} \quad (6.17)$$

The closed dispersion curve is simply a circle which is concentric with the reference orbit $r = \rho$.
The momentum compaction factor is therefore

$$\alpha = \frac{1}{2\pi\rho} \oint \frac{D}{\rho} ds = \frac{1}{1-n}$$

For the vertical plane, we replace $1 - n$ by n

$$\begin{aligned} \beta_z &= \frac{\rho}{\sqrt{n}} = \text{const} \\ Q_z &= \sqrt{n} \end{aligned} \tag{6.18}$$

For $n = \frac{1}{2}$ we have $\beta_x = \beta_z = \rho\sqrt{2}$ and $D = 2\rho$. The following table compares weakly and strongly focusing machines for $\rho = 25 \text{ m}$ and $\rho = 400 \text{ m}$. The weakly focusing machine requires extremely large apertures especially to accommodate the energy spread of the beam. In the strongly focusing case, a phase advance of 60° per cell has been chosen.

$$\text{a) } \begin{aligned} \rho &= 25 \text{ m} \\ \ell &= 5 \text{ m} \end{aligned}$$

$$\text{b) } \begin{aligned} \rho &= 400 \text{ m} \\ \ell &= 20 \text{ m} \end{aligned}$$

weak foc.	strong foc.
$\beta = 35 \text{ m}$	$\hat{\beta} = 17 \text{ m}$
$D = 50 \text{ m}$	$\hat{D} = 5 \text{ m}$

weak foc.	strong foc.
$\beta = 566 \text{ m}$	$\hat{\beta} = 69 \text{ m}$
$D = 800 \text{ m}$	$\hat{D} = 5 \text{ m}$

7 ACKNOWLEDGEMENTS

In preparing these lectures and the notes we have profited greatly from the books and articles quoted in the bibliography.

References

- [1] E.D. Courant and H.S. Snyder: Theory of the Alternating-Gradient Synchrotron, *Annals of Physics* **3**, 1958, 1.
- [2] H. Bruck: *Accélérateurs Circulaires de Particules*, Press Universitaires de France, Paris, 1966; english translation: Los Alamos Report LA-TR-72-10
- [3] M. Sands: The Physics of Electron Storage Rings, SLAC report 121, 1970.
- [4] K. Steffen: Basic Course on Accelerator Optics, Proceedings of the 1984 CERN Accelerator School, CERN 85-19, 1985.
- [5] P. Schmüser: Basic Course on Accelerator Optics, Proceedings of the 1986 CERN Accelerator School, CERN 87-10, 1987
- [6] H. Wollnik: *Optics of Charged Particles*, Academic Press, 1987.
- [7] K. Wille: *Physik der Teilchenbeschleuniger und Synchrotronstrahlungsquellen*, Teubner, Stuttgart, 1992.
- [8] Proceedings of the 1984 CERN Accelerator School, CERN 85-19, 1985.
- [9] R. Brinkmann: Insertions, Proceedings of the 1986 CERN Accelerator School, CERN 87-10, 1987
- [10] K. Steffen: *High Energy Beam Optics*, Interscience, 1965.
- [11] M. Conte, W.W. MacKay: *An Introduction to the Physics of Particle Accelerators*, World Scientific, 1991.
- [12] J. Rossbach: Teilchenbeschleuniger, in: *Handbuch der Vakuumelektronik*, Hrsg. Eichmeier/Heynisch, Oldenbourg, 1989, 343-425.
- [13] F. Willeke, G. Ripken: *Methods of Beam Optics*, DESY 88-114, 1988.
- [14] D. Edwards, M.J. Syphers: *An Introduction to the Physics of High Energy Accelerators*, Wiley-Interscience, 1993.